UNIVERSITÀ DI PARMA

UNIVERSITA' DEGLI STUDI DI PARMA

DOTTORATO DI RICERCA IN BIOTECNOLOGIE E BIOSCIENZE

CICLO XXXVI

Nanobiotechnologies to improve plant protection

Coordinatore:

Prof. Marco Ventura

Supervisore:

Prof. Nelson Marmiroli

Prof.ssa Marta Marmiroli

Tutor:

Prof.ssa Elena Maestri

Co-Tutor:

Prof.ssa Marina Caldara

Dott. Luca Pagano

Dottorando: Silvia Carlo

Anno Accademico 2022 - 2023

Summary

Abstract

The increasing salinization of arable lands exposes crops to abiotic stresses, requiring the adoption of novel, sustainable and efficient technologies to counteract yield reductions. In recent years, prolonged drought conditions contributed to the intrusion of saline water from the sea into rivers and wells, furtherly increasing the overall salinity levels. The use of brackish water from the Po River delta lagoons in Romagna, along with salinized water in the Foggia plains, are examples of common practices for field irrigation in Italian regions. However, this practice has been associated with reduced tomato plant yields and the gradual salinization of the soil. Nano-biotechnological approaches, including Plant Growth Promoting Microorganisms (PGPM) and Engineered Nanomaterials (ENMs) to mitigate salt stress in economically significant crops such as tomato (*Solanum lycopersicum* L.) hold promise to regulate plant responses. In particular, multi-strain inoculants offer the potential to achieve a balanced microbial functional profile capable to induce various plant responses, including resistance to abiotic stresses. In addition, the use of ENMs could be an applied solution as agricultural nanofertilization, due to their unique properties contributing to improve crop performance and to decrease environmental impact, through a diminished usage of conventional fertilizers. The present work aims to assess the effects of PGPMs (microbial consortia) combined with SiO_2 nanoparticles (NPs) on salt stress tolerance during the cultivation of industrial tomato (cv. Heinz 3402). The experiments consisted of different phases: a preliminary study aimed at optimizing experimental conditions, including the determination of the optimal saline concentration and the selection of the most promising consortium. For the treatment the selected consortium was combined with silicon nanoparticles and its physiological and transcriptomic effects in the plant were assessed. A germination test was performed to evaluate the impact of microbial consortia when used as seed coatings at different salinity levels. Given that the microbial consortia seeds coating consistently showed a negative effect on tomato germination, the subsequent pot experiment involved the inoculation of microbial consortia stabilized in zeolite during the transplant phase. Tomato plants were transplanted after 21 days from germination, in soil inoculated with 2 grams of MC_B and MC_D consortia powder in combination with 2 grams of spores of Arbuscular Mycorrhizal Fungi (AMF) (*Rhizophagus intraradices*). One week after transplant other 2 grams of microbial consortia were inoculated and the induction of salt stress started, through 0% (no stress), 0.5% (low), 0.75% (medium) and 1% (high) NaCl solutions and lasted for a total of six weeks. The results indicated a decreased germination rate of seeds coated with MC_D, along with reduced plant biomass, photosynthetic activity and flowering in the pot experiment. Conversely, plants treated with MC_B in combination with AMF exhibited decreased proline content under stress conditions and a

significant increase in root length. After the preliminary assessment of the experimental conditions, tomato plants were transplanted into soil amended with SiO_2 NPs or sodium metasilicate (Na_2SiO_3), in combination with MC_B and AMF inoculum and salt stress (1% NaCl). After 6 weeks of salt stress, samples of roots, shoots, and leaves were collected. Physiological and phenotypic parameters were monitored during plant growth: photosynthetic activity and biochemical assays (lipid peroxidation, cellular respiration, determination of proline content) were performed. Leaves and roots samples were analyzed through scanning electron microscopy (μ-XRF), to obtain X-ray fluorescence elemental maps. Transcriptomic analysis through RNAseq were also performed on leaves and roots samples. The results showed a positive role of SiO_2 NPs in reducing lipid peroxidation of plant roots under salt stress condition, although it did not affect proline content. On the other hand, microbial consortium inoculum appears to play a role in the reduction of salt stress biomarkers, including proline content and lipid peroxidation. However, a comprehensive understanding of these mechanisms requires further investigation. X-ray fluorescence elemental maps analyses showed a greater accumulation of silicon into the stems treated with Na_2SiO_3, as compared to SiO_2 NPs treatment and untreated control, suggesting a greater silicon translocation in its ionic form. The reduced SiO_2 NPs translocation (as compared with sodium metasilicate) results in a differential gene expression regulation. Interestingly, chloroplast functions have been observed in the modulation of silicon-mediated salt stress response. The use of ENMs demonstrated considerable potential, not only for inducing stress tolerance, as exemplified in the case of nano-Si, but also as a sustainable alternative to conventional fertilizers application. In a parallel study, *Zea mays* L. plants were treated with Fe_3O_4 NPs to assess a controlled release of iron, a vital element for plant physiology. Maize plants (V_2 growth stage) were transplanted into Fe_3O_4 NPs or $FeCl_3$ amended soil, and after 5 month (R growth stage) leaves, roots and seeds were harvested. Morphological and physiological parameters, metal uptake in the three tissues and transcriptional responses in leaves and roots, were evaluated. While no significant morphological differences were observed, $FeCl_3$ treated plants showed reduced photosynthetic activity as well as increased stomatal transpiration and lipid peroxidation, while Fe_3O_4 NPs treatments resembled untreated controls and $FeCl_3$ treated plants. Furthermore, the transcriptional analysis via RT-qPCR on target genes in RNA extracted from leaves and roots has revealed an influence of iron treatments on iron transport mechanisms and the response to oxidative stress. The approaches explored on different plants of agri-food interest, utilizing multiple nano-biotechnological strategies (with PGPM, nanofertilizers, or through their combination) showed a high potential of implementation in the modern agricultural practices and scale-up to field experimental conditions. Moreover, the approaches utilized may also contribute to develop and to adopt novel strategies in assessment and in characterization of the risk associated to nano-biotechnological solutions.

Abbreviations list

AAS13	Auxin amido synthetase13
ABA	Abscissic acid
ABRE	ABA-responsive elements
ACC	1-aminocyclopropane-1-carboxylic acid
AMF	Arbuscular Mycorrhizal Fungi
BP	Biological Processes
CAT	Catalase
CC	Cellular Component
CK	Cytokinins
DEGs	Differentially Expressed Genes
DLS	Dynamic Light Scattering
ENMs	Engineered Nanomaterials
FA-AAS	Flame Atomic Absorption Spectrometry
FC	Fold Change
FDR3	Ferric reductase defective3
FPKM	Fragments Per Kilobase of exon per Million mapped fragments
GA	Gibberellins
GI	GIGANTEA
GSI	Germination Stress Tolerance Index
GSR1	Glutathione reductase 1
HSP	Heat Shock Protein
IAA	Indole-3-acetic acid
ISR	Induced Systemic Resistance
JA	Jasmonic acid
JAR1	Jasmonic acid-amido synthetase
MATE	Multidrug and toxic compound extrusion
MC	Microbial Consortia

MDA Malondialdehyde

MF Molecular Function

NA Nicotianamine

NAS Nicotianamine synthase

NPs Nanoparticles

PGPMs Plant Growth Promoting Microorganisms

PGPR Plant Growth-Promoting Rhizobacteria

PI Promptness Index

POX Peroxidase

PRO1 Proline responding 1

PS Phytosiderophores

PSII Photosystem II

ROS Reactive Oxygen Species

SA Salicylic acid

SOD Superoxide dismutase

SOD1 Superoxide dismutase 1

SOS Salt Overly Sensitive

TBAR Thiobarbituric Acid Reactive Substance

TTC 2,3,5-Triphenyltetrazolium chloride

1 Introduction with foreground literature

1.1 Climate change: an emerging agricultural challenge

One of the most debated topics in recent decades is the ongoing climate change and its negative effect. The damages caused are irreversibly creating serious issues in various essential sectors, and the condition is expected to worsen unless immediate international measures are taken to manage and mitigate the damages, with effects the entire industrial system. Global warming has led to a sudden increase in average temperatures by 1.1°C during the period 2011-2020 compared to the last century, with a greater impact on inland areas (+1.6°C) than oceans (+0.9°C). Projections from the Intergovernmental Panel on Climate Change (IPCC, 2023) indicate that if we maintain an intermediate level of emissions as of today, we can expect the average temperature increase that could reach 3°C by 2100 (**Figure 1.1**).

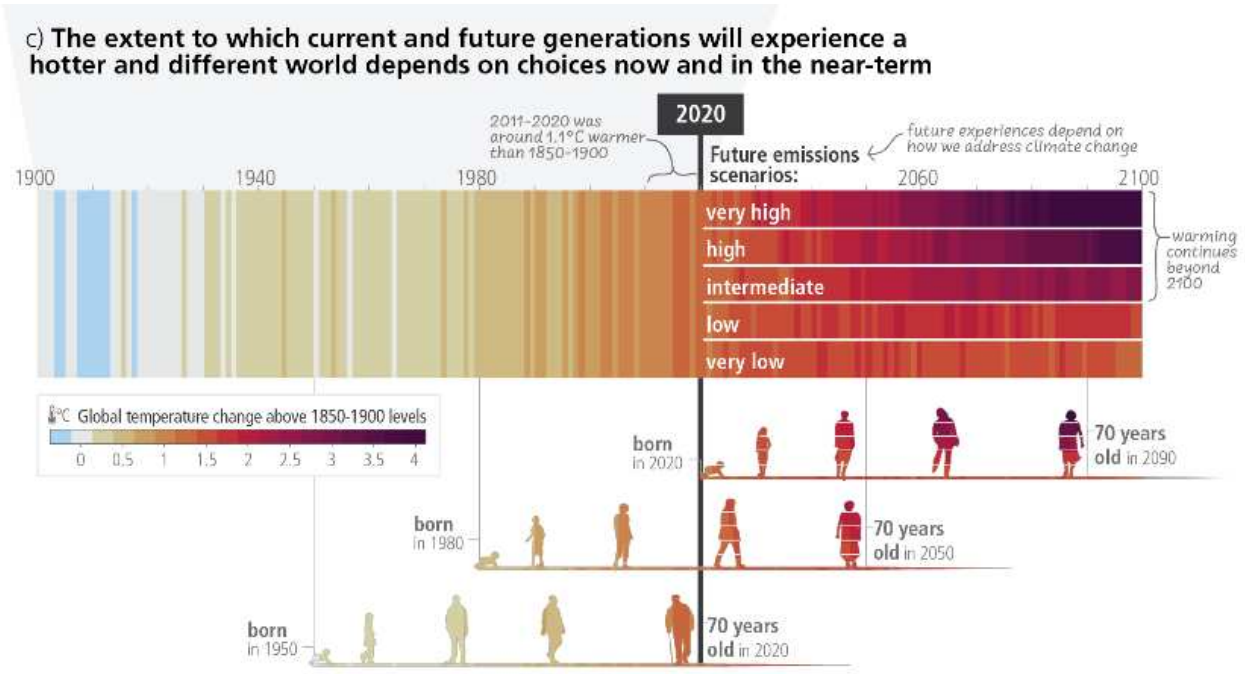

Figure 1.1: The picture is taken from Figure SPM.1 of the United Nations Intergovernmental Panel on Climate Change, AR6 Synthesis Report with partial elaboration. The image depicts the fluctuations in worldwide surface temperature from 1900 to 2020, and its projection up to 2100, and it is showcasing the historical and future changes in climate across the lifespan of three generations (born in 1950, 1980, and 2020). The predicted changes in global surface temperature from 2021 to 2100 are displayed for different emissions scenarios, ranging from very low to very high. The 'climate stripes' represent the fluctuations in yearly global surface temperatures, illustrating the human-induced long-term trends and the ongoing influence of natural variability. The generational icons' colors match the global surface temperature stripes for each year, and the segments within the icons from 2020 to 2100 represent possible future emission scenarios depending on how we address climate change today.

The rise in temperature is having, and will have, an increasingly significant impact on agriculture. On one hand, climate change is reducing the moisture of the soils in various geographic areas, including the Mediterranean region (**Figure 1.2**), and, on the other hand, it is rising sea levels (it is currently 20 cm higher than in 1901, as reported by IPCC). This leads to a subsequent decrease in river levels and a rise in the seawater level, causing to cultivated lands to become generally drier and/or more saline, resulting in significant damages to agriculture. Climate change has already reduced food security, while the average crop production increased over the last 50 years. Approximately half of the global population is currently at risk of severe drought during at least one period of the year due to a combination of climatic and non-climatic factors (IPCC, 2023).

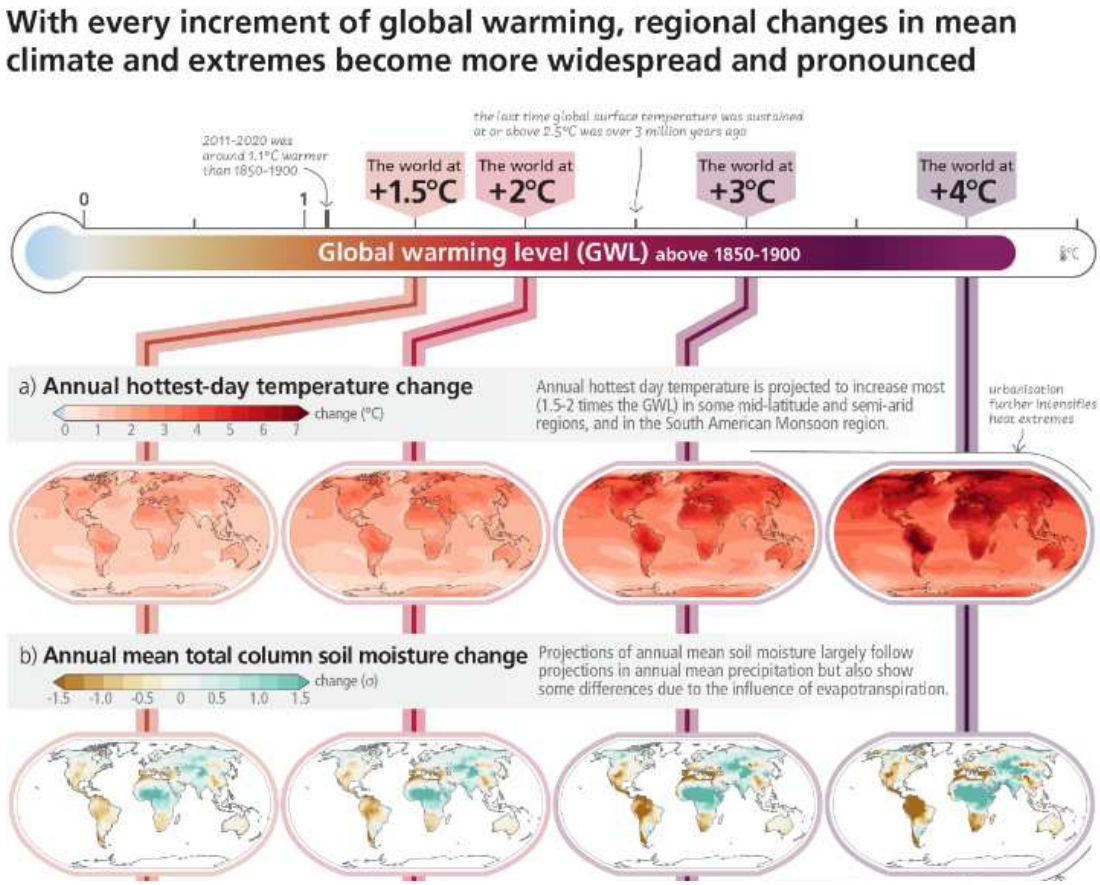

Figure 1.2: The picture is taken from Figure SPM.1 of the United Nations Intergovernmental Panel on Climate Change, AR6 Synthesis Report with partial elaboration. The figure illustrates the projected changes in annual maximum daily temperature and annual mean total column soil moisture at different global warming levels (1.5°C, 2°C, 3°C, and 4°C relative to 1850–1900). In dry regions, large positive relative changes of temperature may correspond to small absolute changes in soil moisture. The unit of measurement for soil moisture change is the standard deviation of interannual variability during 1850–1900, which is commonly used to characterize drought severity.

In Europe, it is estimated that 34.6% of arable lands are subjected to drought, and climate change will further increase this percentage (Prăvălie *et al*., 2021). Globally, some scenarios predict a 7%-23% decrease in the yield of staple food crops, particularly rice and maize (Rezaei *et al*., 2023).

Only in Italy, estimates suggest that climate change will cause by 2100 a reduction in the value of agricultural land ranging from 87-162 billion euros due to drought (Spano *et al*., 2020). In the summer of 2022, an extremely hot and dry period led to a drastic decrease in the water level of the Po River, the main Italian river that provides water for field irrigation across much of the Po Valley, resulting in the intrusion of saltwater into cultivated areas for over 40 km inland (Straffelini & Tarolli, 2023). It is projected that in the future, saltwater intrusions into the Po River will increase by 80% in extent and 100% in persistence (Bellafiore *et al*., 2021), causing serious issues related to the progressive salinization of soils and the consequent reduction in crop yields. This calls for agricultural practices capable of mitigating these harmful effects. According to the United Nations, the planet is projected to accommodate 10.4 billion people, leading to a global increase in food demand that by 2050 should increase from 30% to 62%, compared to 2010 (van Dijk *et al.,* 2021). To meet this growing demand, it will be necessary to increase crop yields, especially to counteract the progressive reduction in cultivable areas. However, the use of conventional fertilizers could cause the accumulation of toxic substances in the soil, exacerbating the environmental situation (Baweja *et al*., 2020). Furthermore, fertilizer production is a significant source of climate-altering gases (Walling & Vaneeckhaute, 2020). Hence, it is crucial to prioritize the development of eco-friendly alternatives to tackle the rising food demand and promote environmental preservation.

1.2 Impact of abiotic stresses on plants

According to various reports, crop productivity is consistently impacted from the changing environmental conditions (Janni *et al.*, 2024). Indeed, cultivations are subjected to increased temperatures, prolonged periods of drought and floods, that are leading to enormous losses with a reduction of nearly 50% of the yield of various crops. In response to abiotic stresses, plants adopt various response strategies such as modulating photosynthetic activity and hormonal homeostasis. However, this leads to an alteration in the plant's biochemical and physiological balance, sometimes resulting in oxidative stress (Khan *et al*., 2012). One of the most critical abiotic stresses is salt stress as it directly reduces crop yield and health. Moreover, salt accumulation in soils progressively makes fields less arable and reduces their use in agriculture (Abdelgawad *et al.,* 2016). The consequences of salt stress on crops pose a global threat, affecting approximately 1.1 billion hectares worldwide (FAO, 2020). In Italy, particularly in the Po Delta region, it is estimated that over the last twenty years, the rise of seawater has reached values of 40 kilometers along the deltaic mouths. This phenomenon, along with the increasingly frequent droughts, enhanced the salinity of the irrigation waters (Agenzia prevenzione ambiente energia emilia-romagna, Arpae, 2023). Plants exposed to salt stress undergo an initial osmotic phase, caused by the influx of salts, primarily sodium ions, into its root cells from

the surrounding soil. This increased concentration of salts creates an osmotic imbalance, leading to a higher solute concentration in the root cells compared to the surrounding soil solution. As a result, water moves out of the plant cells, causing a decrease in turgor pressure and cell dehydration. However, when saline stress persists over a long period of time, the ionic phase follows the osmotic phase. The influx of Na^+ and Cl^- ions determines the plant's response at the cytoplasmic level, triggering different pathways aimed at sequestering ions within the vacuole. This accumulation may lead to an osmotic imbalance within the cell, which could result in tissue damage and interference with the plant's vital biochemical and physiological activities (Munns & Tester, 2008).

1.2.1 Physiological mechanisms in response to salt stress

The onset of drought stress during the osmotic phase triggers a plant response which tries to minimize water loss through stomatal closure, thereby maintaining water balance in plants (Saradadevi *et al*., 2017). However, the low availability of CO_2 in leaf intercellular spaces can lead to the disruption of important biochemical reactions such as photosynthesis, which in turn may induce oxidative damages in tissues. During photosynthesis, excessive light absorption and low CO_2 availability promotes electron transfer to O_2, resulting in the generation of singlet oxygen and the subsequent induction of oxidative stress (Nadarajah, 2020). Under salt and drought stress conditions, respiration increases to compensate for the reduced energy rate in chloroplasts, contributing to a further increase in oxidative stress (Atkin & Macherel, 2009). The overproduction of reactive oxygen species (ROS) causes oxidative damage to membrane lipids, proteins, DNA, and nucleic acids (Gill & Tuteja, 2010). Polyunsaturated fatty acids (PUFA), such as linoleic acid, are particularly susceptible to ROS attack, leading to the formation of alkoxyl radicals, aldehydes (malondialdehyde), alkanes, epoxides, and alcohols (Davies, 2000). Following ROS generation, hydrogen peroxide synthesis stimulates a transduction cascade that activates detoxification mechanisms, including enzymatic and non-enzymatic components capable of preventing cellular damages. Enzymatic components include superoxide dismutase (SOD), catalase (CAT), and peroxidase (POX), involved in reducing singlet oxygen ($^1O_2$) to hydrogen peroxide (H_2O_2). Non-enzymatic components include ascorbic acid, α-tocopherol, flavonoids, glutathione, carotenoids, lipids, and phenolic compounds, components that can effectively mitigate oxidative damage by reducing ROS activity or working in conjunction with the enzymatic components mentioned above (Gill & Tuteja, 2010). Exposure of plants to NaCl-rich soils can lead to the accumulation of Na^+ and Cl^- ions in the apoplast or in the vacuole. If ion accumulation occurs in the apoplast, the osmotic gradient between the cell interior and exterior increases, promoting water diffusion into the intercellular spaces and a progressive dehydration which could lead to cell death. Alternatively, if ion accumulation occurs in the cellular vacuole, salt stress

tolerance is enhanced (Volkmar *et al.*, 2011). Indeed, ion compartmentalization in the vacuole creates a strong osmotic gradient across the vacuolar membrane, balanced by an increased synthesis of low molecular weight biochemical molecules in the cytoplasm, known as osmolytes and osmoprotectants. Osmolytes play a role in stabilizing internal osmotic potential, increasing protein stability, and protecting the macromolecular structures (Yancey, 2005). Osmoprotectants are categorized into various groups, including amino acids, sugars, and sugar alcohols (Läuchli & Grattan, 2011). Salt stress alters the biosynthesis, accumulation, and distribution of various phytohormones, including abscisic acid (ABA) (Calestani *et al.*, 2015; Ruotolo *et al.*, 2018), jasmonic acid (JA), salicylic acid (SA), indole-3-acetic acid (IAA), gibberellins (GA), and cytokinins (CK). Abiotic stress in plants leads to ethylene overproduction, which can inhibit roots and shoots proliferation and leaf senescence, thereby reducing plant growth and development. ABA is a key hormone in regulating the response to salt stress, playing a major role during the osmotic stress phase. In leaves, ABA regulates transpiration by promoting stomatal closure and inducing the expression of many genes involved in abiotic stress tolerance (Fujita *et al.*, 2013). Another example of hormonal regulation is the induction of salt stress tolerance by salicylic acid, the latter is involved in maintaining ion homeostasis by promoting osmolyte accumulation and detoxification from reactive oxygen species (Elhakem, 2020).

1.2.2 Molecular mechanisms in response to salt stress

The molecular mechanisms underlying the plant response to salt stress involve various signal transduction pathways triggered by environmental stimuli capable of disrupting biochemical and physiological balance. Among the primary consequences of Na^+ ion accumulation are alterations in intracellular Ca^{2+} levels and the production of ROS. The increase in cytosolic Ca^{2+} caused by Na^+ accumulation induces changes in cellular osmotic pressure, activating Ca^{2+} channels and, consequently, initiating the Ca^{2+} signaling transduction cascade, as described more in details in **Figure 1.3**.

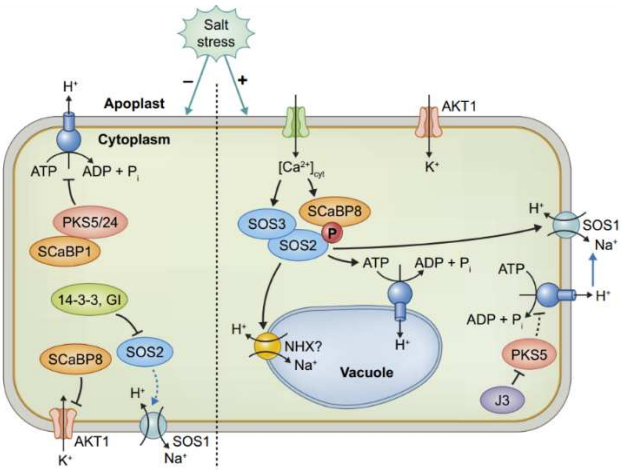

Figure 1.3: The picture is taken from Yang Y. & Guo, 2018 with partial elaboration. Comparison of cellular homeostatic regulation in the presence and absence of salt stress. The kinase activity of SOS2 is repressed under unstressed conditions by 14-3-3 and GIGANTEA (GI) proteins, preventing the transport of H^+ through the ATPase. When salt stress is induced, the concentration of Ca^{2+} ions in the cytoplasm increases, and SCaBP8, which under unstressed conditions acts as a repressor of the K^+ transporter AKT1, gets phosphorylated, activating the SOS pathway. Gradients that allow the internalization of Na^+ into the vacuole through the Na^+/H^+ antiport are then generated.

The rise in ROS levels also contributes to trigger the Ca^{2+} signaling pathway: for instance, hydrogen-peroxide-induced Ca^{2+} increases 1 (HPCA1), a kinase receptor located in the plasma membrane capable of sensing H_2O_2 increase and induce stomatal closure through Ca^{2+} influx (Zhao *et al.*, 2021). The accumulation of Na^+ ions under salt stress conditions also leads to a disruption of cellular ion homeostasis, potentially causing severe cytotoxic damage. The efflux of Na^+ from the cytoplasm is mediated by Na^+/H^+ antiports that transport Na^+ to the apoplast, if located in the plasma membrane, or to the vacuole, if located in the vacuolar membrane. This regulation is mediated by the Salt Overly Sensitive (SOS) signaling pathway, that prevent the cytosolic Na^+ concentration from reaching toxic levels (Yang Y. & Guo, 2018). The production of osmolytes such as proline, polyols, and sugars results in a reduction of cytosolic osmotic potential, contributing to alleviating the cytotoxic effects induced by salt stress. Simultaneously, these osmolytes serve as signaling molecules for the regulation of ABA-mediated signaling. The interaction with ABA-responsive elements (ABREs) modulates the expression of various genes responsible for salt stress tolerance, with the involvement of ABRE-binding protein/ABRE-binding factor (AREB/ABF) transcription factors (**Figure 1.4**). Furthermore, the disruption of cellular balance caused by salt stress can also lead to damages of the cell membrane, requiring a specific regulatory system for its biosynthesis.

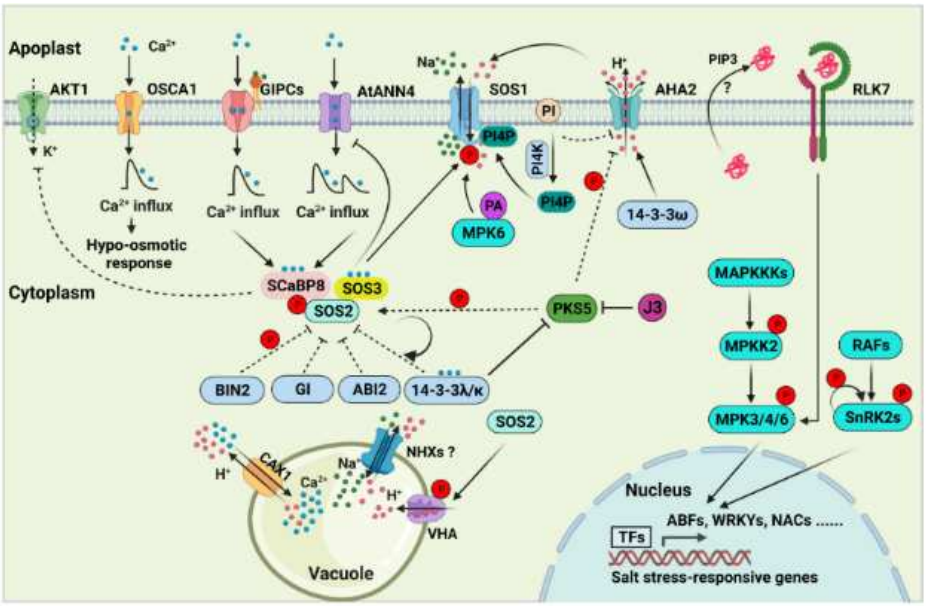

Figure 1.4: The picture is taken from Ma L. *et al*. 2022 with partial elaboration. The increase in cellular Na^+ is sensed by the GIPCs sensor, which, by binding to Na^+, mediates Ca^{2+} influx. The accumulation of Ca^{2+} activates the SOS pathway. To ensure the plant response to salt stress in the long term, calcium influx is then maintained through the modulation of AtANN4 by the SOS pathway. The interaction between PIP3 and RLK7, which accumulate under salt stress conditions, activates MPK3/6, initiating a signal transduction cascade mediated by MAP kinases. As a result of this signal transduction, various transcription factors activate the expression of genes involved in the plant's response to salt stress (e.g., ABFs, WRKYs, NACs) at the nuclear level.

In addition to ABA-mediated regulation of secondary wall biosynthesis, other key players such as the Homeobox HD-ZIP Class III (HD-ZIPIII) transcription factor, as well as the MYB46/MYB83 transcription factor, play a crucial role (Zhao *et al*., 2021). There are also evidences of a correlation between the plants response to salt stress and light signaling, highlighting the negative influence of salt stress on the photosynthetic system. For instance, there are reports of the translocation in cytosol of constitutive photomorphogenic1 (COP1) protein in plants exposed to salt treatments, which is typically controlled by light signal. Additionally, the proline pathway, which is typically modulated under salt stress conditions, shows regulation by light signaling at the P5CS1 gene level. Furthermore, the modulation of the expression of salt-dependent genes linked to diurnal cycles and the circadian clock has been observed (Ma L. *et al.,* 2022).

1.3 Nano-biotechnological approaches to improve plant growth

1.3.1 Engineered nanomaterials (ENMs)

Nanotechnologies attract the interest of numerous companies in diverse sectors because of the wide-ranging applicability, and unique properties, of nanoscale materials. According to the European Commission, nanomaterials, whether natural or synthetic, are defined as solid particles wherein at least 50% of their composition falls within the range of 1 nm to 100 nm. Alternatively, if they exhibit an elongated or plate-like shape, one dimension should be less than 1 nm, and the other dimensions should exceed 100 nm (EU Commission, 2022). Operating at the nanoscale exploits unique physicochemical properties, such as highly specific surface area, enhanced dissolution and reactivity rates, and strong absorption capabilities. These distinguish nanoparticles significantly from their bulk counterparts. Adhering strictly to the definition of NPs enables the identification of various types of NPs in nature, including biological (viral NPs) and non-biological (volcanic powders). However, naturally occurring NPs often exhibit irregular structures and size variabilities. In contrast, the synthesis of ENMs allows for greater uniformity and the design of well-defined nanostructures, making them applicable in various technological sectors (Elmer & White, 2018). Classification systems of ENMs are dependent on both the morphology and the chemical composition of nanoparticles (**Figure 1.5**). The morphology of ENMs is influenced during their production by the material and synthesis techniques, allowing the creation of specific shapes (e.g., spherical, needle, cubic, nanotubes) tailored to the intended application (Buzea & Pacheco, 2017).

In recent decades, many studies in the field of plant pathology have involved the use of metalloids and metallic oxides to be used as bactericides/fungicides, nanofertilizers or protectant against abiotic stress (Elmer & White, 2018). The use of ENMs such as metal oxide or functionalized carbon-based NPs, enables the gradual and targeted release of fertilizers, pesticides, and herbicides, reducing their widespread application and optimizing the administration of micronutrients (P. Wang *et al*., 2016). Numerous studies have demonstrated the potential use of NPs as nutritional sources to support plant growth (Marmiroli et al., 2017; Pavlicevic, Pagano, et al., 2023). However, potential concentration-dependent phytotoxic effects remain to be investigated (Ma C. *et al.*, 2018). For example, it is reported that SiO_2 nanoparticles can be used as fertilizers, insecticides, and herbicides (Goswami & Mathur, 2022). It has been shown that nano-Si could have a beneficial impact on plant growth, attributed to an increase in photosynthesis, transpiration, and photochemical efficiency (Rastogi *et al.*, 2019). Additionally, silicon-based nanomaterials are known for their ability to induce resistance and enhance plant stress tolerance through a wide range of mechanisms, including mechanical reinforcement of defensive structures and activation of biochemical defenses (Fellet *et al*., 2021). Several studies also indicate that Fe_3O_4 nanoparticles can have positive effects on plant growth and development (Palmqvist *et al.*, 2017; Servin *et al*., 2017), offering promising prospects for their potential application in agriculture as nanofertilizers. For example, it has been demonstrated that the application of iron nanoparticles can lead to an increase in the chlorophyll content in leaves, improving the photosynthetic activity of plants (Ghafariyan et al., 2013; Jalali et al., 2016, 2017; Souad A. Elfeky, 2013).

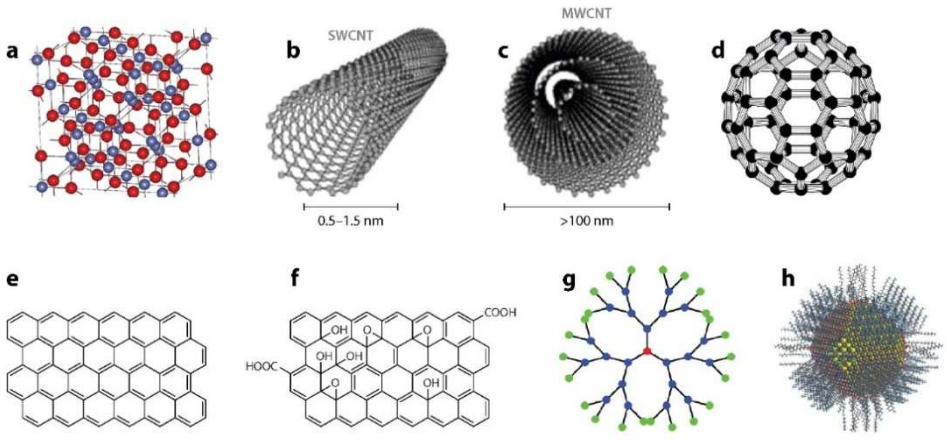

Figure 1.5: The picture is taken from Elmer & White, 2018 with partial elaboration. The schematic diagrams illustrate the various types of nanoparticles utilized in phytopathology. These include molecular arrangements of metal oxide nanoparticles, single-walled carbon nanotubes (SWCNT), multiwalled carbon nanotubes (MWCNT), fullerenes, graphene nanoparticle sheets, graphene-oxidized nanoparticle sheets, dendrimers, and quantum dots.

The small size and high surface area-to-volume ratio of nanomaterials make them ideal to pass through cellular barriers and interact with intracellular structures, but this may also increase the potential for genotoxic and cytotoxic effects (Ma C. *et al*., 2015; Rico *et al.*, 2011). Potential toxic effects of nanomaterials on plants can be caused by a variety of factors, including dissolution and release of metallic ions, size and morphology-dependent injuries or obstructions from NPs, production of ROS, and oxidation of biomolecules through catalytic reactions. The nature of interactions between plants and NPs strongly depends on the intrinsic properties of the ENM (Burello & Worth, 2015; P. Wang *et al*., 2016). To enhance the understanding of interactions between ENMs and plants, several models have been proposed, describing the pathways through which nanomaterials can penetrate plant tissues. These includes binding to carrier proteins, endocytosis, or binding to organic compounds present in the plants growth medium (**Figure 1.6**).

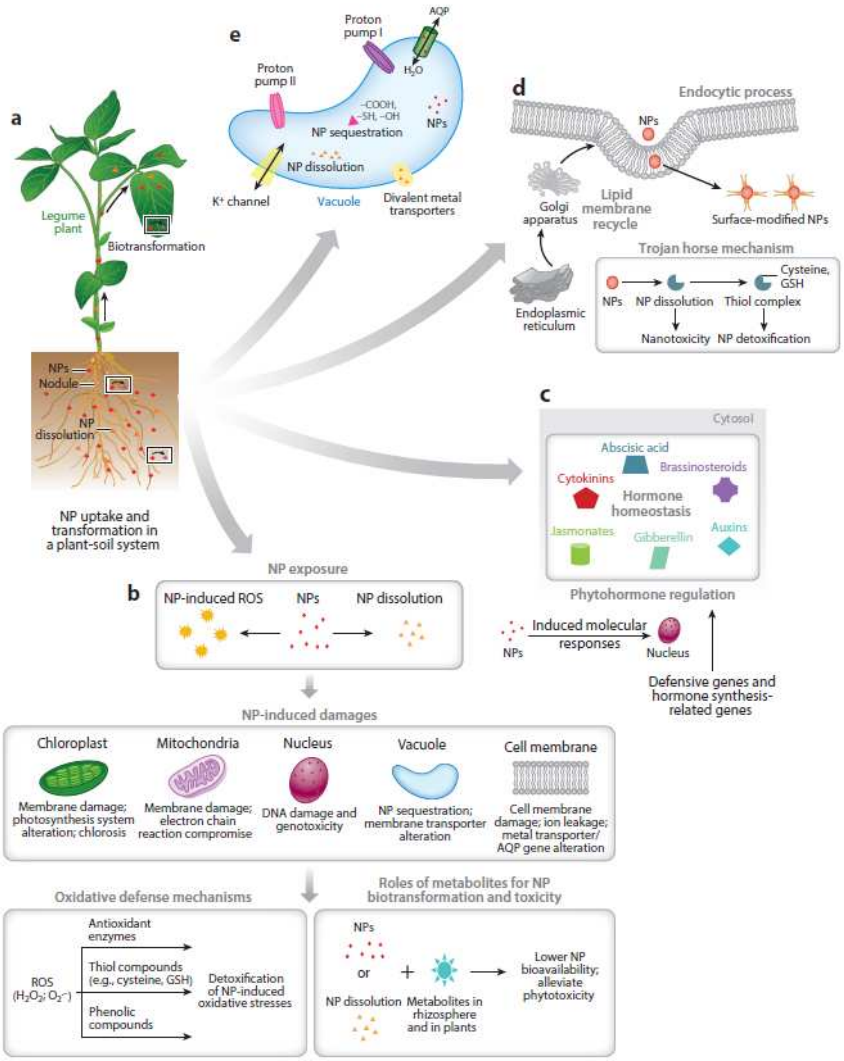

Figure 1.6: The picture is taken from Ma C. *et al*., 2018 with partial elaboration. Graphic representation of the plant response to exposure to nanoparticles (NPs) and potential internalization pathways in plant tissues. Once internalized at the root level, NPs can accumulate in the vacuole or be translocated to the aerial parts, either maintaining their structure or undergoing biotransformations. Internalization can occur through endocytosis followed by accumulation inside the plant cell, thereby exhibiting potential cytotoxicity. However, nanotoxicity at the cellular level can be mitigated by sequestration in the vacuole. The induction of cytotoxicity can be caused by oxidative stress, leading to increased levels of ROS, activating antioxidant defense mechanisms and regulating the plant's hormone-mediated response, both at the biochemical and molecular level.

They can also form complexes with membrane transporters or root exudates and subsequently be transported into the plant (Rico *et al*., 2011). The assessment of potential toxic effects of ENMs is crucial for establishing reliable regulations for their use. A significant factor when approaching nanotoxicological studies is understanding the effects of the material in its various physical forms, to determine whether any toxicity is distinctively caused by the nanostructured material, the bulk material, or the release of the metallic ion (Rico *et al*., 2011). For example, when designing an experiment for the study of nanomaterials, it is advisable to treat the organism with both the ENM and its respective salt under the same conditions, to assess whether any toxic effects or tolerance are exclusive to the nanostructured material or not (Marmiroli et al., 2014). This type of studies would also provide a more comprehensive and wide-ranging understanding of the action of NPs in complex systems (Pagano *et al.*, 2017). In this context, some of the challenges related to the ecotoxicology of nanomaterials are common to conventional ecotoxicology, while others present unique characteristics. Traditional ecotoxicology for example refers to the effective dose of a toxic substance capable of crossing the cell membrane and disrupting essential processes. However, when investigating ENMs, the effective dose could vary based on the conditions in which the suspension is found or due to dynamic physico-chemical interactions between receptors and the toxic substance, as well as biotic and abiotic transformations (Holden *et al.*, 2016). The accumulation of nanomaterials and the potential trophic transfer are influenced by several factors: chemical-physical and biological, which are generally analyzed separately, despite the need for a robust characterization of the complex interaction among all these parameters within the ecosystem. In the context of promoting a secure and sustainable application of ENMs in agriculture, with the aim of implementing strategies to optimize processes and production in the agri-food chain and mitigate damages resulting from climate change, it becomes essential to conduct specific studies on nanomaterials in cultivated plants that are economically significant.

Characterizing the modes of internalization and accumulation in different plant tissues is crucial, especially when dealing with edible plants. It is important to thoroughly understand the molecular and physiological mechanisms underlying the interaction between nanomaterials and plants. This approach seeks to broaden the understanding of these mechanisms to ensure safe use, both for environmental introduction and for the end consumer. In this way, a good balance between implication and application in the use of nanomaterials in agriculture can be established, opening a promising scenario for sustainable alternatives to conventional fertilization methods.

1.3.2 Plant Growth Promoting Microorganisms (PGPM)

An alternative strategy to the use of chemical fertilizers could involve the use of microorganisms able to interact with plants, generating positive effects on both growth and tolerance to abiotic and biotic stresses. PGPMs include a wide variety of microorganisms, such as AMF and rhizobacteria, present both in the rhizosphere and inside root tissues (Ma Y. *et al*., 2011). AMF are filamentous fungi that colonize roots and the rhizosphere in the form of branched filaments. After initial contact with root epidermal cells mediated by root exudates, hyphae reach cortical cells and branch into arbuscules, allowing enhanced nutrient assimilation by the plant. Nutrient absorption occurs due to the presence of extraradical mycelium, nitrogen, phosphorus, zinc, and potassium assimilation (Jacott *et al.*, 2017). The influence of AMF treatments on mitigating detrimental effects of salt stress has been documented, involving mechanisms such as increased nutrient availability, greater accumulation of osmolytes and antioxidant enzymes, and important physiological alterations, such as an improved photosynthetic efficiency and increased ABA accumulation (Evelin *et al*., 2009). Bacteria capable of colonizing plant root systems and promoting growth are referred to as Plant Growth-Promoting Rhizobacteria (PGPR). PGPR can be distinguished into internal PGPR (iPGPR), symbiotic bacteria living inside plant cells through nodule production, and external PGPR (ePGPR), bacteria colonizing the rhizosphere (Gray & Smith, 2005). The interaction of PGPR with plants promotes plant growth and development and enhances resistance to abiotic and biotic stresses through both direct and indirect mechanisms (**Figure 1.7**). Generally, PGPR mechanisms influencing plants include improved nutrient acquisition through nitrogen fixation and potassium and phosphate solubilization, as well as hormone synthesis. Common symbiotic nitrogen-fixing bacteria belong to the genera *Rhizobium, Sinorhizobium, Mesorhizobium, Frankia, Bradyrhizobium, Burkholderia*, while common non-symbiotic nitrogen-fixing bacteria include *Azoarcus, Herbaspirillum, Gluconacetobacter, Azospirillum,* and *Azotobacter*. Among the common phosphate-solubilizing bacteria are *Bacillus circulans, Agrobacterium* spp, *Pseudomonas* spp, *Rhizobium, Burkholderia, Azotobacter,* and *Enterobacter* (Shah *et al*., 2021).

In addition to enhancing nutrient availability, other direct mechanisms include the synthesis of hormone-like molecules (**Figure 1.8**). Many rhizospheric bacteria can synthesize indole-3-acetic acid (IAA) from tryptophan present in root exudates, which is absorbed by plants, promoting auxin synthesis and stimulating plant growth and cell proliferation (Ilangumaran & Smith, 2017). Indirect mechanisms include the bio-protective action of microorganisms against phytopathogens through antibiotic and antifungal synthesis or induced systemic resistance (ISR) by the activation of the plant's defense mechanisms, preparing it to resist and respond more rapidly and effectively to future pathogenic attacks.

PGPR-induced ISR stimulates signal transduction pathways dependent on jasmonic acid and ethylene, enhancing the plant's basal defense level against phytopathogens (Choudhary et al., 2007; Pavlicevic, Elmer, et al., 2023).

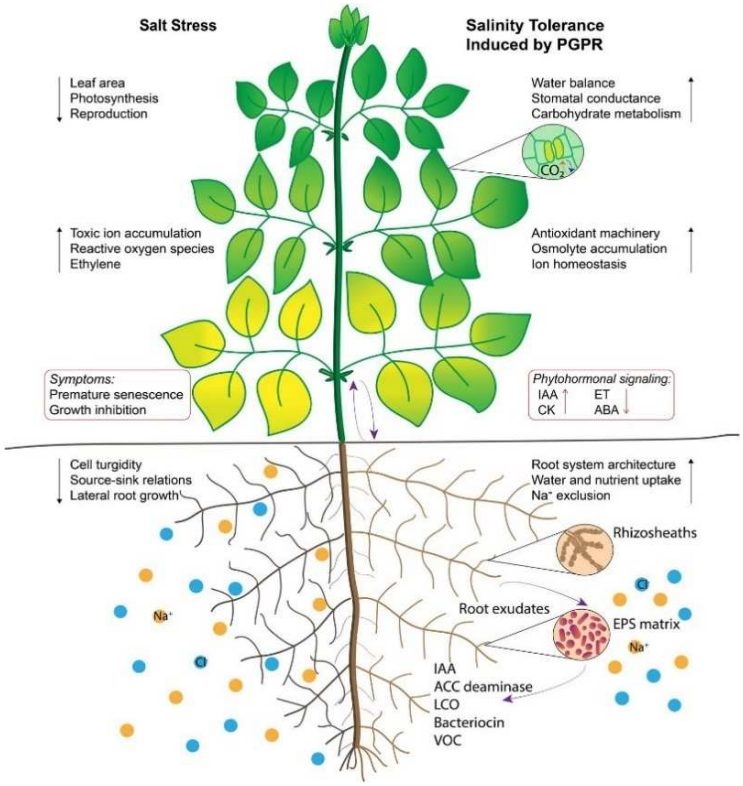

Figure 1.7: The picture is taken from Ilangumaran & Smith, 2017 with partial elaboration. Graphical representation of various mechanisms triggered by Plant Growth Promoting Rhizobacteria (PGPR) to mitigate the effects induced by abiotic stress, specifically salt stress. The action includes both direct effects at the root level, and influence on communication between the root and aerial parts through hormone-mediated signaling, as well as the regulation of physiological processes and the plant's water balance.

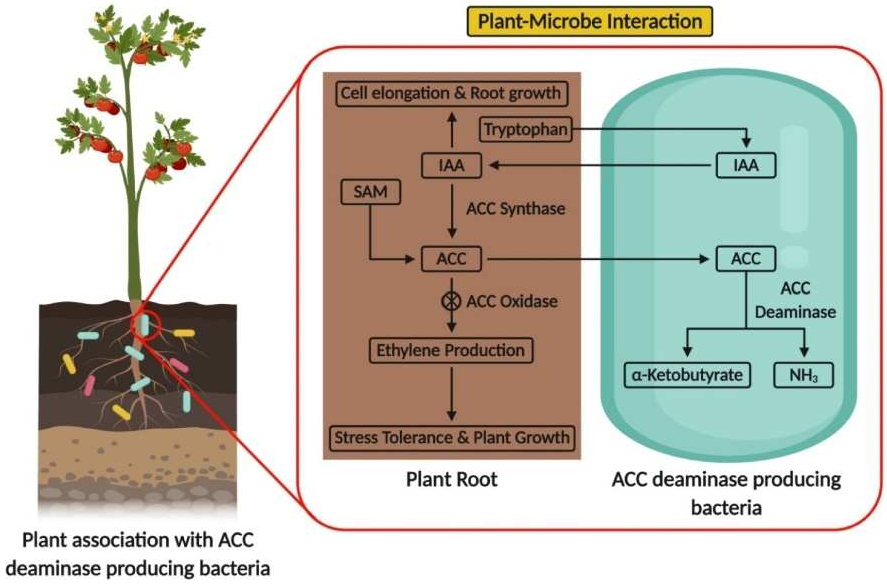

Figure 1.8: The picture is taken from Murali *et al*., 2021 with partial elaboration. Regulation of the ethylene pathway mediated by the production of ACC deaminase by root-associated PGPR. Mechanisms of action for enhancing plant and root growth and mitigating the effects induced by abiotic stress.

In the context of abiotic stress resistance, a key role is played by 1-aminocyclopropane-1-carboxylic acid (ACC)-deaminase, capable of regulating ion homeostasis and osmolyte accumulation by hydrolyzing ACC and thus decreasing ethylene concentration (Murali *et al*., 2021). Ethylene is a well-known hormone important in regulating many morphological and physiological plant processes, and it is overproduced in the presence of high exposure to abiotic stress. Its overproduction can inhibit root and shoot proliferation and increase leaf senescence, hindering plant growth and development. Another mechanism of stress response induced by microorganisms is the regulation of ionic homeostasis (**Figure 1.9**). It is reported that inoculation with certain PGPR prevents excessive Na^+ accumulation under salt stress conditions, increasing the K^+/Na^+ ratio in shoots, enhancing Na^+ exclusion through roots by enhancing high-affinity K^+ transporters (Sunita *et al*., 2020).

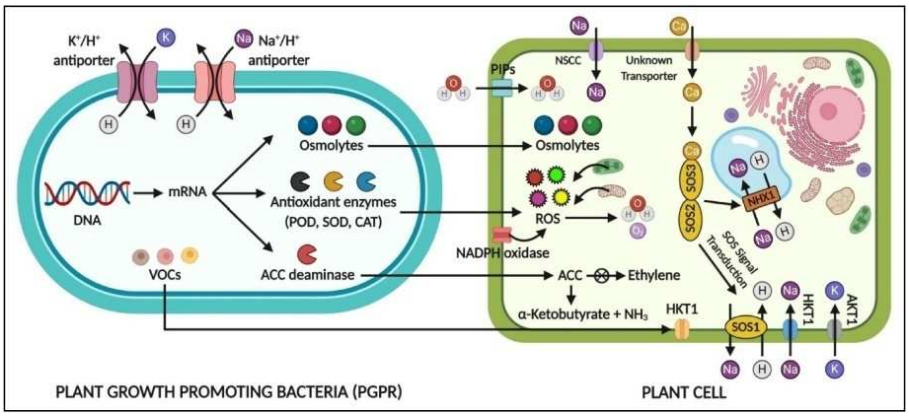

Figure 1.9: The picture is taken from Murali *et al*., 2021 with partial elaboration. Salt stress cellular response mediated by PGPR through the production of ACC deaminase and the regulation of ionic homeostasis.

1.4 Microbial Consortia

Microbial consortia, composed by communities of bacteria, fungi, and other microorganisms, have emerged as promising tools for enhancing plant growth and health in agricultural systems. The relationships between plants and their associated microbiota play a pivotal role in shaping plant development, nutrient acquisition, and stress responses. For these reasons, the potential of microbial consortia for plant biostimulation represents a sustainable and eco-friendly approach in modern agriculture. Unlike single-strain inoculations, microbial consortia leverage the synergistic interactions among diverse microbial species, creating a complex web of relationships that can positively influence plant performance. In this study, potential effects of PGPMs on salt stress mitigation were investigated with three different microbial consortia (MC): MC_B (*Bacillus amyloliquefaciens* LMG 9814, *Pseudomonas fluorescens* DR54, *Ranhella aquatilis* BB23/Tad, *Bacillus* sp. BV84, *Azotobacter vinelandii* DSM2289), MC_C (*Bacillus amyloliquefaciens* LMG9814, *Pseudomonas fluorescens* DR54, *Ranhella aquatilis* BB23/Tad, *Bulkholderia ambifaria* MCl7, *Azotobacter*

chrococcum LS132) and MC_D (*Paenibacillius amylolyticus* Sp949, *Microbacterium oxydans* Sp951, *Stenotrophomonas rhizophila* Sp952, *Xanthomonas retroflexus* Sp95). Microbial consortia MC_B and MC_C were produced during the Horizon 2020 project "Sustainable Innovation of Microbiome Applications in Food System" (SIMBA), to the unit of Biotechnology of the Department of Chemistry, Life Science and Environmental Sustainability (SCVSA - University of Parma) and described by Tabacchioni *et al.* (2021) with a bottom-up approach: microorganisms with different plants stimulating functions (nitrogen fixation, phosphorus solubilization, biocontrol, auxin production, amylolytic activity) were selected from a broad panel of PGPMs and their ability to coexist in consortia was verified through *in vitro* compatibility tests. The most promising combinations of microbial species were then used to formulate synthetic microbial consortia. Economically significant plants including tomato, wheat, and corn treated with MC_B and MC_C, revealed the involvement of microbial consortia in both biomass yield and productivity. Additionally, these studies demonstrated the modulation of gene expression in critical pathways governing the physiological and metabolic regulation of the plant. The results highlighted a root-level crosstalk between plants and microorganisms, leading to a systemic plant response (Caldara *et al.*, 2024; Graziano *et al*., 2022; Vassura *et al.*, 2023). The four strains comprising MC_D were identified from soil samples collected from a Danish agricultural field (De La Cruz-Perera *et al*., 2013). Their ability to form biofilms was verified, revealing distinct properties in the microbial consortium compared to individual strains (Ren *et al*., 2014). MC_D was then tested on *Arabidopsis thaliana* L. (Heyhn) exposed to drought stress. Inoculation with MC_D influenced chlorophyll content, abscisic acid signaling and root microbiota, resulting in an improvement in the response to drought stress. The contribution of MC_D appears to be attributed to the formation of a robust biofilm at the root level, which could lead to increased water retention and nutrient supply (Yang N. *et al*., 2021).

For greenhouse experiments, microbial consortia were stabilized on zeolite powder (Hett *et al.,* 2023) and inoculated in soil during the transplant. The use of PGPMs stabilized on zeolite rather than liquid inoculum, can offer significant advantages in agricultural applications. Zeolites are alumino-silicates characterized by an ordered and microstructured framework. In addition to their easy use for field applications, zeolites possess intrinsic properties that enhance water retention in the soil and promote its gradual release. The microstructured nature of zeolites enables their use as PGPMs carriers, increasing their survival potential throughout the plant's life cycle.

1.5 *Solanum lycopersicum* L. (cv. Heinz 3402)

The cultivation of tomato (*Solanum lycopersicum* L.) for industrial transformation is widely practiced worldwide, ranking as the second most important plant in horticulture after potatoes, with a production of approximately 180 million tons/year (FAO, 2020).

Italy is the third-largest global producer after California and China, with cultivation spanning about 67 thousand hectares of land, with 54% of the cultivation concentrated in Northern Italy and 41% in Southern Italy. The composition of macro and micronutrients in tomatoes, like all horticultural products, is strongly influenced by factors such as cultivar type, agronomic practices, sunlight exposure, and soil characteristics. Considered a health-promoting food, tomatoes have rich nutritional quality due to the presence of secondary metabolites such as lycopene, alpha- and beta-carotene, flavonoids, vitamin C, and hydroxycinnamic acid derivatives. Tomato has reached enormous popularity in recent years, particularly with the discovery of the antioxidant and anticancer activities of lycopene (Raiola *et al*., 2014) and the high content of vitamins B and C.

Tomatoes belong to the *Solanaceae* family, which also includes potatoes and eggplants, constituting one of the most important species in terms of food production. Since its introduction in Europe, tomatoes were initially underutilized for food due to the presence of small golden berries like other toxic *Solanaceae* varieties, i.e. mandrake. Between the 17th and 18th centuries tomatoes use in cuisine began thanks to progressive domestication, which led to a drastic reduction in genetic variability (Bergougnoux, 2014). The first complete genome sequence of the tomato (cv. Heinz 1706) was published in 2012 as part of the international Tomato Genome Consortium, providing a valuable resource for understanding plant biology and developing new varieties (Sato *et al.*, 2012). The study of the tomato genome as a model organism over the years has facilitated the investigation of interesting pathways and molecular markers in the plant biology. Thanks to this, biomarkers related to the regulation of the transition from vegetative to reproductive states, fruit maturation, and response to abiotic and biotic stresses have been identified and characterized (W. Liu *et al*., 2022).

1.6 *Zea mays* L. (cv. Pioneer P0837)

Maize (*Zea mays* L.) is widely cultivated in many regions around the world and together with wheat, rice and soybean represent one of the most important cereals in terms of production and distribution. In Italy, maize is the leading national crop both in terms of production, amounting to approximately 8.5 million tons, and yields. It generates an annual value of €2.1 billion for direct consumption, and an overall value of €36.2 billion for derived livestock productions, including over €6.0 billion from Protected Designation of Origin (PDO) and Protected Geographical Indication (PGI) excellence productions (Ministero dell'agricoltura, della sovranità alimentare e delle foreste (MASAF), 2019).

Currently, over 80% of maize is allocated for animal feed, while the portion designated for human consumption does not exceed 5%. The remaining part is utilized for industrial purposes (biogas production) and for starch production (ISTAT, 2013). The main constituents of maize kernel are carbohydrates (with a high presence of starch), lipids, proteins, and minerals (with a high iron content, though it is poorly bioavailable). Moreover, phenolic compounds, which exert antioxidant, antimicrobial, and anti-inflammatory effects, are the characteristic active compounds (Formenti A. *et al*., 2004). Interestingly, the beginning of maize (*Zea mays* ssp. *mays*) domestication can be traced back to Mexico around 9000 years ago, originating from the wild ancestor *Zea mays* spp. *parviglumis*. Considering that it was then exported from Mexico to various regions in South America, genetic variability has significantly diversified over the centuries, adapting to different domestication pathways and climatic conditions, leading to the development of numerous landraces. The CIMMYT collection, for instance, documents over 300 maize races (Andorf *et al.*, 2019).

Improving maize cultivation for enhanced production and nutritional qualities necessitates in-depth phenotyping, which is challenging due to the dispersion of specific traits related to resistance to abiotic stress or nutritional properties among different landraces. The complete genome sequencing of maize has been conducted on B73 and Palomero (Jiao *et al*., 2017). Characterizing maize germplasm with targeted traits is crucial to increase crop yield in the agri-food chain, but this requires international networks (e.g., "Seeds of Discovery" (SeeD) promoted by CIMMYT) that provide accurate and systematic characterization of genetic diversities (Prasanna, 2012).

1.7 Aim of the project

This project aims at enhancing eco-sustainable innovations in the agri-food system through the evaluation of nano-biotechnological solutions. In the context of food and climate emergencies, the use of biostimulants could improve agricultural practices, providing sustainable alternative strategies for better soil management. Biostimulants are substances or microorganisms applied to plants or soil to enhance nutrient uptake, nutrient efficiency, tolerance to abiotic stress, and overall plant performance (du Jardin, 2015). Unlike traditional fertilizers that provide essential nutrients directly to plants, they stimulate natural processes within the plant or the surrounding soil microbiome. Their mechanisms of action may involve improving nutrient availability, promoting root development, enhancing stress tolerance, and modulating various physiological processes. The use of biostimulants is gaining significance in sustainable agriculture as they contribute to more efficient resource utilization, reduce the environmental impact of agricultural practices, and offer potential solutions for mitigating the effects of climate change on crop productivity.

Among the emerging problems associated with climate change, the salinization of irrigation water following prolonged drought periods led to a severe reduction in crop yields. This is happening in the Po river delta and in many area of the Po valley, causing significant economic losses. The application of biostimulants able to mitigate the reduction in crop yields mediated by salt stress could be a potential strategy, increasing the availability of arable land. However, the use of nanomaterials, whether to mitigate adverse responses to abiotic stresses or as nanofertilizers, may pose several challenges related to potential accumulation in the environment, biomagnification, and biotransformation (Pagano *et al.*, 2023), increasing the need to clarify aspects related to their potential eco-toxicity. A clear understanding of the mode of action of nanomaterials on crops, both from a physiological and molecular perspective and in terms of their internalization in plant tissues, is a crucial goal for their implementation and application within the agri-food production context. These aspects were investigated in this work.

2 Materials and Methods

2.1 Experimental design: *Solanum lycopersycum* L. – preliminary experiments

2.1.1 Germination Test

To assess the effectiveness of a potential seed coating with microbial consortia under salt stress conditions, tomato seeds were coated and exposed to various concentrations of saline solution to evaluate key parameters for germination efficiency. In this study, the cultivar Heinz 3402 tomato variety was used, known for its good-sized fruits and thick, excellent-textured pulp. The individual bacteria strains of microbial consortia MC_B (*Bacillus amyloliquefaciens* LMG 9814, *Pseudomonas fluorescens* DR54, *Ranhella aquatilis* BB23/Tad, *Bacillus* sp. BV84, *Azotobacter vinelandii* DSM 2289), MC_C (*Bacillus amyloliquefaciens* LMG 9814, *Pseudomonas fluorescens* DR54, *Ranhella aquatilis* BB23/Tad, *Bulkholderia ambifaria* MCl 7, *Azotobacter chrococcum* LS132), and MC_D (*Paenibacillius amylolyticus* Sp949, *Microbacterium oxydans* Sp951, *Stenotrophomonas rhizophila* Sp952, *Xanthomonas retroflexus* Sp95) were grown on LB (Luria-Bertani) agar cultures (Triptone 10 g/L, Yeast Extract 5 g/L, NaCl 10 g/L, agar 15 g/L) and incubated in 3 mL of LB broth (Triptone 10 g/L, Yeast Extract 5 g/L, NaCl 10 g/L) for 24 hours at 28°C. Considering the relationship between OD_{600} and colony forming units (CFU), a volume of microbial culture corresponding to 10^8 CFU/mL for each strain was collected and mixed in a tube in order to obtain the desired consortium. The mix was centrifuged at 6000 rpm for 3 minutes. The resulting pellet was resuspended in 100 µL of ddH_2O and transferred to 3 mL of 1% methylcellulose. The seeds were sterilized with a 10% sodium hypochlorite solution for 10 minutes and then washed three times for 20 minutes with sterile deionized water (ddH_2O). The seeds were transferred to methylcellulose alone (untreated control) or supplemented with microbial consortia, incubated for 1 hour with agitation at room temperature, and dried for 24 hours in a sterile environment (Rocha *et al*., 2019). The seeds were then sown in 10 cm Petri dishes (10 seeds per plate, for a total of 100 seeds per condition) on sterile Whatman filter paper (grade 1) impregnated with 1.5 mL of ddH_2O (unstressed condition), 0.3% NaCl solution and 0.6% NaCl solution (salt stressed conditions). The plates were then incubated in the dark in a growth chamber for 6 days (temperature 24/19°C, 16h/8h light cycle). Germination monitoring was conducted from the third day after sowing up to the sixth day, with daily counts of germinated seeds. Seeds with a root length longer than 2 mm were considered germinated.

The Promptness Index (PI), which provides an indication of seed germination speed, and the Germination Stress Tolerance Index (GSI), which relates the germination speed of treated seeds to that of untreated seeds, were calculated as follow (Tanveer *et al*., 2020):

PI = gpT3 (1.00) * gpT4 (0.75) * gpT5 (0.50) * gpT6 (0.25)

GSI (%) = (PI treated seeds/PI control seeds) * 100

Where gp represents the germination percentage calculated after Tn days from sowing.

2.1.2 Pot experiment

After the germination test, a greenhouse pot experiment was conducted to assess the effects of microbial consortia at different salinity levels to identify the most promising conditions for further investigation. (**Figure 2.1**).

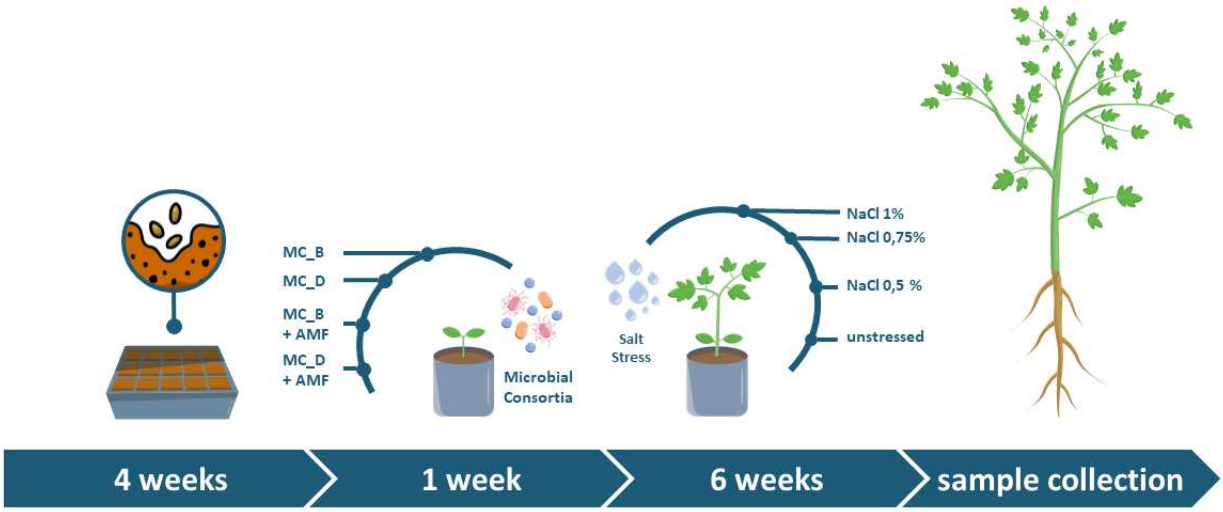

Figure 2.1: Graphical abstract of the experimental setup: timeline and conditions. Tomato seeds cv. Heinz 3402 were used. Four weeks seedlings were transplanted into pots and inoculated with microbial consortia stabilized in zeolite powder MC_B (*Bacillus amyloliquefaciens* LMG 9814, *Pseudomonas fluorescens* DR54, *Ranhella aquatilis* BB23/Tad, *Bacillus* sp. BV84, *Azotobacter vinelandii* DSM2289) and MC_D (*Paenibacillius amylolyticus* Sp949, *Microbacterium oxydans* Sp951, *Stenotrophomonas rhizophila* Sp952, *Xanthomonas retroflexus* Sp95) alone or combined with Arbuscular Mycorrhizal Fungi (AMF) *Rhizophagus intraradices.* After one week, salt stress with 0.5%, 0.75% and 1% NaCl solutions was started. Salt stress was induced for 6 weeks.

Tomato seeds were sterilized with 10% sodium hypochlorite solution, sown in seedbed and germinated for 4 weeks. The obtained seedlings were transplanted into pots containing 1.5 kg of soil and inoculated with 2 grams of microbial consortia stabilized in zeolite powder (Hett *et al*., 2023). Briefly, microbial consortia powder produced during the year 2020 was made by incubation of consortia strains in nutrient medium, then centrifugated and suspended in water at a concentration of 10^9 CFU/mL. The strains were then mixed in a 1:1 ratio and stabilized on micronized zeolite *(*Hett *et*

al., 2022). The production during the next year was made following the Magarelli *et al.* (2022) approach: after the incubation, strains were dehydrated by freeze-drying and the lyophilized bacteria were stabilized on zeolite in a 1:1 ratio between strains. Microbial consortia MC_B and MC_D were used individually and in combination with 2 grams of the AMF *Rhizophagus intraradices* (commercial product from MycAgroLab, France). After one week of stabilization, a microbial reinforcement of an additional 2 grams has been applied and salt stress was induced using NaCl solutions at low (0.5% NaCl), medium (0.75% NaCl), and high (1% NaCl) concentrations. The stress was induced watering plants with 150 mL of tap water (unstressed condition) or saline solutions twice a week for 6 weeks, after which morphological and physiological analyses were conducted, followed by sample collection. The plants were grown in greenhouse at a temperature of 24°C with a 16/8 h photoperiod. The experimental conditions under analyses were: untreated control, MC_B, MC_D, AMF, MC_B + AMF and MC_D + AMF for unstressed condition, while these six treatments where also combined with NaCl solutions at low, medium and high salinity level for stressed conditions, for a total of 24 different experimental conditions performed in triplicate for a total of 72 pots.

2.2 Experimental design: *Solanum lycopersycum* L. treatment combining ENMs and PGPMs

The highest concentration of NaCl solution and the microbial consortium MC_B in combination with AMF were selected as the most promising conditions for further analysis. The next year, an additional experiment was set up. The microbial consortium treatment was combined with a nano-Si treatment under salt stress condition (**Figure 2.2**). Three weeks tomato seedlings were transplanted into pots with 1 kg of soil (same volume used in the preliminary experiment) and exposed to different treatments: plants were inoculated with 2 g of microbial consortium MC_B stabilized in zeolite powder combined with *Rhizophagus intraradices* (MycAgroLab, France), while soil was also amended with 500 mg/kg of SiO_2 NPs (previously suspended in ddH_2O and sonicated to inhibit the potential formation of aggregates) or 2.37 g/kg of the silicon salt Na_2SiO_3 as an additional control to evaluate the potential effect of ion dissolution. Salt stress (1% NaCl solution) was induced after 1 week from the transplant with 150 mL of saline solution twice a week for 6 weeks (42 days). The plants were grown in greenhouse at a temperature of 24°C with a 16h/8h photoperiod. There were 10 experimental conditions: untreated control, MC_B+AMF, SiO_2 NPs, Na_2SiO_3, MC_B+AMF + SiO_2 NPs for unstressed condition, while these five treatments were combined with 1% NaCl solution for stressed condition, each performed with 5 replicates.

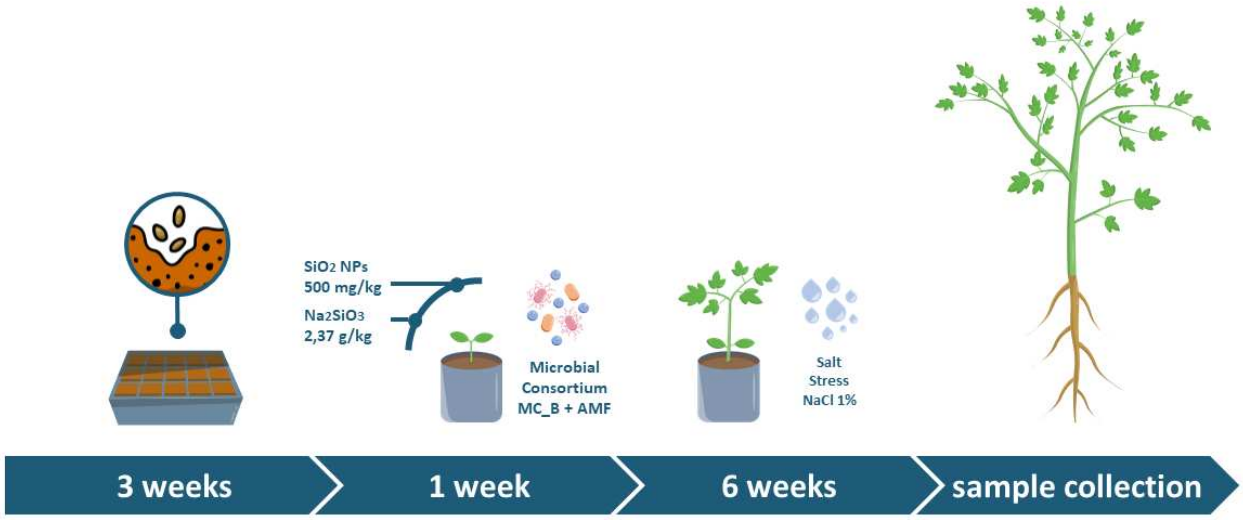

Figure 2.2: Graphical abstract of the experimental setup: timeline and conditions. Tomato seeds cv. Heinz 3402 were used. Three weeks seedlings were transplanted into pots and inoculated with microbial consortium MC_B stabilized in zeolite powder (*Bacillus amyloliquefaciens* LMG9814, *Pseudomonas fluorescens* DR54, *Ranhella aquatilis* BB23/Tad, *Bacillus* sp. BV84, *Azotobacter vinelandii* DSM2289) combined with Arbuscular Mycorrhizal Fungi (AMF) *Rhizophagus intraradices*. Soil was also homogenized with SiO_2 NPs or the silicon salt Na_2SiO_3. After one week, salt stress (1% NaCl solution) was started. Salt stress was induced for 6 weeks.

2.3 Experimental design: *Zea mays* L.

The maize cultivar under examination in this study is Pioneer P0837, known for its exceptional productive potential in terms of yield and biomass, making it ideal for central and eastern areas of Emilia-Romagna where the focus is on maximizing silage production. Maize seeds were sown in vermiculite after sterilization with 10% sodium hypochlorite solution. After 11 days, V_2 (two visible leaf collars) growth stage seedlings were transplanted in pots with 3.5 kg of soil, to ensure a sufficient amount of soil to support the plant until the reproductive phase and grown in greenhouse at 24°C (16h/8h photoperiod). Before transplant, the soil of treated conditions was homogenized with 500 mg/kg of Fe_3O_4 NPs (previously suspended in ddH_2O and sonicated to inhibit the potential formation of aggregates) or 75 mg/kg of the iron salt $FeCl_3$ as an additional control to evaluate the potential effect of ion dissolution (Pagano *et al.*, 2022). Three months after the germination, flowering started (Vt phase) and assessments for stomatal transpiration, photosynthetic activity and plant height were made. Five months after germination, cobs were formed and the analysis of morphological and physiological parameters was conducted, followed by the collection of samples from roots, shoots, and seeds.

2.4 Nanomaterials characterization

When planning experiments involving engineered nanoparticles, the characterization to assess their stability (ion dissolution, tendency to form aggregates) is essential for a better understanding of their effects on the targeted organism. Nanoparticles can undergo chemical and physical variations that not only influence their mode of action on organisms and the environment, but also impact their internalization and the physiological and molecular response of the plant. In this work, SiO_2 NPs (Sigma-Aldrich, Merck, Darmstadt, Germany) and Fe_3O_4 NPs (synthesized by IMEM-CNR, Parma, Italy and characterized by Pagano *et al.* 2022) suspended in water were homogenized in soil after sonication to inhibit aggregate formation. The tendency of nanomaterials to form aggregates was determined through Zeta (ζ) potential and the aggregate size (hydrodynamic diameter) by Dynamic Light Scattering (DLS), while dissolution percentage was obtained through Flame Atomic Absorption Spectrometry (FA-AAS) (Marmiroli *et al*., 2021; Pagano *et al.*, 2022). Zeta potential and hydrodynamic diameter were measured with 1 mL of nanoparticle suspension in ddH_2O at 200 mg/L concentration and the Zetasizer Nano (Malvern Instruments Ltd., Enigma Business Park, Grovewood Road, Malvern, United Kingdom) was used. In DLS the sample placed in a polystyrene cuvette is illuminated with a laser light, and the light scattered in all directions by the particles is detected. Zeta potential is determined using a combination of electrophoresis and Laser Doppler Velocimetry. In this study, measurements were conducted by placing the sample in a polystyrene cuvette with the Universal 'Dip' cell (ZEN1002), designed for the application of an electric field to the analyzed sample (Zetasizer Nano Series User Manual).

2.5 Physiological and Morphological analysis

2.5.1 Morphological analysis

To monitor the growth of tomato and maize plants, the length of both shoots and roots for each sample was measured using a meter. Shoots measurements were taken from the collar to the apical leaf, while root measurements were taken from the collar to the terminal portion of the root apex. At the end of the plant treatment period, the shoots were cut and measured, and the roots were cut and washed with tap water to remove rhizospheric soil, taking care not to damage them. The roots were then laid out and measured to obtain their total length. The measurement of fresh weight and dry weight allows the determination of the final yield of the plant. Fresh weight refers to the total weight of the freshly harvested plant, including water and other fluids present inside.

Dry weight represents the weight of the plant after water removal through evaporation or drying. Samples of shoots and roots, once collected, were weighed using a precision balance to collect data on fresh weight. Subsequently, they were dried in an oven at 70°C for 48 hours before another measurement on the precision balance to determine their dry weight.

2.5.2 Photosynthetic activity and stomatal transpiration

Total chlorophyll content was measured using an SPAD-502 (Konica Minolta Business Solution Italia S.p.a., Milan). Measurements were taken on three young leaves in different nodes (from the youngest fully expanded leaf to the oldest, corresponding to the 1st, 2nd, and 3rd nodes) for each plant. Ten measurements were taken per leaf to ensure adequate representativeness of the total chlorophyll content value. Stomatal transpiration was measured using a porometer (AP4-porometer, Delta-T Devices Ltd, 130 Low Road, Burwell, Cambridge, CB25 0EJ, UK) on three leaves in different nodes (youngest fully expanded leaves) for each sample. The value of stomatal resistance, which is the reciprocal of stomatal conductance, was measured.

2.5.3 Cellular respiration in leaves (TTC assay)

Cellular respiration was determined in tomato leaves using the TTC assay (Marmiroli M. *et al*., 2020). Immediately after sample collection, the leaves were cut into discs and weighed. For each sample 0.1 g of leaves tissue was incubated for 15 hours at 30°C in the dark with 0.18 M TTC solution (2,3,5-Triphenyltetrazolium chloride, Sigma-Aldrich, St. Louis, Missouri, USA). During incubation, TTC is reduced to formazan by electrons from metabolically active tissues, originating from the electron transport chain in the cellular respiration process. After the 15-hour incubation, two washes with water were performed, followed by extraction of the produced formazan with 5 mL of 95% ethanol for 10 minutes at 80°C. The extracted formazan was then quantified through spectrophotometric reading (Pharmacia type Novaspec II, Prinses Beatrixlaan 301, 7312 DG Apeldoorn, The Netherlands) at 530 nm wavelength.

2.5.4 Lipid peroxidation in roots (TBARs assay)

To quantify the concentration of malondialdehyde (MDA) from potential peroxidation of polyunsaturated membrane lipids, plants roots were frozen in liquid nitrogen and ground with a mortar and pestle until their reduction to powder (Marmiroli *et al*., 2020; Pagano *et al.*, 2022). For each sample, 100 mg of roots powder was homogenized in 1 mL of 0.1% trichloroacetic acid (TCA) to extract MDA from the tissue. Each homogenized sample was centrifuged at a speed of 12,000 rpm for 15 minutes. After centrifugation, 0.5 mL of supernatant (extract) was collected, and 1 mL of

reaction buffer (0.5% Thiobarbituric Acid (TBA) dissolved in a 20% TCA solution) was added and incubated at 95°C for 30 minutes to allow the reaction between MDA and TBA. The mixture was then rapidly cooled on ice to stop the reaction. Absorbance at 532 nm was measured using a spectrophotometer to determine the concentration of the MDA-TBA complex (Hodges *et al.*, 1999; Murshed *et al*., 2014). MDA concentration within the tissue was determined through interpolation with the calibration curve (0 µM – 2.5 µM – 5 µM – 10 µM – 20 µM – 50 µM).

2.5.5 Proline content in leaves

Tomato leaves were harvested and immediately frozen in liquid nitrogen. The frozen tissue was ground using a mortar and pestle, and three technical replicates for each condition were prepared. Proline was extracted from 100 mg of ground leaves homogenized in the extraction buffer (3% sulfosalicylic acid). The homogenate was then centrifuged for 10 minutes at 1,400 rpm to separate the extract from the tissues. The supernatant was collected and kept on ice.

The reaction buffer containing ninhydrin (Sigma-Aldrich, St. Louis, Missouri, USA) dissolved in glacial acetic acid and 100 mM PBS (pH = 7) was mixed with 3% sulfosalicylic acid and 50 µl of proline extract were added (T. Chen & Zhang, 2016). The reaction mix was then incubated at 100°C for 15 minutes. The reaction was stopped on ice for 5 minutes, and the absorbance at 520 nm was measured using a spectrophotometer (Pharmacia type Novaspec II, Prinses Beatrixlaan 301, 7312 DG Apeldoorn, The Netherlands) (Marmiroli *et al.*, 2022). The proline content (µg per gram of fresh weight) for each sample, was derived by a calibration curve obtained with the absorbance measured at 520 nm of standard proline solutions (0 µg/mL – 0.5 µg/mL – 1 µg/mL - 1.5 µg/mL – 2 µg/mL - 2.5 mg/mL – 3 µg/mL).

2.6 Molecular analysis

2.6.1 RNA extraction and Quality Control

Roots and leaves samples of *Z. mays* and *S. lycopersicum*, after the end of the treatments period, were collected and immediately frozen in liquid nitrogen. Tissues were stored at -80°C until their use for molecular analysis. Frozen tissues were reduced to powder using a mortar and pestle, avoiding thawing thanks to the use of liquid nitrogen. Subsequently, 100 mg of tissue powder was aliquoted for RNA extraction. Total RNA extraction was performed using the RNeasy Plant Mini Kit (RNeasy® Mini Kit, QIAGEN) following the manufacturer's instructions.

After elution of RNA with sterile RNAse-free water, quality control was carried out to verify both the concentration of nucleic acids in the eluate and the integrity of the extracted RNA. The concentration of nucleic acids and the purity of the sample were determined using the NanoDrop™ 2000/2000c spectrophotometer (Thermo Fisher Scientific). Absorbance at 260 nm, 280 nm, and 230 nm was measured from 1 µL of extract (factor 40), and samples with good 260/280 and 260/230 ratios were used for next steps. For the assessment of RNA integrity, a 2% agarose gel was prepared, and 1 µL of extract was run at 70 V for 45 minutes. Samples showing visible bands corresponding to the 28S and 18S rRNA were considered to have passed the quality control.

2.6.2 Gene expression analysis

In *S. lycopersicum* exposed to silicon treatments, gene expression of roots and leaves samples was investigated through RNA-seq analysis. Samples with 260/280 ratio greater than 1.8 and with 18S and 28S prominent bands, were aliquoted (minimum: total amount 1 µg, concentration 50 ng/µL, volume 20 µL), stored in dry ice and sent to IGATech (IGA Technology Services, Udine, Italy) for total RNA sequencing. The Universal Plus mRNA-Seq kit (Tecan Genomics, Redwood City, CA) was used for library preparation according to the manufacturer's instructions (library type: fr-secondstrand). RNA samples were quantified and quality tested by Agilent 2100 Bioanalyzer RNA assay (Agilent technologies, Santa Clara, CA). Final libraries were checked using both Qubit 2.0 Fluorometer (Invitrogen, Carlsbad, CA) and Agilent Bioanalyzer DNA. Libraries were then prepared for sequencing and sequenced on paired-end 150 bp mode on NovaSeq 6000 (Illumina, San Diego, CA). Base calling, demultiplexing and adapter masking were conducted using Illumina BCL Convert v3.9.31. Adapter sequences were masked during the demultiplex with BCL-Convert. Trimming involved removing lower quality bases and adapters by ERNE2 software. Reads were aligned to the reference genome GCF_000188115.5_SL3.1 using STAR3, a splice junction mapper for RNA-Seq reads. STAR3 aligns RNA-Seq reads to genomes and then analyzes the mapping results to identify splice junctions between exons. Transcripts count were determined by assembling and quantitation of full-length transcripts representing multiple spliced variants for each gene locus by Stringtie4. RSeqQC5 package was used to perform statistics on "strandness" of reads, on genome coverage and read distribution.

Gene expression in *Z. mays* was analyzed with Real Time qPCR (RT-qPCR) for relative quantification of target genes (Appendix). The extracted RNA (1 µg) was converted to cDNA using QuantiNova™ Reverse Trascription Kit (QIAGEN). Key genes able to elucidate the interaction between maize and iron nanoparticles were selected, then the primers were designed (Appendix) using Primer-BLAST

web tool (National Center for Biotechnology Information – NCBI). After the primers test in end-point PCR, relative quantification for gene expression analysis was performed using SYBR® Green PCR Kit (QIAGEN), 10 ng of cDNA for each sample and a primer concentration of 250 nM, on a BIO-RAD CFX96™ Touch Real-Time PCR Detection System. The relative quantity of target genes was obtained with comparative C_T method with actin2 (Zm00001d012277) as housekeeping gene.

2.7 Elemental quantification and distribution

2.7.1 Determination of iron content on *Zea mays*

For the determination of the iron content in corn tissues, roots, shoots and seeds samples were dried in oven at 70°C for 48 h. When completely dry, 200 mg of tissue were digested with 4 mL of HNO_3 for 20 minutes at 165°C using a VELP DK20 digester (VELP Scientifica, Usmate, Italy). The digested sample was further diluted with distilled water (dilution 1:20).

The concentration of iron in the solution was measured using FA-AAS Varian AA240FS (Agilent Technologies, Santa Clara, CA, USA). A calibration curve with standard iron solutions at known concentrations (0 ppm, 0.1 ppm, 0.5 ppm, 1 ppm, 5 ppm) was created and the iron content of the samples was calculated (Marmiroli *et al*., 2020, 2021).

2.7.2 Preparation of samples for synchrotron analysis

For μ-XRF (TwinMic beamline, ELETTRA synchrotron, Trieste, Italy) tomato freshly collected samples of leaves and roots, were immediately frozen in liquid nitrogen and then included in wax. With the use of cryomicrotome, 3 μm slices were cut and placed on ultralene film and attached to a sample holder. For the μ-XRF analysis on maize roots, leaves and seeds, samples were cut and fixed in 3% glutaraldehyde triphosphate for three days. After dehydration in gradients of alcohol (from 25% to 100%), samples were embedded in epoxy resin (Technovit® 7100) following the manufacturer's instructions, cut in 10 μm slices and placed a sample holder in ultralene film (Marmiroli *et al.*, 2021, 2022).

2.8 Data analysis

2.8.1 Analysis of data from germination test

To assess the significance of the effects resulting from salt exposure and the contribution of microbial consortia during the germination phase, statistical analysis was conducted. The χ^2 test was employed to compare the germination percentages obtained in the analyzed treatments. The analysis of seedlings lengths from coated and un-coated seeds under various salt stress conditions was compared through one-way analysis of variance (ANOVA). Post hoc Tukey's Honestly Significant Difference (HSD) test for pairwise multiple comparisons was then applied using the PAST software (Paleontological Statistics, https://past.en.lo4d.com/windows).

2.8.2 Analysis of physiological and morphological data

Statistical significance in both morphological and physiological analysis was obtained with analysis of variance (ANOVA, p-value < 0.05). To analyze the data collected from the preliminary experiment in *S. lycopersicum*, two-way ANOVA was applied to determine the influence of both salt stress and the application of microbial consortia, as well as the interaction between these two variables. On the other hand, when combining consortia treatment in stressed condition with silicon treatments, three-way ANOVA was used to better understand the significance of multiple interactions between all the variables under analysis.

Physiological and morphological data related to the treatments of *Zea mays* with nano-Iron, one-way ANOVA was applied. Pairwise multiple comparisons were also performed using Tukey's HSD test, utilizing the PAST software (https://past.en.lo4d.com/windows).

2.8.3 Analysis of data from RT-qPCR

The analysis of gene expression using RT-qPCR was performed in triplicate, including a no-template control. The relative quantity of each gene for all the treatments under analyses was determined by calculating the ΔC_T (target gene C_T – housekeeping gene C_T) difference between the treated samples and the control, resulting in $\Delta\Delta C_T$. The modulation of gene expression is represented by $2^{-\Delta\Delta CT}$, indicating the fold change that means how many times the target gene expression is increased or decreased in treated conditions compared to the control.

2.8.4 Analysis of data from RNA sequencing

The RNA sequencing analysis was conducted on tomato roots and leaves exposed to silicon-based treatments (control, SiO_2 NPs, Na_2SiO_3, salt stress, SiO_2 NPs + salt stress). Distribution of FPKM values obtained for all samples were done, and their normality was verified. For the selection of Differentially Expressed Genes (DEGs), genes with an FPKM value greater than 100 in at least one of the two conditions (treated vs untreated) were considered, aiming to avoid genes with extremely low gene expression. DEGs with log_2 Fold Change (FC) greater than 0.6, 2, and 3 were identified for both tissues. Considering the DEGs count, a log_2FC cut-off of 3 was chosen for roots (FC=8) and log_2FC=0.6 for leaves (FC=1.5). Analyses were performed, and graphs were generated using R statistical software (www.r-project.org) and Microsoft Excel. The resulting DEGs from the four treatments were compared, identifying common and unique ones among treatments (diagrams generated with Venny bioinformatics tool http://bioinfogp.cnb.csic.es/tools/venny/). DEGs were utilized for enrichment analysis, functional annotation was performed with Database for Annotation, Visualization and Integrated Discovery (DAVID – Huang *et al.*, 2008; Sherman *et al*., 2022) and gene ontology classes were identified. Genes with higher FC and FPKM values, showing interesting differences between treatments in both enrichment and modulation analyses, were selected and visualized in heatmaps using R software. Among these, a more restricted panel of genes was chosen for future validation through RT-qPCR.

3 Results and Discussion

3.1 Nanoparticles characterization

Nanoparticles and nanomaterials possess different and unique properties compared to bulk materials. These properties, in addition to the high surface-to-volume ratio responsible for their remarkable reactivity, are undoubtedly connected to other important physical and chemical characteristics that significantly influence their interaction with biological matrices. These characteristics make nanomaterials interesting for the scientific community, which, in addition to developing various synthesis methods and innovative strategies for their production, requires an increasingly detailed understanding of the relationship between the physicochemical nature of nanoparticles and the effects of their application on living organisms, especially through accurate characterization. This represents a valid strategy for understanding the behavior of different nanomaterials in the environment and their interactions with various living organisms (Mourdikoudis *et al.*, 2018). The surface charge and the sizes of SiO_2 NPs and Fe_3O_4 NPs aggregates were evaluated using DLS and determination of the Zeta potential in deionized water suspensions at pH=7, as described in more detail in the "Materials and Methods" section. **Table 3.1** reports the sizes of the particles, their purity, the percentage of the element within the molecule, the values of hydrodynamic diameter (dh) and Zeta potential (ζ) obtained from the characterization analyses. Additionally, **Figure 3.1** shows the images obtained via TEM of the two nanoparticles used in this work.

NPs	*Size (nm)*	*Purity (%)*	*(ζ) Z-potential (mV)*	*(dh) Hydrodynamic range (nm)*
SiO_2 NPs	<20	99.5	- 27.0	399
Fe_3O_4 NPs	< 10	98.5	- 21.1	452

Table 3.1: Characterization of ENMs used in this work: particle size (nm), purity (%), Zeta potential (ζ) (mV), hydrodynamic range (dh) (nm), percentage of elements in SiO_2 and Fe_3O_4 NPs in deionized water suspension at pH=7.

a) **b)**

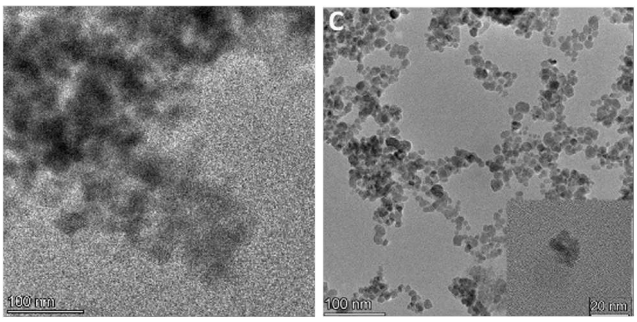

Figure 3.1:

Trasmission Electron Microscope (TEM) images of SiO_2 NPs (**a**) and Fe_3O_4 NPs (**b**) used in this work (the picture 3.1-b is taken from Pagano *et al.* (2022) with partial elaboration).

3.2 *Solanum lycopersicum* L. – preliminary experiment

3.2.1 Effect of seed coating in salt stress conditions

Germination is a crucial phase in plant development and is the first growth stage that is sensitive to salt stress. High salinity results in a decrease of osmotic potential, leading to a subsequent reduction in seed imbibition. It also disrupts biochemical processes such as respiration and energy production, as well as causing hormonal imbalances, resulting in delayed, or inhibited, seed germination (Uçarlı & Uçarlı, 2020). To assess the impact of salt stress on germination and the potential influence of seed coating with microbial consortia, two different levels of salt stress (NaCl solutions 0.3% and 0.6%) were used. Seeds were coated with methylcellulose inoculated with MC_B, MC_C, or MC_D and seeds coated with un-inoculated methylcellulose, were used as untreated control. Germination percentage and seedlings length were measured on the sixth day after sowing.

As expected, the results showed a reduction in the germination percentage with increasing salt stress, but no significant differences dependent on the seed coating with microbial consortia were observed (**Figure 3.2**). The seedlings length was also reduced with increasing salt stress, but in this case, there is also an influence of the treatments with the microbial consortia. Indeed, the seedlings length after six days from sowing was significantly reduced as compared to the untreated control when the seeds were coated with methylcellulose inoculated with the three MC, both in unstressed and in stressed conditions at a 0.3% NaCl concentration (**Figure 3.3**).

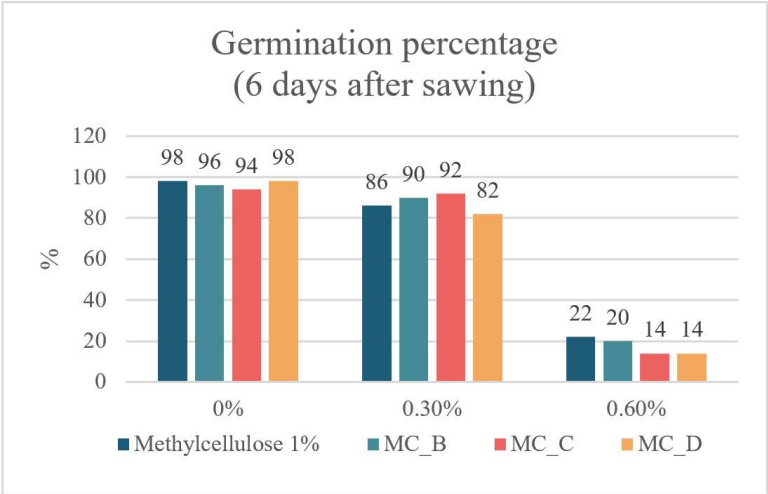

Figure 3.2: Germination percentage measured on the sixth day after sowing of Heinz 3402 tomato seeds. The observed results for seeds coated with 1% methylcellulose (control condition) are compared with seeds coated with methylcellulose inoculated with the microbial consortia MC_B, MC_C, MC_D under unstressed conditions (0%) and two levels of salt stress (NaCl solutions 0.3% and 0.6%). The significance of the differences was obtained using the Chi-Square (χ^2) test.

Starting from the third day after sowing, a monitoring of germination was carried out to evaluate the potential influence of salt stress or treatment with microbial consortia on the germination speed. The PI and GSI were calculated as described by Tanveer *et al*. (2020).

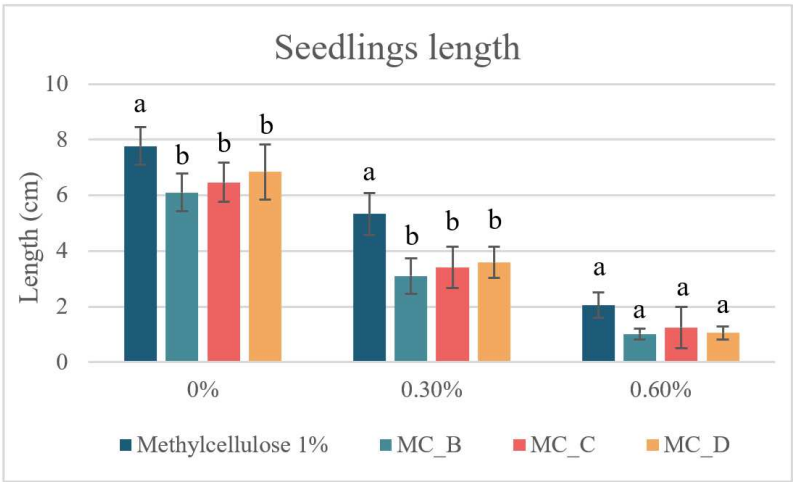

Figure 3.3: Means and standard deviations of seedlings length values obtained on the sixth day after sowing of Heinz 3402 tomato seeds. The observed results for seeds coated with 1% methylcellulose (control condition) are compared with seeds coated with methylcellulose inoculated with the microbial consortia MC_B, MC_C, MC_D under unstressed conditions (0%) and two levels of salt stress (NaCl solutions 0.3% and 0.6%). The letters (a and b) represent significant differences was obtained using One-way analysis of variance (ANOVA) followed by Tukey's HSD (Honestly Significant Difference)

The results show a reduction in GSI with increasing salinity, which is not mitigated by treatments with microbial consortia. Conversely, the germination speed was reduced by about 50% compared to the stressed control for both levels of salinity when the seeds were coated with MC_D. There is also a reduction in germination speed even under unstressed conditions, but with a more pronounced effect in the condition of MC_D coated seeds (**Table 3.2**). Therefore, the hypothesis is that the MC_D consortium used during germination had inhibitory effects in this phase, causing increased sensitivity to salt stress. In general, the results of the germination test did not show promising evidence, so for the subsequent greenhouse experiments, microbial consortia were inoculated exclusively during the transplanting phase.

Salinity	***Methylcellulose 1%***	***MC_B***	***MC_C***	***MC_D***
NaCl 0%	-	95.61 %	93.27 %	61.87 %
NaCl 0.3%	60.14 %	72.24 %	63.16 %	30.04 %
NaCl 0.6%	7.48 %	6.63 %	4.29 %	2.99 %

Table 3.2: *Germination Stress Tolerance Index* (**GSI %**) of seeds coated with microbial consortia MC_B, MC_C, MC_D under unstressed conditions (NaCl 0%) and two levels of salt stress (NaCl solutions 0.3% and 0.6%). The significance of the differences was obtained using the Chi-Square (χ^2) test.

3.2.2 Morphological and physiological effects of different PGPMs at different salinity levels

To assess the most promising microbial treatments at the level of salinity that would have more pronounced effects on the plant, a greenhouse experiment was set up by inoculating tomato plants with the microbial consortia MC_B and MC_D at the transplanting stage, both individually and in combination with arbuscular mycorrhizal fungi (AMF). In previous studies (Graziano *et al*., 2022; Vassura *et al*., 2023) the use of MC_B for field application showed a beneficial impact on plants growth. Therefore, given the similarity in composition of MC_C with MC_B, it was not used during the pot experiment. Three different salinity levels were chosen for this purpose: low (0.5%), medium (0.75%), and high (1%). Morphological and physiological parameters were measured in tomato shoots and roots after 6 weeks of salt stress induction, to assess the impact of the microbial treatments on salt stress mitigation.

Stomatal transpiration

The stomatal transpiration is one of the key parameters which explain the plant response to osmotic stress caused by exposure to saline environments. The latter is the resistance imposed by guard cells to counteract the outward flow of water vapor through the stomatal opening. The measurement was carried out using a porometer before sampling, 6 weeks after stress induction (**Figure 3.4**). The results show an increase in resistance (and thus a reduction in conductance) with increasing salt concentration. This behavior aligns with the type of response to salt stress documented in the literature, as inhibiting the loss of water vapor through the closure of the stomatal opening promotes the maintenance of water balance in the plant (Saradadevi *et al.*, 2017). On the other hand, at the highest salinity level, a distinction was evident in two significantly different groups: one group comprising the control and plants inoculated with the two individual consortia, which shows significantly higher stomatal resistance values compared to the second group comprising all treatments containing mycorrhizae (AMF, MC_B+AMF, MC_D+AMF). From this analysis, it is evident that the contribution of mycorrhizae results in lower stomatal resistance, leading to greater stomatal opening. Numerous studies demonstrate that the application of AMF leads to a reduction in stomatal closure under water stress conditions (Augé *et al.*, 2015). Two main hypotheses emerge from the literature as a result of this phenomenon: the greater supply of water and nutrients due to the greater extension of hyphae (Smith & Read, 2008) and the possible influence of mycorrhizal components in regulating hormonal homeostasis (Birhane *et al.*, 2012).

Furthermore, plants inoculated with consortia in combination with mycorrhizae also show lower stomatal resistance values, which could be due to the induction of greater colonization by mycorrhizae. Literature reports that some PGPR can improve mycorrhizal colonization and thus increase their influence on plant response (Hashem *et al.*, 2019).

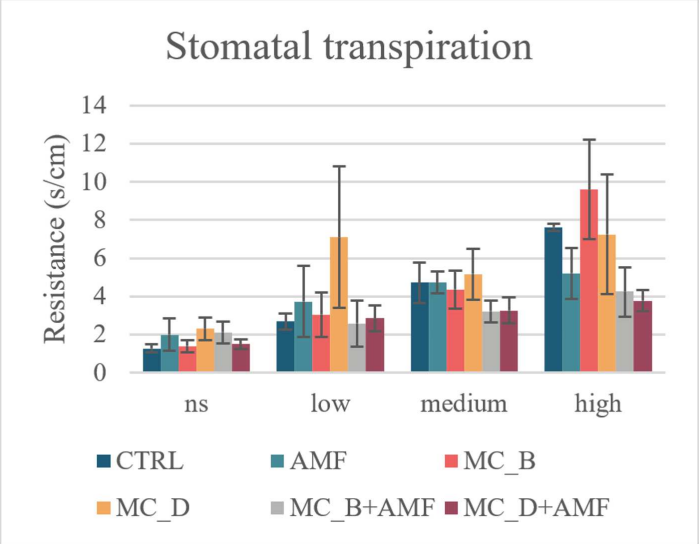

	F value	*p value*
Salt Stress	92.522	2.00E-16
Consortia	10.85	1.91E-10
Salt Stress * Consortia	5.298	5.80E-10

Figure 3.4: Means and standard deviations of stomatal resistance values obtained after six weeks of salt stress induction on tomato plants. Stomatal resistance is the inverse of stomatal conductance: increased values of stomatal resistance indicate decreased stomatal transpiration. The results obtained from the untreated plants (control condition) are compared with those obtained from plants inoculated with microbial consortia MC_B, MC_D, and AMF alone and in combination, under unstressed conditions (ns), as well as under three levels of salt stress: NaCl solutions at 0.5% (low), 0.75% (medium), and 1% (high). In the table below, results of Two-way analysis of variance (ANOVA) are shown. The significance of the differences was assessed by Tukey's HSD (Honestly Significant Difference)

Photosynthetic activity

Another key parameter in monitoring salt stress in plants is the measurement of chlorophyll content, which allows evaluating the plant's physiological response to oxidative stress by modulating photosynthetic activity. The measurement of photosynthetic pigment content using the SPAD technique is a non-invasive method that enables the quantification of total chlorophyll content by measuring leaf absorbance in the red and infrared region. The results highlight a dependence of photosynthetic activity on treatments with microbial consortia, while the influence of salt stress is moderate, despite significant interactions between the two variables (**Figure 3.5**).

While in unstressed condition the differences between microbial treatments are negligible, under stress conditions, especially at higher concentrations, photosynthetic activity is reduced in plants inoculated with MC_D. These results suggest a greater sensitivity to salt stress in plants inoculated with MC_D compared to the control group. The decreased photosynthetic activity at high stress condition, is in line with the reduction in photosynthetic input and the concentration of photosynthetic pigments typically triggered by salt stress (Taïbi *et al.*, 2016).

On the other hand, consortium D has been studied in *Arabidopsis thaliana* L. (Heyhn) exposed to drought stress, where it showed an increase in photosynthetic pigment content compared to non-inoculated plants (Yang N. *et al.*, 2021). Hypothetically, the reduction in photosynthetic activity may be a consequence of ionic stress due to the accumulation of Na^+ and Cl^-, rather than water stress caused by salt stress, or it could be dependent on the species under analysis.

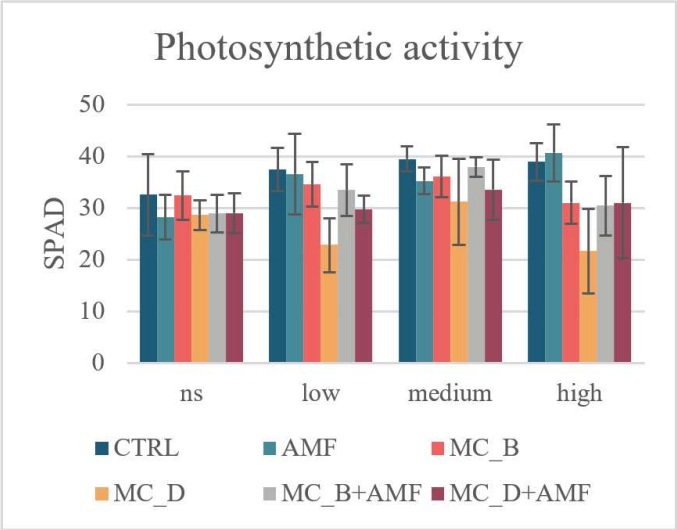

	F value	*p value*
Salt Stress	3.689	0.0128
Consortia	13.293	8.33E-13
Salt Stress * Consortia	3.672	2.25E-06

Figure 3.5: Means and standard deviations of chlorophyll content (SPAD units) values obtained after six weeks of salt stress induction on tomato plants. The results obtained from the untreated plants (control condition) are compared with those obtained from plants inoculated with microbial consortia MC_B, MC_D, and AMF alone and in combination, under unstressed conditions (ns), as well as under three levels of salt stress: NaCl solutions at 0.5% (low), 0.75% (medium), and 1% (high). In the table below, results of Two-way analysis of variance (ANOVA) are shown. The significance of the differences was assessed by Tukey's HSD (Honestly Significant Difference)

Proline content

The quantification of proline content is useful for understanding how plants respond to changes in cellular osmotic balance caused by salt stress. Proline is a well-known osmolyte synthesized in response to the perturbation of osmotic balance caused by the compartmentalization and accumulation of ions inside the vacuole. Its function is to stabilize the internal osmotic potential, increase protein stability, and protect cellular integrity (Yancey, 2005). Proline was extracted from leaves and then quantified spectrophotometrically. An increase in proline content was observed, depending on increasing salinity levels, particularly pronounced in plants exposed to medium and high salt stress (**Figure 3.6**). However, the type of response to salt stress is modulated by the type of consortia used, especially at high salinity level. In fact, in plants inoculated with MC_D and MC_B+AMF, no increase in proline concentration was observed under high stress condition compared to the unstressed control.

Conversely, plants inoculated with AMF alone respond to abiotic stress by increasing proline concentration more than the other tested conditions, indicating a greater plant response to salt stress. It is reported that inoculation with AMF increases proline concentration, allowing for greater regulation of osmotic potential or suggesting a greater need to promote an antioxidant response (Sharifi *et al.*, 2007). Proline also plays an antioxidative role by promoting the detoxification of hydroxyl radicals and inhibiting lipid peroxidation (Trovato *et al.*, 2008).

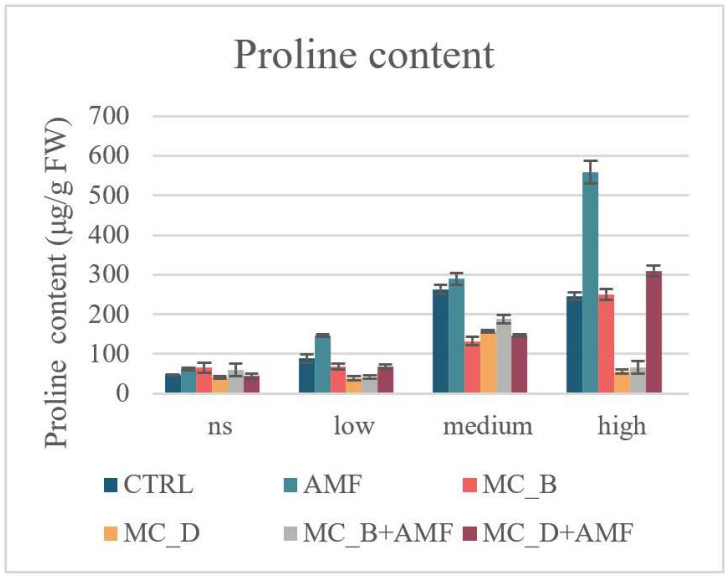

	F value	*p value*
Salt Stress	1.29E+03	2E-16
Consortia	361.6	2E-16
Salt Stress * Consortia	148.7	2E-16

Figure 3.6: Means and standard deviations of proline content values obtained after six weeks of salt stress induction on tomato plants. The results obtained from the untreated plants (control condition) are compared with those obtained from plants inoculated with microbial consortia MC_B, MC_D, and AMF alone and in combination, under unstressed conditions (ns), as well as under three levels of salt stress: NaCl solutions at 0.5% (low), 0.75% (medium), and 1% (high). In the table below, results of Two-way analysis of variance (ANOVA) are shown. The significance of the differences was assessed by Tukey's HSD (Honestly Significant Difference)

From the presented results, it seems that plants inoculated with MC_B combined with AMF acquire the ability to respond more effectively to higher stress conditions. However, the increase or decrease in proline under stress conditions may depend on a multitude of combined physiological and molecular variables. A more in-depth analysis, including the examination of other biomarkers and the modulation of gene expression, is necessary to understand more fully the physiological mechanisms underlying the observed variations.

Cellular respiration

Cellular respiration is one of the biochemical mechanisms that is altered when plants are exposed to salt stress. In particular, respiration usually increases during salt stress to compensate for the reduction in the energy rate in the chloroplasts (Atkin & Macherel, 2009). This increases the generation of oxidative stress through the transfer of electrons to oxygen.

However, in this case no significant differences between treatments are recorded, either regarding the response to salt stress, the response dependent on microbial inoculation and the interactions between the two variables (**Figure 3.7**).

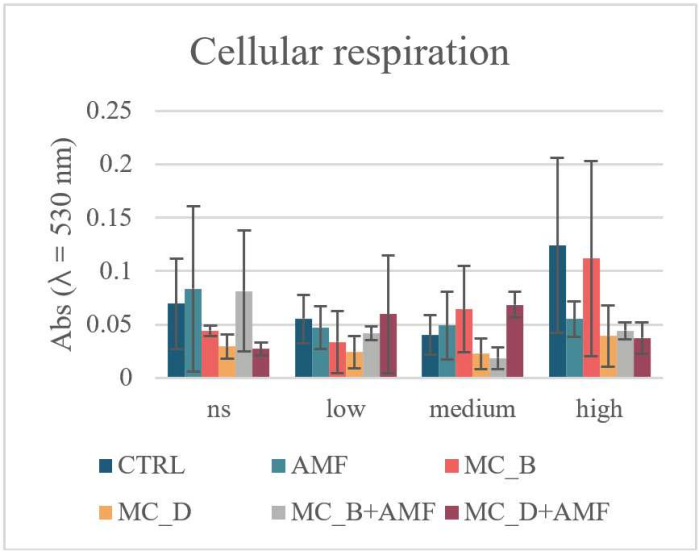

Figure 3.7: Means and standard deviations of formazan absorbance obtained after six weeks of salt stress induction on tomato plants. The results obtained from the untreated plants (control condition) are compared with those obtained from plants inoculated with microbial consortia MC_B, MC_D, and AMF alone and in combination, under unstressed conditions (ns), as well as under three levels of salt stress: NaCl solutions at 0.5% (low), 0.75% (medium), and 1% (high). In the table below, results of Two-way analysis of variance (ANOVA) are shown. The significance of the differences was assessed by Tukey's HSD (Honestly Significant Difference)

	F value	*p value*
Salt Stress	1.918	0.137
Consortia	1.174	0.135
Salt Stress * Consortia	1.266	0.246

Biometric analyses

The plant's growth and consequently its yield were evaluated through various biometric analyses at both root and shoots levels, such as length, fresh weight, and dry weight. In all cases, the plant's response for these parameters was not significantly influenced by salt stress, but it was dependent on the type of microbial treatment (**Figure 3.8** and **3.9**). Specifically, a distinction in plant height emerges in two significantly different groups: one group comprising the control group and the plants treated with AMF and MC_B, another group comprising plants inoculated with MC_D, MC_B+AMF, and MC_D+AMF (**Figure 3.8-a**). In this case, a possible interaction with hormones involved in plant growth and development could be hypothesized. From the results obtained, it is observed that plants treated with MC_D show a significant reduction in height compared to the other conditions tested, which is more pronounced when the plants are exposed to the highest level of salinity. There could be different possible causes for this behavior: in the literature it is reported that the possible growth-promoting effect depends on the composition of the consortia, the type of plant under analysis, and the composition of the soil nutrients (Santoyo *et al.*, 2021).

It is known that the production of secondary metabolites by bacterial consortia can influence the plant's hormones balance. Furthermore, the pronounced reduction in height following treatment with MC_D at the highest saline concentration suggests that this response is a possible plant escape mechanism following the induction of stress, aimed at reducing energy demands. At the root growth level, despite the absence of an observed influence of salt stress, plants treated with MC_B+AMF, especially under low and medium salt stress conditions, showed an increase in root length (**Figure 3.8-b**). This parameter also emphasized a certain degree of influence of the MC_B consortium in stimulating the response to stress when used in combination with mycorrhizae.

a)

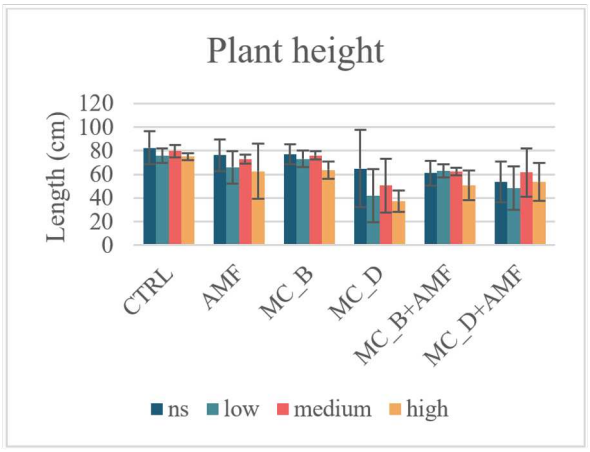

b)

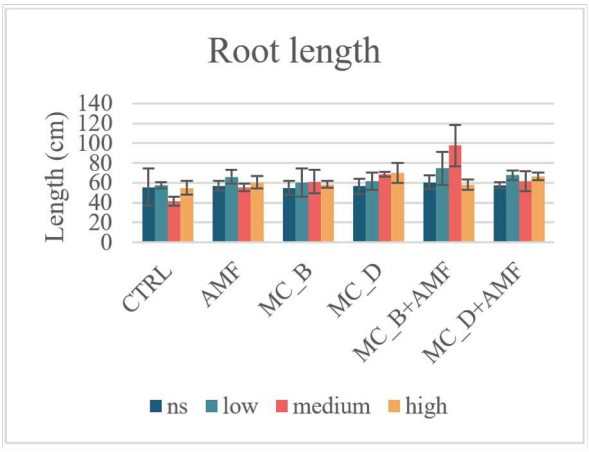

	F value	*p value*
Salt Stress	2.659	0.057
Consortia	5.238	0.00024
Salt Stress * Consortia	0.434	0.9734

	F value	*p value*
Salt Stress	1.81	0.157
Consortia	4.13	0.0017
Salt Stress * Consortia	2.26	0.0104

Figure 3.8: Means and standard deviations of plants height (**a**) and roots length (**b**) after six weeks of salt stress induction on tomato plants. The results obtained from the untreated plants (control condition) are compared with those obtained from plants inoculated with microbial consortia MC_B, MC_D, and AMF alone and in combination, under unstressed conditions (ns), as well as under three levels of salt stress: NaCl solutions at 0.5% (low), 0.75% (medium), and 1% (high). In the table below, results of Two-way analysis of variance (ANOVA) are shown. The significance of the differences was assessed by Tukey's HSD (Honestly Significant Difference)

Parameters like fresh and dry weight allows to quantify the final yield of the plant, providing an estimate of the ability of microbial consortia to promote its growth. The results showed a statistically significant variation depending on the microbial consortia used. In particular, the fresh weight of the roots in the control group is significantly greater than the fresh weight of the roots of plants inoculated with MC_D+AMF (**Figure 3.9-b**). This result is confirmed by roots dry weight, which also shows a significant difference between plants inoculated with MC_D and the control group (**Fig. 3.9-d**), highlighting a considerable reduction in root biomass induced by both treatments with MC_D.

Shoots fresh and dry weight also show a significant reduction in biomass in plants treated with MC_D, MC_D+AMF, and MC_B+AMF compared to the control group (**Figure 3.9-a** and **3.9-c**).

a)

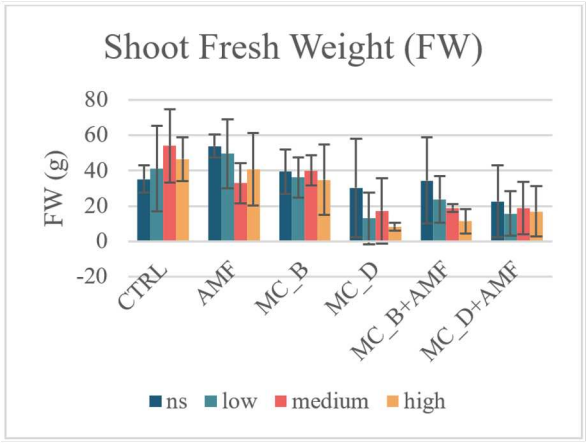

	F value	*p value*
Salt Stress	1.516	0.22
Consortia	6.556	2.77E-05
Salt Stress * Consortia	0.67	0.825

b)

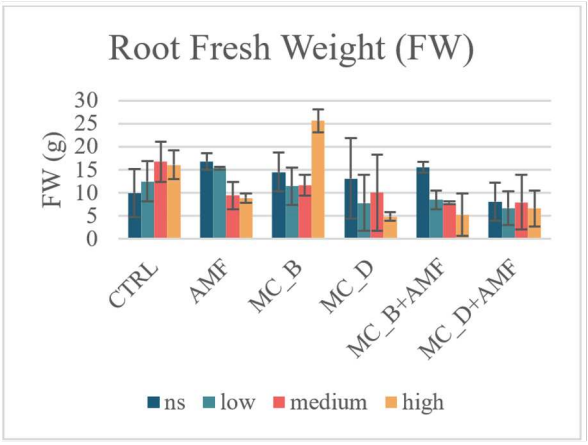

	F value	*p value*
Salt Stress	0.895	0.4495
Consortia	2.996	0.0131
Salt Stress * Consortia	1.07	0.4044

c)

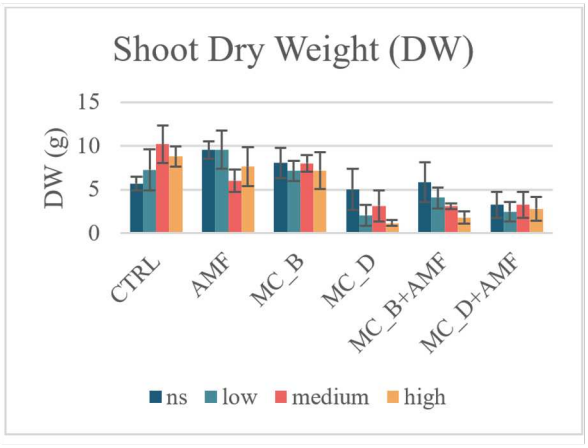

	F value	*p value*
Salt Stress	0.819	0.489
Consortia	7.175	1.04E-05
Salt Stress * Consortia	0.727	0.77

d)

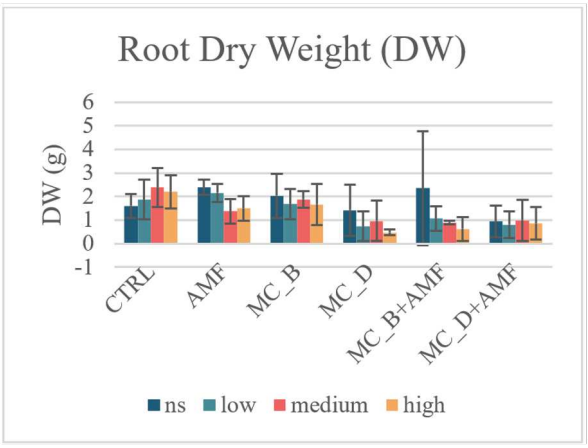

	F value	*p value*
Salt Stress	1.917	0.137
Consortia	4.468	0.00092
Salt Stress * Consortia	0.699	0.7975

Figure 3.9: Means and standard deviations of shoots fresh and dry weight (**a** and **c**) and roots fresh and dry weight (**b** and **d**) after six weeks of salt stress induction on tomato plants. The results obtained from the untreated plants (control condition) are compared with those obtained from plants inoculated with microbial consortia MC_B, MC_D, and AMF alone and in combination, under unstressed conditions (ns), as well as under three levels of salt stress: NaCl solutions at 0.5% (low), 0.75% (medium), and 1% (high). In the table below, results of Two-way analysis of variance (ANOVA) are shown. The significance of the differences was assessed by Tukey's HSD (Honestly Significant Difference)

Therefore, it seems that the analyzed microbial consortia not only do not have a significant positive impact in terms of plant growth, but they could even have detrimental effects, especially in the case of the treatment with MC_D. Given the results obtained, the most promising microbial combination would seem to be MC_B+AMF, considering that unlike MC_D, it has not shown detrimental effects on the plant, but on the contrary, for some parameters, it seems to trigger a response to salt stress, with more pronounced effects at the highest salinity level (NaCl solution 1%).

3.3 *Solanum lycopersicum* L. – combining ENMs and PGPMs

The results obtained during the preliminary experiment highlighted a potential positive influence of the treatment with MC_B combined with AMF in modulating the response of tomato plants to salt stress, especially at the highest salinity level (NaCl 1%). Next, the experiment was repeated under the same environmental conditions to confirm the morphological and physiological results obtained the previous year and to further investigate the molecular response of the plants in terms of gene expression. Considering the extensive documented potential of silicon-based nanoparticles, we also decided to compare the effects of these two types of technologies (i.e. SiO_2 NPs and microbial consortia), individually assessing their applicative potential or their synergy in the response to salt stress mediated by their combination.

For this purpose, tomato plants treated with MC_B+AMF and with SiO_2 NPs (or Na_2SiO_3 as an additional control) were exposed to salt stress (1% NaCl) for 6 weeks (**Figure 3.10**). At the end of salt stress induction, physiological and morphological analyses were conducted, and mRNA from leaves and roots was extracted for gene expression analysis through RNA-seq. Furthermore, leaves and roots samples were analyzed at the TwinMic beamline of the Trieste Synchrotron to obtain X-ray fluorescence elemental maps, providing insights into the internalization and distribution of elements within various plant tissues.

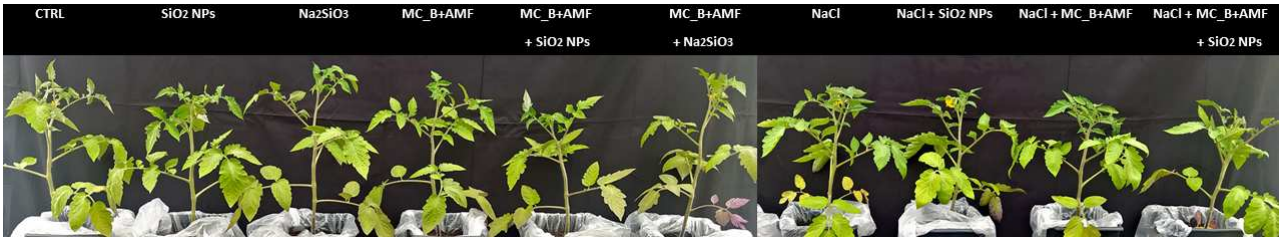

Figure 3.10: Tomato plants cv. Heinz 3402 after six weeks of salt stress. During the transplant, plants were inoculated with microbial consortium MC_B stabilized in zeolite powder (*Bacillus amyloliquefaciens* LMG9814, *Pseudomonas fluorescens* DR54, *Ranhella aquatilis* BB23/Tad, *Bacillus* sp. BV84, *Azotobacter vinelandii* DSM2289) combined with Arbuscular Mycorrhizal Fungi (AMF) *Rhizophagus intraradices*. Soil was also homogenized with SiO_2 NPs or the silicon salt Na_2SiO_3. Salt stress induction was performed with saline water irrigation (NaCl 1%) two times/week.

3.3.1 Morphological and physiological effects of PGPMs combined with nano-Si in tomato plants exposed to salt stress

The treatments with PGPMs and nano-Si do not lead to a significant change in the height of the plants, which is instead affected by salt stress. In stressed conditions, the plant height resulted reduced compared to the unstressed condition for nearly all the treatments under analysis. On the other hand, the growth of the root system does not appear to be directly influenced by the individual variables being studied. However, the results indicate an interaction between them: tomato plants treated with a combination of PGPMs and nano-Si would promote greater root growth in terms of length under unstressed conditions compared to the same treatment under salt stress.

a)

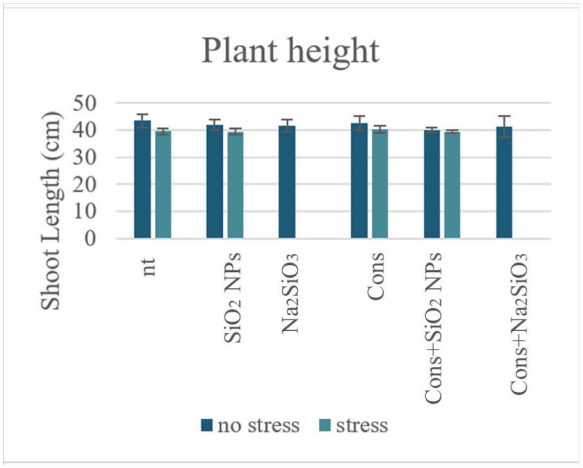

	F value	*p value*
SiO2 NPs	2.328	0.10815
Consortia	0.448	0.64161
Salt Stress	16.156	0.0002
SiO2 NPs * Consortia	0.536	0.46756
SiO2 NPs * Salt Stress	1.473	0.23065
Consortia * Salt Stress	2.28	0.13748
SiO2 NPs * Salt Stress * Consortia	0.005	0.94618

b)

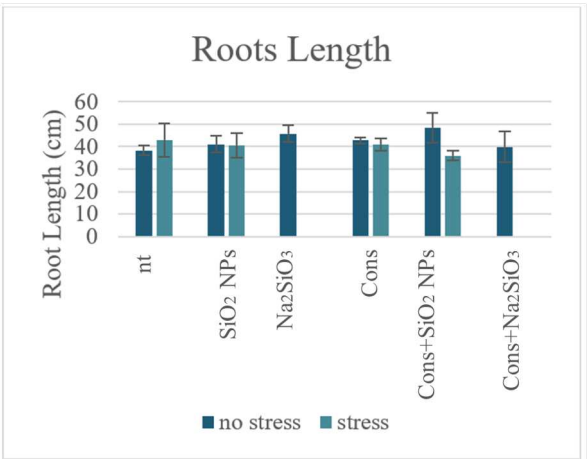

	F value	*p value*
SiO2 NPs	0.372	0.692
Consortia	2.442	0.09989
Salt Stress	2.934	0.09447
SiO2 NPs * Consortia	0.01	0.92025
SiO2 NPs * Salt Stress	7.04	0.01138
Consortia * Salt Stress	9.341	0.00398
SiO2 NPs * Salt Stress * Consortia	0.822	0.36993

Figure 3.11: Means and standard deviations of plants height (**a**) and roots length (**b**) after six weeks of salt stress induction on tomato plants. The results obtained from the untreated plants (nt) are compared with those obtained from plants inoculated with MC_B+AMF (cons), SiO_2 NPs or Na_2SiO_3 under stressed and unstressed conditions. In the table below, results of Three-way analysis of variance (ANOVA) are shown. The significance of the differences was assessed by Tukey's HSD (Honestly Significant Difference)

It is reported that silicon plays a positive role in the development of plant roots, stems, and leaves (Roohizadeh *et al.*, 2015). This effect may be attributed to its fundamental role in improving the plant's water status (Romero-Aranda *et al.*, 2006). Furthermore, it is interesting to note that silicon also has the capacity to promote the formation of secondary and tertiary cells of the endodermis, which are directly involved in the development of a more extensive root system (Hattori *et al.*, 2005).

a)

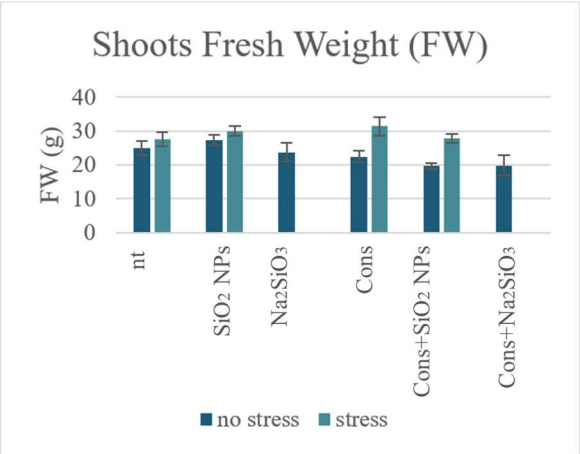

	F value	*p value*
SiO2 NPs	21.179	5.93E-07
Consortia	9.56	0.00042
Salt Stress	76.282	1.02E-10
SiO2 NPs * Consortia	18.528	0.00011
SiO2 NPs * Salt Stress	0.099	0.75439
Consortia * Salt Stress	20.843	4.88E-05
SiO2 NPs * Salt Stress * Consortia	0.094	0.76021

b)

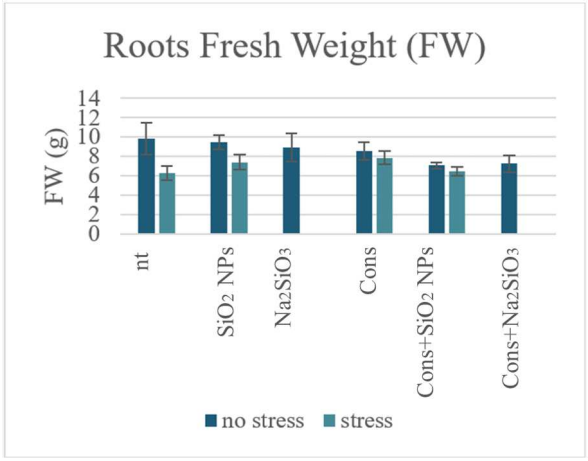

	F value	*p value*
SiO2 NPs	2.381	0.10546
Consortia	7.686	0.0015
Salt Stress	28.95	3.50E-06
SiO2 NPs * Consortia	10.605	0.0023
SiO2 NPs * Salt Stress	2.36	0.13232
Consortia * Salt Stress	14.203	0.00053
SiO2 NPs * Salt Stress * Consortia	0.815	0.37205

c)

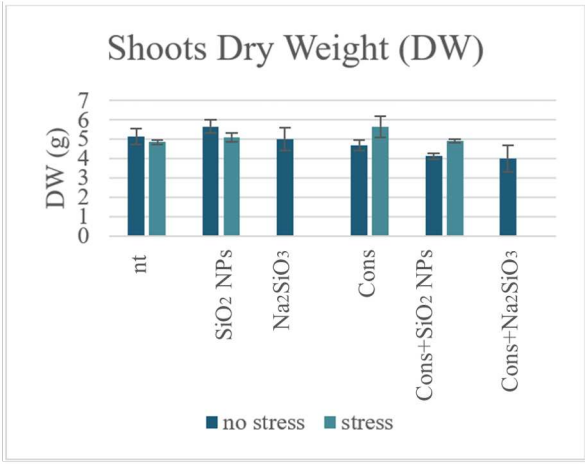

	F value	*p value*
SiO2 NPs	6.272	0.00427
Consortia	10.837	0.00017
Salt Stress	2,564	0.11719
SiO2 NPs * Consortia	18.708	9.86E-05
SiO2 NPs * Salt Stress	0.206	0.65238
Consortia * Salt Stress	30.825	2.01E-06
SiO2 NPs * Salt Stress * Consortia	0.015	0.90371

d)

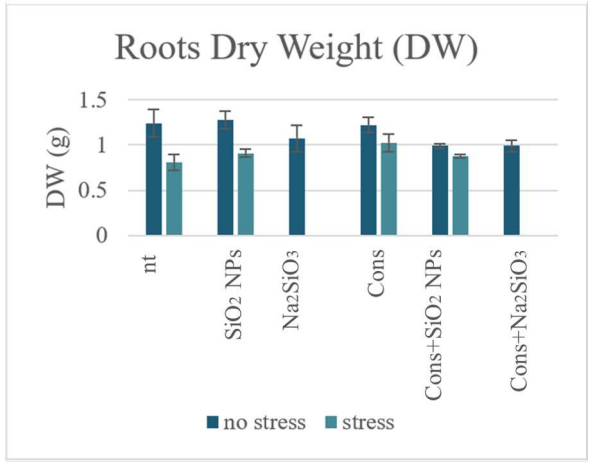

	F value	*p value*
SiO2 NPs	2.027	0.14502
Consortia	1.538	0.22733
Salt Stress	92.134	6.21E-12
SiO2 NPs * Consortia	19.009	8.86E-05
SiO2 NPs * Salt Stress	1.89	0.17689
Consortia * Salt Stress	17.376	0.00016
SiO2 NPs * Salt Stress * Consortia	0.029	0.8651

Figure 3.12: Means and standard deviations of shoots fresh and dry weight (**a** and **c**) and roots fresh and dry weight (**b** and **d**) after six weeks of salt stress induction on tomato plants. The results obtained from the untreated plants (nt) are compared with those obtained from plants inoculated with MC_B+AMF (cons), SiO_2 NPs or Na_2SiO_3 under stressed and unstressed conditions. In the table below, results of Three-way analysis of variance (ANOVA) are shown. The significance of the differences was assessed by Tukey's HSD (Honestly Significant Difference)

The yield of plants exposed to treatments with silicon and PGPMs was assessed by measuring the fresh and dry weights of shoots and roots (**Figure 3.12**). In untreated plants, salt stress does not appear to interfere with the biomass of the shoots, both in terms of fresh and dry weights. However, when plants are inoculated with the microbial consortium (both in the presence and absence of nano-Si), an increase in biomass is observed under salt stress compared to the non stressed condition (**Figure 3.12-a** and **3.12-c**). Conversely, root length is reduced in untreated plants under salt stress compared to the unstressed control. This reduction is mitigated when plants are inoculated with the microbial consortium (**Figure 3.12-b** and **3.12-d**). In terms of yield, therefore, a direct influence appears to be exclusively mediated by PGPMs treatments, which in this case have a greater impact in mitigating salt stress compared to silicon-based treatments. Contradictory results are reported in the literature regarding the effect of SiO_2 NPs on plant growth. Studies, have reported that nano-Si can be beneficial or ineffective on plants, either supporting growth or with no impact (Bao-shan *et al.*, 2004; Siddiqui & Al-Whaibi, 2014; Suriyaprabha *et al*., 2014), while in other studies, a negative impact has been observed (Slomberg & Schoenfisch, 2012). The different growth conditions and a species-specific response may explain these differences.

As previously described, both osmotic imbalance induced by salt stress and the use of nanomaterials may lead to the formation of ROS in plants, causing oxidative damage. The disturbance of the cell's redox state thus affects the proper functioning of both the photosynthetic system and cellular respiration. The photosynthetic activity at the end of salt stress induction was assessed by measuring the chlorophyll content using the SPAD method, while cellular respiration was measured on leaves through the TTC assay. The photosynthetic activity (**Figure 3.13-a**) did not show a significant difference under salt stress conditions compared to the unstressed control in untreated plants. Conversely, for both treatments analyzed (MC_B+AMF and SiO_2 NPs), a significant increase in photosynthetic activity under stress conditions compared to the unstressed condition within the same treatment was reported, with no treatment-specific differences observed. It appears that neither nano-Si nor the microbial consortium play a role in the response to salt stress in terms of chlorophyll concentration. However, these results still need to be clarified through molecular analysis, as pigment content alone is not sufficient to fully describe the integrity of the photosynthetic apparatus. In contrast, it has been demonstrated that silicon may play a role in increasing chlorophyll content in leaves, contributing to the maintenance of chloroplast integrity and ultrastructure, by increasing enzymes involved in chlorophyll biosynthesis or reducing enzymes that degrade it (Liang *et al.,* 2007). On the other hand, cellular respiration (**Figure 3.12-b**) does not appear to be significantly influenced by salt stress in plants untreated with PGPMs and nano-Si.

However, when the plant's soil is supplemented with SiO_2 NPs, there is an increase in cellular respiration in leaves of unstressed plants, while under stress conditions, the respiration returns to levels similar to the untreated control. Cellular respiration is a vital process for energy production in plants, and an increase in response to SiO_2 NPs treatment could be interpreted as an adaptation or defense strategy induced by nanoparticles.

a)

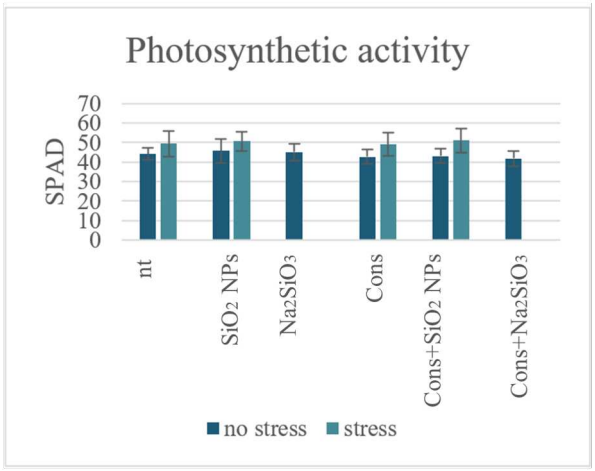

	F value	*p value*
SiO2 NPs	7.369	0.00085
Consortia	2.422	0.09186
Salt Stress	46.387	1.63E-10
SiO2 NPs * Consortia	0.128	0.72078
SiO2 NPs * Salt Stress	0.285	0.59403
Consortia * Salt Stress	1.894	0.17058
SiO2 NPs * Salt Stress * Consortia	0.099	0.75297

b)

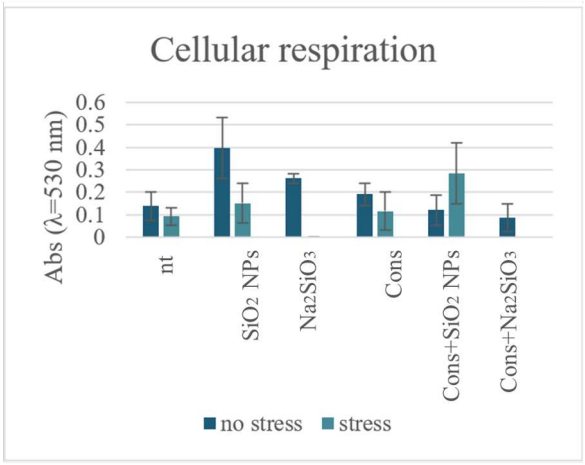

	F value	*p value*
SiO2 NPs	5.796	0.01279
Consortia	3.606	0.07576
Salt Stress	4.254	0.05579
SiO2 NPs * Consortia	3.044	0.0758
SiO2 NPs * Salt Stress	0.185	0.67322
Consortia * Salt Stress	5.251	0.03584
SiO2 NPs * Salt Stress * Consortia	12.231	0.00298

Figure 3.13: Means and standard deviations of Means and standard deviations of chlorophyll content (SPAD units) values (**a**) and formazan absorbance (**b**) after six weeks of salt stress induction on tomato plants. The results obtained from the untreated plants (nt) are compared with those obtained from plants inoculated with MC_B+AMF (cons), SiO_2 NPs or Na_2SiO_3 under stressed and unstressed conditions. In the table below, results of Three-way analysis of variance (ANOVA) are shown. The significance of the differences was assessed by Tukey's HSD (Honestly Significant Difference)

The cytoplasmic proline content is a key parameter for understanding the plant's response to the accumulation of ions in the vacuole induced by salt stress, as an increase in its production suggests a heightened plant response to restore cellular osmotic balance. As expected, the proline content increases under salt stress conditions while it remains at low levels in the absence of stress, with no significant differences observed among the silicon and consortium treatments (**Figure 3.14-a**). Conversely, under stress conditions, a treatment-dependent modulation of proline content is observed. Plants inoculated with the microbial consortium exhibit a reduction in proline content compared to the untreated plants under stress conditions, confirming the results obtained during the preliminary experiment. On the other hand, the use of SiO_2 NPs induces an increase in proline content under stress conditions compared to the untreated plant.

However, the reasons behind the increase or decrease in proline content requires additional analyses for accurate interpretation. This includes both the molecular mechanisms underlying this response and a quantitative analysis of ions accumulated within the plant cell. It is not clear whether the variation in proline content is due to modulation of the plant's response interconnected with other pathways responding to abiotic stresses or whether it may indicate a reduced accumulation of ions in the vacuole, hence a diminished osmotic unbalance at the cellular level.

a)

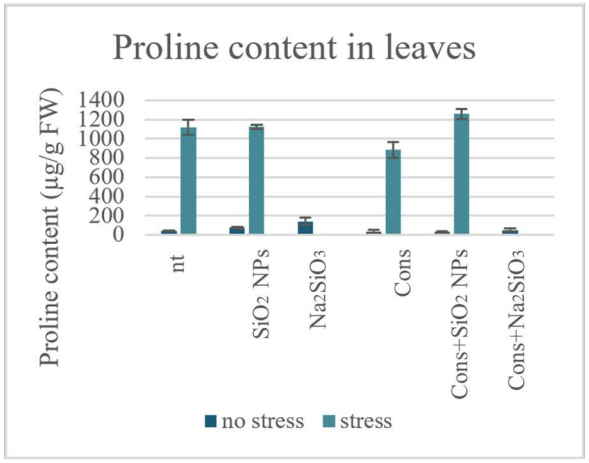

	F value	*p value*
SiO2 NPs	328.509	5.06E-16
Consortia	9.900	0.00508
Salt Stress	3,783.352	< 2e-16
SiO2 NPs * Consortia	12.760	0.000268
SiO2 NPs * Salt Stress	26.259	5.17E-05
Consortia * Salt Stress	0.577	0.456248
SiO2 NPs * Salt Stress * Consortia	36.257	6.91E-06

b)

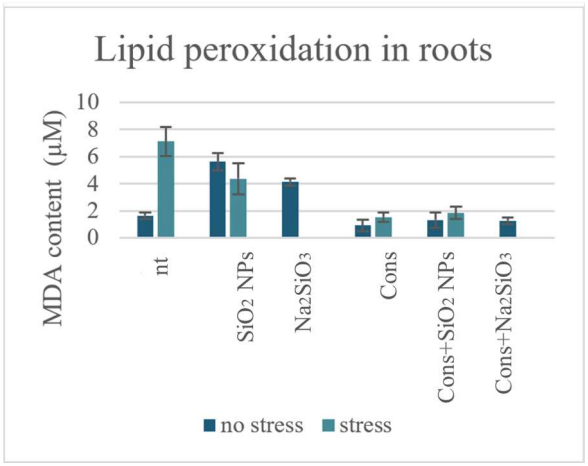

	F value	*p value*
SiO2 NPs	2.440	0.11268
Consortia	198.430	7.62E-12
Salt Stress	27.820	3.67E-05
SiO2 NPs * Consortia	0.400	0.67406
SiO2 NPs * Salt Stress	44.700	1.66E-06
Consortia * Salt Stress	9.280	0.00638
SiO2 NPs * Salt Stress * Consortia	42.740	2.27E-06

Figure 3.14: Means and standard deviations of proline content in leaves (**a**) and malondialdehyde (MDA) content in roots (**b**) after six weeks of salt stress induction on tomato plants. The results obtained from the untreated plants (nt) are compared with those obtained from plants inoculated with MC_B+AMF (cons), SiO_2 NPs or Na_2SiO_3 under stressed and unstressed conditions. In the table below, results of Three-way analysis of variance (ANOVA) are shown. The significance of the differences was assessed by Tukey's HSD (Honestly Significant Difference)

The production of MDA is due to the degradation of polyunsaturated membrane lipids, induced by the attack of ROS. Quantifying its content, especially in the root system where the plant first enters in contact both NaCl, SiO_2 NPs and microbial consortia, provides an indication of the oxidative damage caused at the cellular level. In plants untreated with silicon or the microbial consortium, the MDA content significantly increases under salt stress conditions compared to the unstressed control, confirming the destructive impact of NaCl infiltration at the cellular level (**Figure 3.14-b**). This stress-induced increase is significantly modulated when plants are treated with SiO_2 NPs. However, despite the stress-improving response induced by nano-Si, in unstressed conditions an increase in lipid peroxidation is observed for all the silicon treatments, suggesting a silicon-dependent oxidative effect. The use of silicon at the concentrations under analysis could therefore lead to the formation of

free radicals and to the disruption of membrane integrity. These results align with other studies documenting an increase in lipid peroxidation in various plant species following treatment with SiO_2 NPs (Hussain *et al.,* 2020; Metzler *et al.*, 2012; Salajegheh *et al.*, 2020). However, in a study conducted by Ashkavand *et al.* (2015) on drought resistance mediated by nano-Si in hawthorn plants, it is reported that under stress conditions, the amount of MDA decreases with an increase in silicon NPs concentration. It can be hypothesized that SiO_2 NPs might enhance the activity of certain antioxidant systems in some cases. According to Zarafshar *et al*. (2015), silicon nanoparticles significantly increase the activity of SOD, POX and CAT which are among the key enzymatic antioxidants in plants, promoting the scavenging capacity of ROS (Kumar Tripathi *et al.*, 2017), thus contributing to the potential induction of resilience to abiotic stresses.

Interestingly, while silicon mitigates oxidative damage under salt stress conditions but induces oxidative damage itself in the absence of salt stress, a different pattern is observed for treatments with the microbial consortium. In this case, there seems to be no negative impact on membrane integrity in unstressed conditions. Moreover, under salt stress conditions, the MDA content is significantly comparable to that of unstressed plants, suggesting a protective role of the microbial consortium (MC_B) combined with AMF in the response to oxidative stress, both AMF in the presence and absence of silicon. For instance, a combined use of PGPR such as *Pseudomonas libanensis* and AMF like *Claroideoglomus claroideum* has been reported to reduce the MDA content in plants exposed to salt stress compared to non-inoculated plants. This demonstrates their ability to protect against cellular damage induced by oxidative stress (Y. Ma et al., 2019). Furthermore, a study conducted on tomatoes showed a reduction in MDA content induced by inoculation with a microbial consortium under drought stress conditions (Krishna *et al.*, 2022). In this case, the analysis of antioxidant enzymes revealed a correlation between the reduction in MDA content compared to non-inoculated plants, and an increase in antioxidant enzymes involved in ROS scavenging.

3.3.2 Gene expression analysis through RNA-seq in roots and leaves tissues

The use of SiO_2 NPs in agriculture has been reported to potentially provide benefits in terms of enhancing plant growth and yield, mitigating the effects of abiotic stress, boosting the plant's defense system, and improving water status (El-Kady *et al*., 2017; Mukarram *et al*., 2022; Rajput *et al.*, 2021; Zmeeva *et al*., 2017). However, the potential harm that these particles may cause when interacting with plants or being translocated into the fruit, particularly if consumed by humans, remains to be investigated. Indeed, understanding both the risks associated with the use of nanoparticles in agriculture and the mechanisms through which nanoparticles exert their function is essential to grasp the long-term implications of their use in agriculture (Iavicoli *et al.*, 2017; Okeke *et al.*, 2023; Rastogi

et al., 2019). For this reason, in the analysis of gene expression through RNA-seq, we focused on treatments with nanoparticles and salt stress to obtain a comprehensive overview of the mechanisms involved in mitigating salt stress and the effects mediated by silicon-based treatments. In the future, the analysis of the expression of key genes identified during this initial phase will also be extended to plants treated with microbial consortia. For the RNA-seq analysis, the GCF_000188115.5_SL3.1 genome provided by the International Tomato Genome Sequencing Project (Sol Genomics Network) was used for alignments. It encompasses 34,075 protein-coding genes, with functional annotations assigned to 29,532 genes and 4,794 novel genes. In addition, over 98.94% of its sequences are anchored to 12 chromosomes, offering a comprehensive resource for RNA-seq alignments and other genomic analyses (Sato *et al*., 2012; Su *et al.*, 2021).

The FPKM values obtained from RNA-seq were processed to derive log_2FC values, where $log_2FC=log_2(treated)-log_2(untreated)$. From the box plots and violin plots, a higher density of log_2FC values close to 0 was observed in leaves in the presence of SiO_2 NPs compared to other conditions. Conversely, in the presence of salt stress with the addition of SiO_2 NPs, log_2FC values appeared more dispersed compared to other conditions (**Figure 3.15-a**). In roots, a higher frequency of log_2FC values between 0 and 1 was observed in the two unstressed conditions compared to the two stressed conditions (**Figure 3.15-b**). For the analysis of DEGs, genes were selected if the FPKM value was greater than 100 in at least one of the two conditions (treated vs untreated). This was done to avoid including genes with a too low expression level, which could lead to potential errors in the evaluation of DEGs (a very high fold change between very small values is less reliable than the same fold change for high FPKM values, as it is more susceptible to potential errors). The number of DEGs falling within different fold change ranges was identified for both leaves and roots, and based on these results, an ideal cut-off was selected (**Figures 3.16 and 3.17**). In leaves, we focused on DEGs with $log_2FC>0.6$ (1.5-fold change), while in roots, the analysis was restricted to DEGs with $log_2FC>3$ (8-fold change). In fact, from the number of modulated genes under the analyzed conditions, a greater variation in gene expression is evident in the roots compared to the leaves. The number of genes modulated within the range $0.6 < log_2FC < 2$ is approximately 9-times higher in plants treated with nano-Si and about 4-times higher for other treatments. Additionally, unlike in the roots where there is a strong modulation of gene expression even in the presence of nano-Si, in the leaves, it appears that nanoscale silicon has an impact of more than two times lower than silicate salt and from 3 to 4 times lower in the presence of salt stress.

a) Leaves

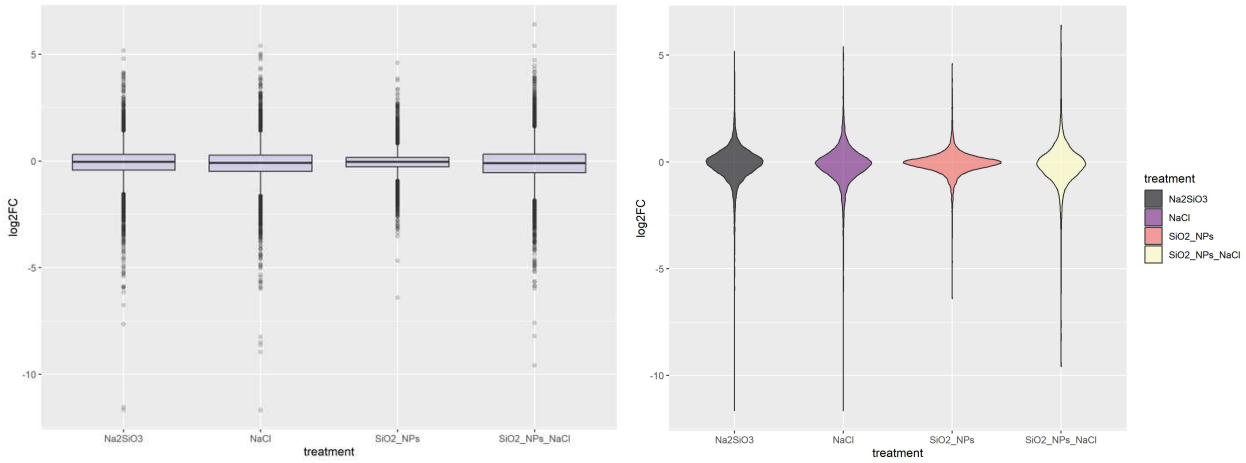

b) Roots

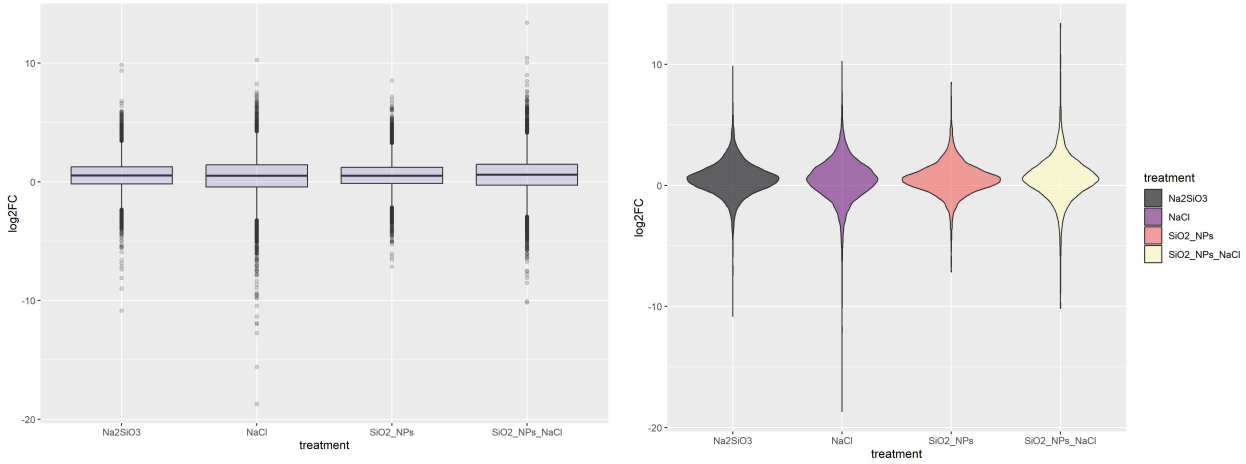

Figure 3.15: Box plot (left) and violin plot (right) representing the statistics of expressed genes in leaves (**a**) and roots (**b**) of tomato plants treated with Na_2SiO_3 (2.37 g/kg) and SiO_2 NPs (500 mg/kg) under unstressed and stressed conditions (NaCl 1%). The values are expressed in log_2 and normalized to the control condition.

a) Leaves

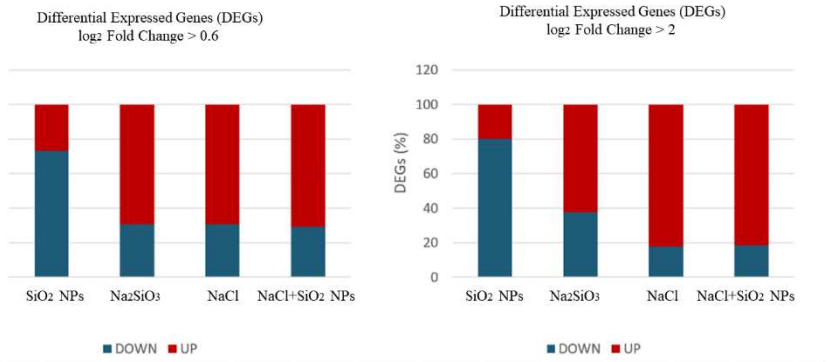

DEGs count	SiO2 NPs	Na2SiO3	NaCl	NaCl + SiO2 NPs
0.6<log2FC<2	85	204	333	396
2<log2FC<3	5	8	17	11
log2FC>3	0	2	4	2

Figure 3.16-a: Comparison of the percentage of up-regulated and down-regulated genes in leaves of tomato plants treated with Na_2SiO_3 (2.37 g/kg) and SiO_2 NPs (500 mg/kg) under unstressed and stressed conditions (NaCl 1%). Differentially Expressed Genes (DEGs) were selected using different ranges of log_2 fold change (0.6, 2, and 3 log_2FC, corresponding to 1.5-FC, 4-FC, 8-FC), the percentage is on the total DEGs count.

b) Roots

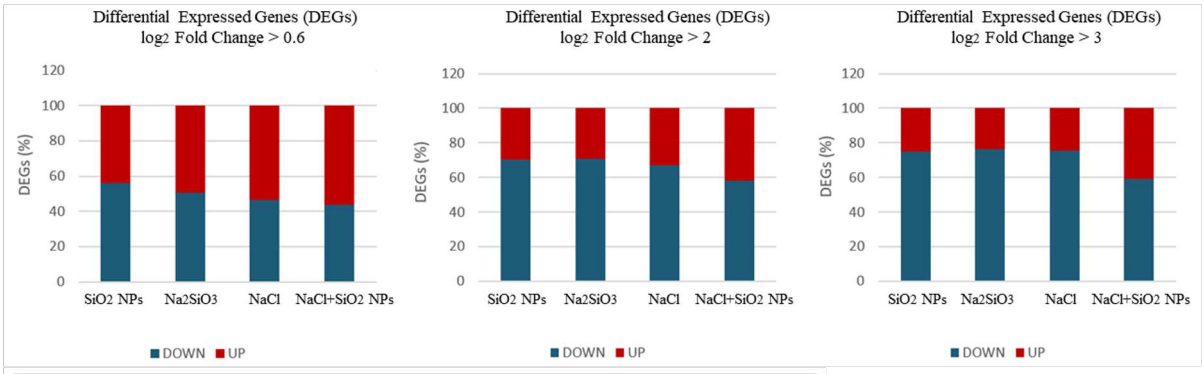

DEGs count	SiO2 NPs	Na2SiO3	NaCl	NaCl + SiO2 NPs
0.6<log2FC<2	909	994	1289	1236
2<log2FC<3	281	282	521	483
log2FC>3	115	119	284	264

Figure 3.16-b: Comparison of the percentage of up-regulated and down-regulated genes in roots of tomato plants treated with Na_2SiO_3 (2.37 g/kg) and SiO_2 NPs (500 mg/kg) under unstressed and stressed conditions (NaCl 1%). Differentially Expressed Genes (DEGs) were selected using different ranges of log_2 fold change (0.6, 2, and 3 log_2FC, corresponding to 1.5-FC, 4-FC, 8-FC), the percentage is on the total DEGs count.

a) Leaves

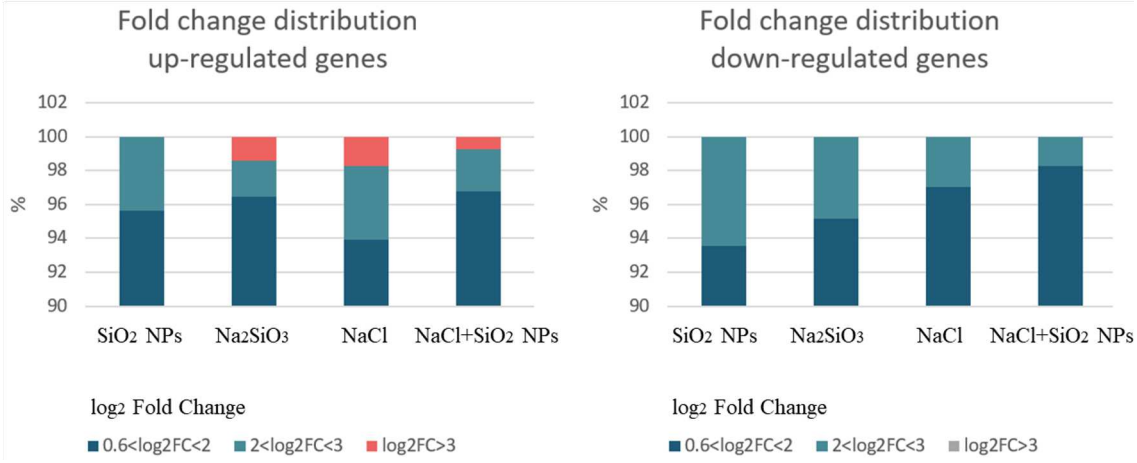

Figure 3.17-a: Percentage of the number of genes that exhibit, for each condition, a log_2 fold change between 0.6 and 2, between 2 and 3, greater than 3 (corresponding to 1.5-fold change, 4-fold change, 8-fold change), in leaves of tomato plants treated with Na_2SiO_3 (2.37 g/kg) and SiO_2 NPs (500 mg/kg) under unstressed and stressed conditions (NaCl 1%).

b) Roots

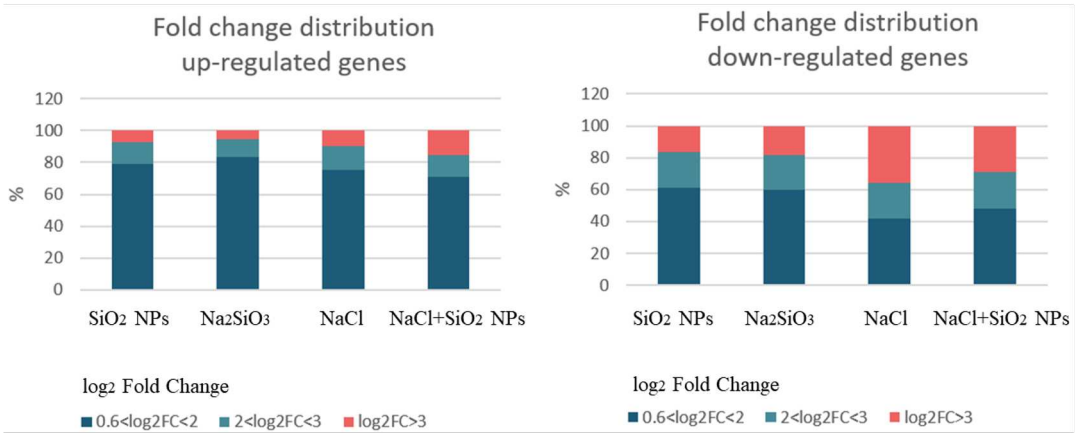

Figure 3.17-b: Percentage of the number of genes that exhibit, for each condition, a log_2 fold change between 0.6 and 2, between 2 and 3, greater than 3 (corresponding to 1.5-fold change, 4-fold change, 8-fold change), in roots of tomato plants treated with Na_2SiO_3 (2.37 g/kg) and SiO_2 NPs (500 mg/kg) under unstressed and stressed conditions (NaCl 1%).

The DEGs obtained for the four conditions using a $log_2FC>0.6$ for leaves and $log_2FC>3$ for roots were compared. In leaves, 15 genes were modulated in all conditions, 32 genes were typical of the nano-Si treatment in unstressed conditions, and 96 genes were modulated in the nano-Si treatment in stressed conditions (**Figure 3.18-a**). In roots, 95 genes modulated in all conditions, and 71 typical of the nano-Si treatment were found, including 2 in unstressed conditions, 68 in stressed conditions, and 1 in common (**Figure 3.18-b**). The heatmaps represent the modulation of the common DEGs to all treatments (**Figure 3.18-c**, value reported in Appendix).

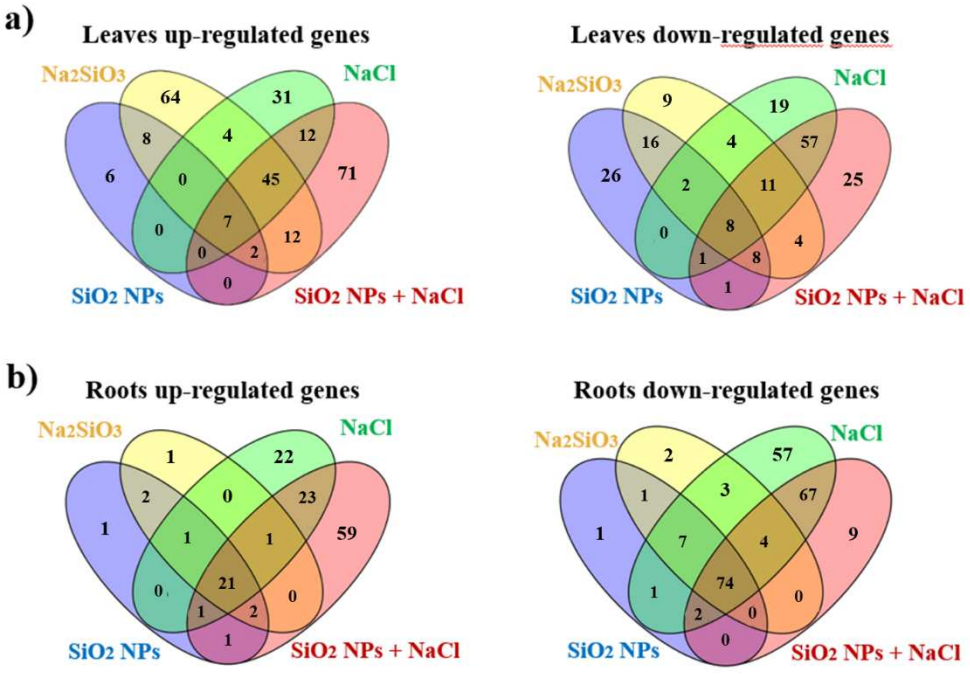

Figure 3.18: Venn diagrams of DEGs upregulated and downregulated in leaves (**a**) and roots (**b**) of tomato plants treated with SiO_2 NPs (blue), Na_2SiO_3 (yellow), NaCl 1% (green) and SiO2 NPs + NaCl 1% (red). The heatmaps represent the modulation of gene expression of common DEGs in leaves and roots (expressed as log_2FC).

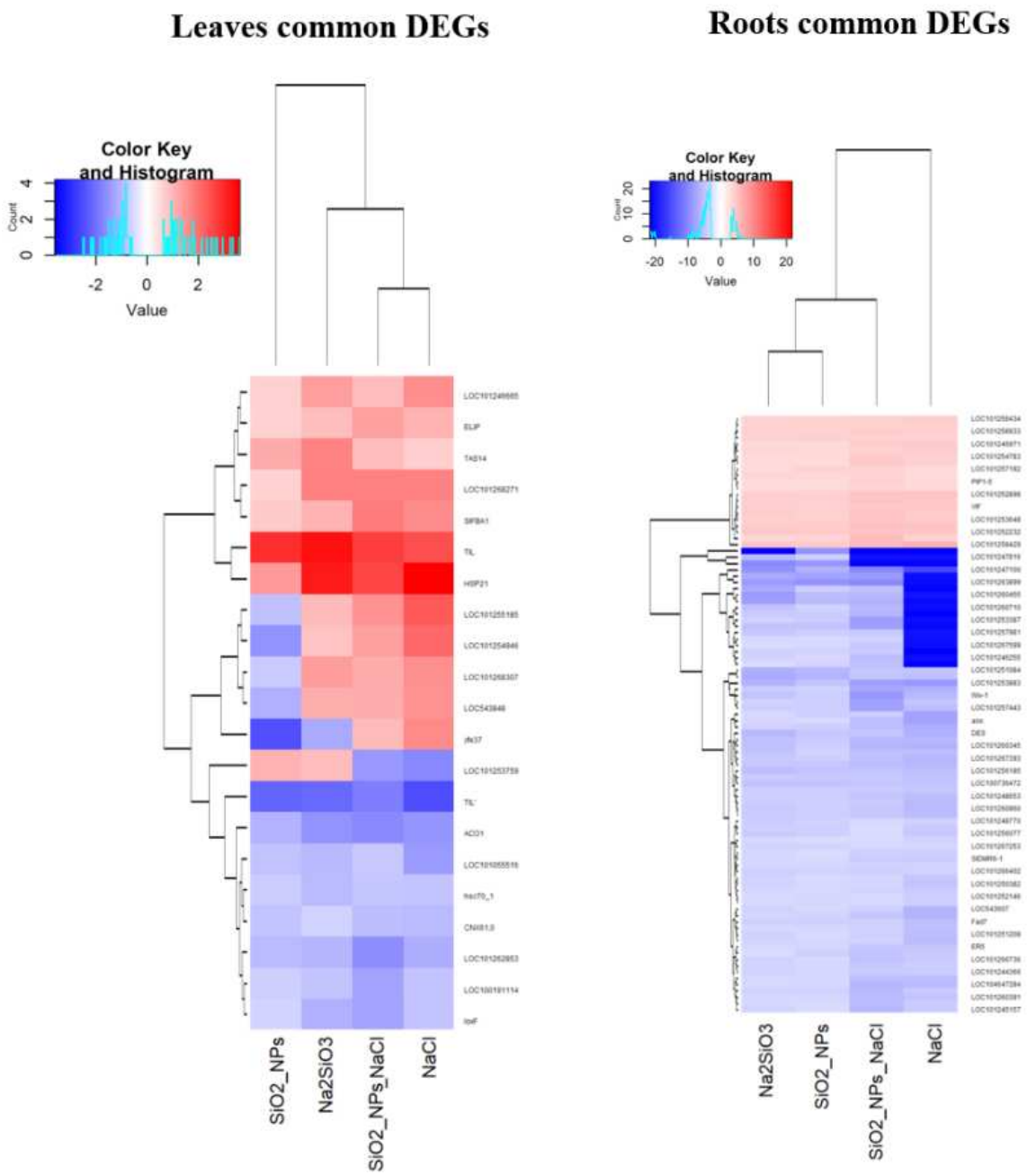

Figure 3.18-c: The heatmaps represent the modulation of gene expression of common DEGs in leaves and roots (expressed as log_2FC).

In leaves, it is possible to identify two genes (LOC101253759, yfe37) that show modulation related to salt stress, with down-regulation in stress conditions and up-regulation in unstressed conditions for the first gene, and the opposite for the second gene. The gene LOC101253759 encodes for MLO-like protein 2 (MLO2), which is part of the MLO protein family, transmembrane proteins involved in plant immunity and response to host-pathogen interactions. Four genes (LOC101254946, LOC101255185, LOC101268307, HSP17-6), all encoding for heat shock proteins, are down-regulated only in the leaves of plants treated with nano-Si in unstressed conditions, while they are up-regulated for all other conditions. In roots, there are no differences in the modulation pattern of

common genes between treatments, but a panel of 15 genes strongly down-regulated in the salt stress condition is observed, with their strong down-regulation mitigated when SiO_2 NPs is applied in stress conditions. Among these, there are, for example, genes that encode for ethylene response factor, calcium-binding protein, and TIFY protein, highlighting the involvement of nano-Si in the variation of the plant's response to salt stress.

In leaves, DEGs with a log_2FC greater than 0.6 were used for enrichment analysis using DAVID to obtain the most relevant functional annotations. In **Figure 3.19**, cluster frequencies are depicted, categorically divided into biological processes (BP), molecular function (MF), and cellular component (CC). While in leaves of tomato plants treated with SiO_2 nanoparticles, sets of genes predominantly localized in the cytoplasm are modulated, in plants treated with salts (both Na_2SiO_3 and NaCl), the modulation of genes localized in the chloroplast and mitochondria is also observed, suggesting an involvement of organelle functions in the response to the salt treatments (Pagano *et al*., 2022). Notably, only in plants exposed to salt stress (both in the presence and absence of nano-Si), an involvement of the photosystem II oxygen-evolving complex is observed, suggesting the initiation of a plant response to oxidative stress mediated by salt. The involvement of organelles in the salt stress response is further reinforced by the modulation of key biological processes and molecular functions related to photosynthetic processes, stabilization of photosystems, as well as sugar metabolism.

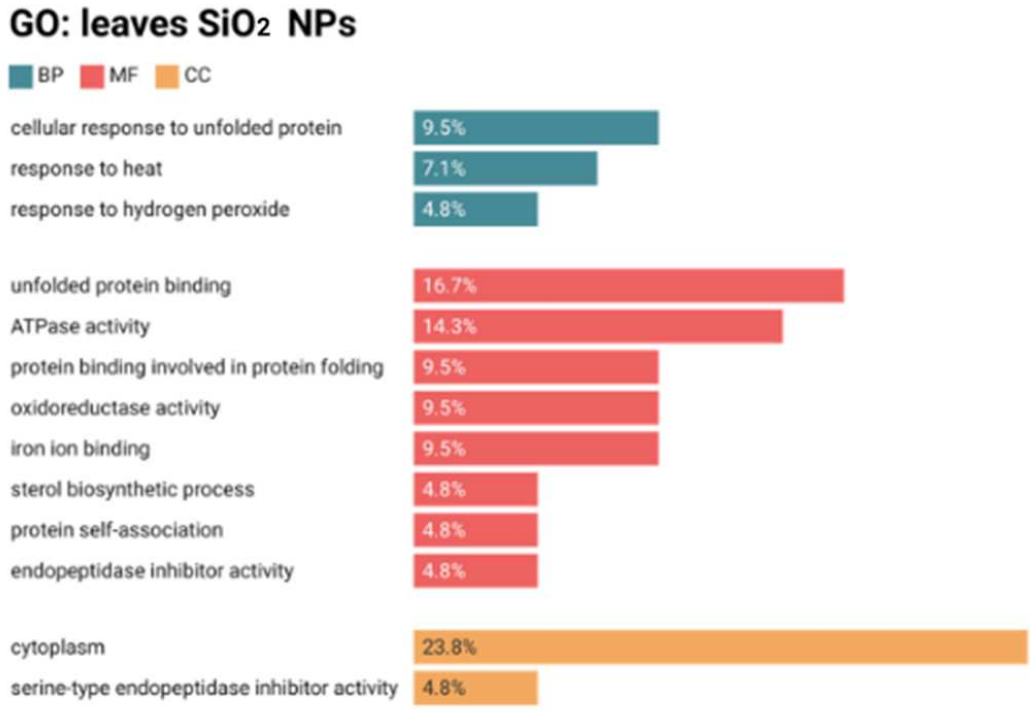

Figure 3.19-a: Cluster frequency (%) of GO enrichment performed with the Database for Annotation, Visualization, and Integrated Discovery (DAVID) of Differential Expressed Genes (DEGs) on tomato leaves ($log_2FC>0.6$). Category of Biological Processes (BP, blue), Molecular Function (MF, pink) and Cellular Component (CC, yellow) are represented for the SiO_2 NPs condition.

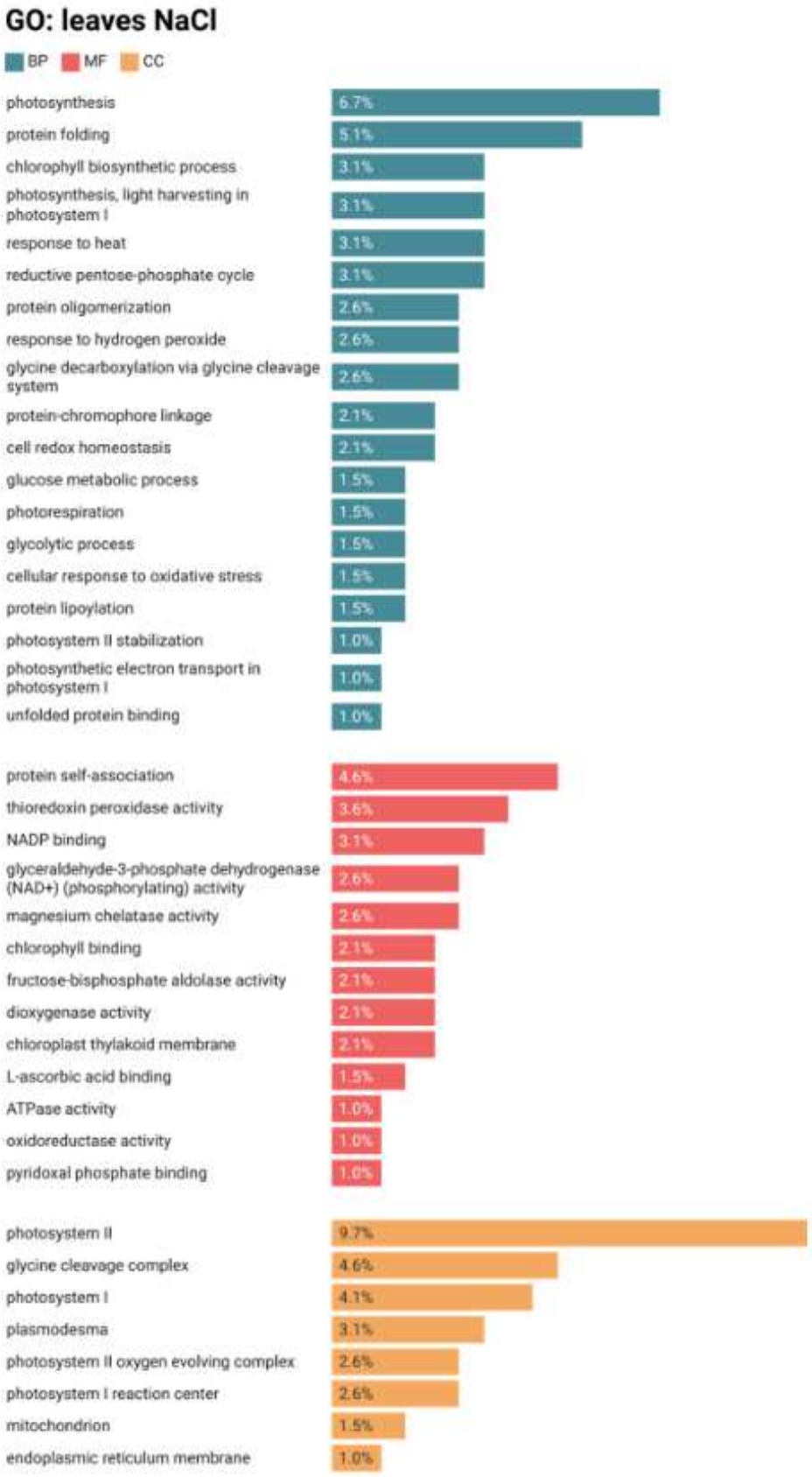

Figure 3.19-b: Cluster frequency (%) of GO enrichment performed with the Database for Annotation, Visualization, and Integrated Discovery (DAVID) of Differential Expressed Genes (DEGs) on tomato leaves ($log_2FC>0.6$). Category of Biological Processes (BP, blue), Molecular Function (MF, pink) and Cellular Component (CC, yellow) are represented for the NaCl condition.

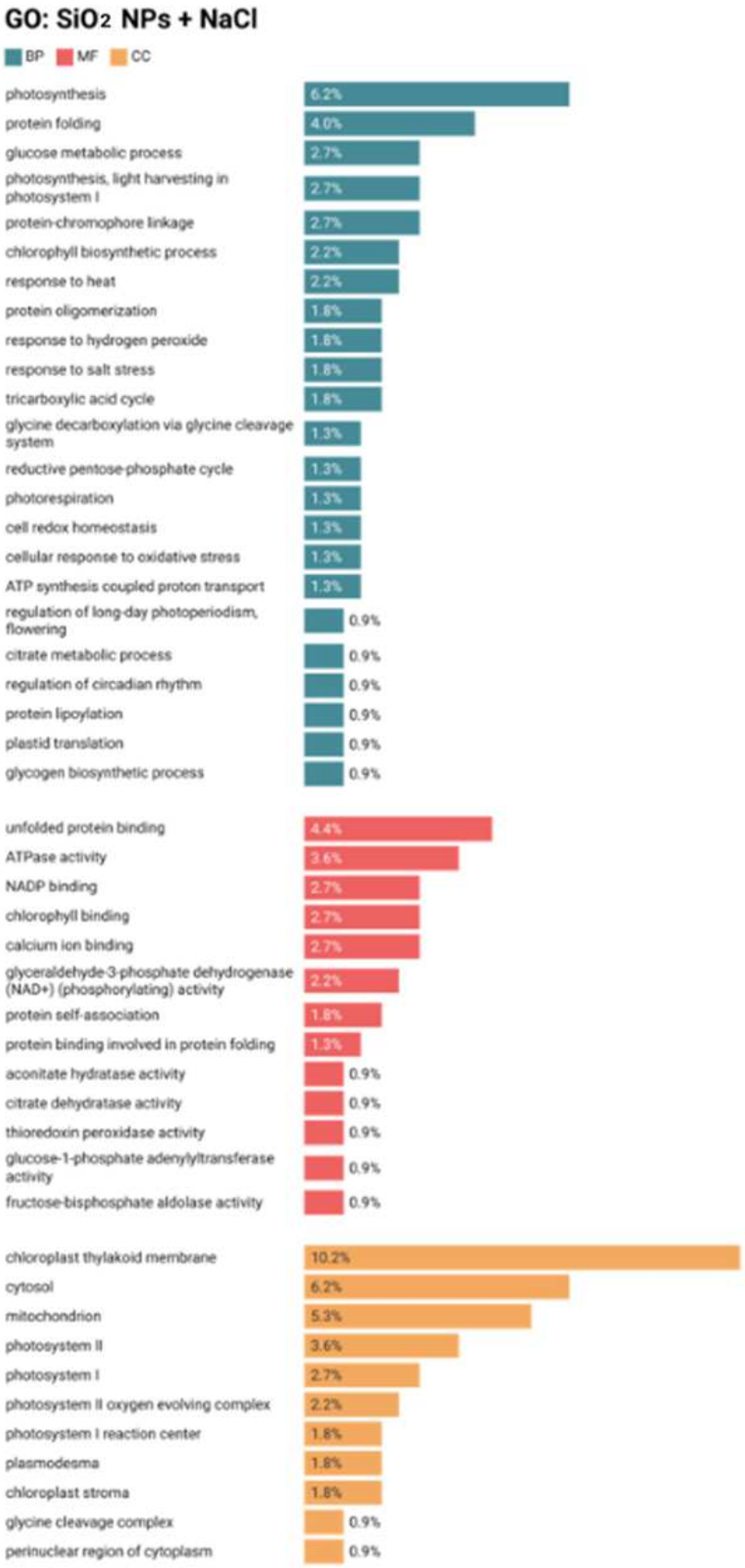

Figure 3.19-c: Cluster frequency (%) of GO enrichment performed with the Database for Annotation, Visualization, and Integrated Discovery (DAVID) of Differential Expressed Genes (DEGs) on tomato leaves ($log_2FC>0.6$). Category of Biological Processes (BP, blue), Molecular Function (MF, pink) and Cellular Component (CC, yellow) are represented for the SiO_2 NPs + NaCl condition.

Figure 3.19-d: Cluster frequency (%) of GO enrichment performed with the Database for Annotation, Visualization, and Integrated Discovery (DAVID) of Differential Expressed Genes (DEGs) on tomato leaves ($log_2FC>0.6$). Category of Biological Processes (BP, blue), Molecular Function (MF, pink) and Cellular Component (CC, yellow) are represented for the Na_2SiO_3 condition.

Pathways involved in maintaining cellular homeostasis are also modulated. In particular, from the heatmap in **Figure 3.20-a**, it can be observed that genes involved in photosynthetic activity, such as PSBQ, PSBR, PSBS (responsible for the regulation and assembly of the photosystem II (PSII) complex, essential for the light-dependent reactions of photosynthesis and involved in protecting PSII from photodamage and oxidative stress), RBCS1, RBCS4 (encoding the small subunit of ribulose-1,5-bisphosphate carboxylase/oxygenase, Rubisco), and CAB13, CAB6A (associated with the production of chlorophyll a/b-binding proteins), are strongly up-regulated only under salt stress conditions. However, the presence of nano-Si does not influence the mitigation of this response. This observation supports physiological data, where the content of photosynthetic pigments increased under salt stress conditions but was not affected by the presence of SiO_2 NPs. The same trend is observed for GIGANTEA (GI) proteins, which are significantly down-regulated under both salt stress conditions. GI proteins act as regulators of flowering and modulate the plant's transition from the vegetative to the reproductive stage. Interestingly, it has been demonstrated that GI proteins may also play a role in the response to salt stress, crucially regulating the SOS pathway (Park *et al.*, 2016). It has been shown that the down-regulation of GI contributes to enhancing the plant's response to cellular ion accumulation, increasing the export of sodium ions from the cell (Ke *et al.*, 2017; Kim *et*

al., 2008). It is noteworthy, however, that although the leaves do not exhibit an influence of nano-Si on the plant's response to salt stress, the down-regulation of several HSP is observed when plants are treated with nano-Si in the absence of stress. In any case, despite the well-documented effects of nano-Si in mitigating various types of abiotic stress in plants (Parveen *et al.*, 2022; Verma *et al.*, 2022), the direct effect on the modulation of HSP remains to be clarified.

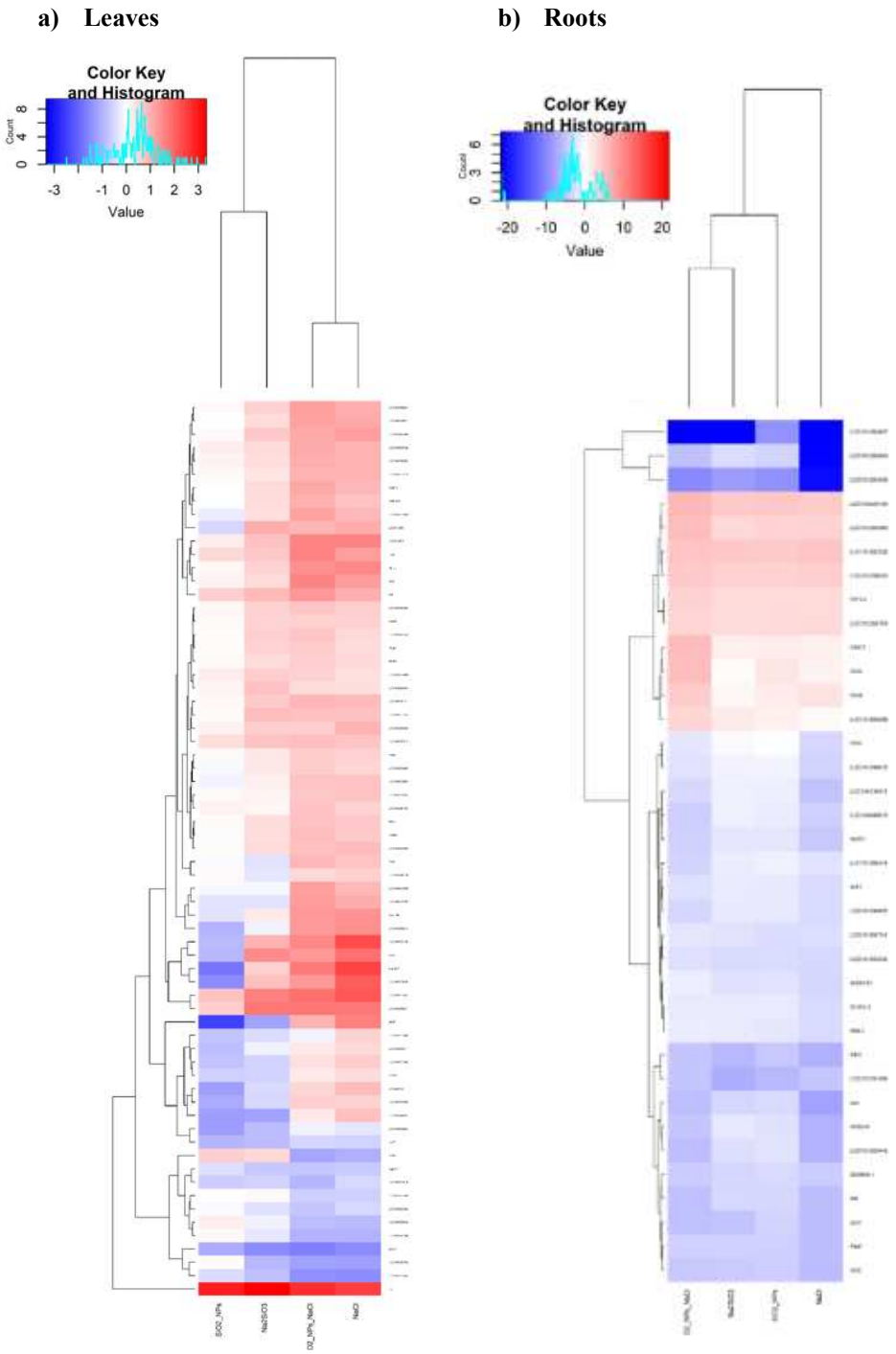

Figure 3.20: Modulation of leaves (**a**) and roots (**b**) genes that, in at least one of the four conditions (SiO_2 NPs, Na_2SiO_3, NaCl, SiO_2 NPs + NaCl), fall within functional annotations with high frequency. Log_2 Fold Change values are depicted.

In roots, the enrichment analysis was conducted with DEGs having a log_2FC greater than 3 (**Figure 3.21**). In this scenario, the most represented cellular component gene ontology classes are the extracellular region and the anchored component of the plasma membrane. At the root level, the main pathways across all conditions included the defense response, with modulation of the jasmonate and ethylene pathways, as well as the response to water deprivation and osmotic stress. Specifically, genes with water channel activity, monooxygenase and oxidoreductase activity, as well as ion binding, were modulated. This suggests an involvement in the response to osmotic stress, which at the root level appears to be triggered by all conditions under analysis.

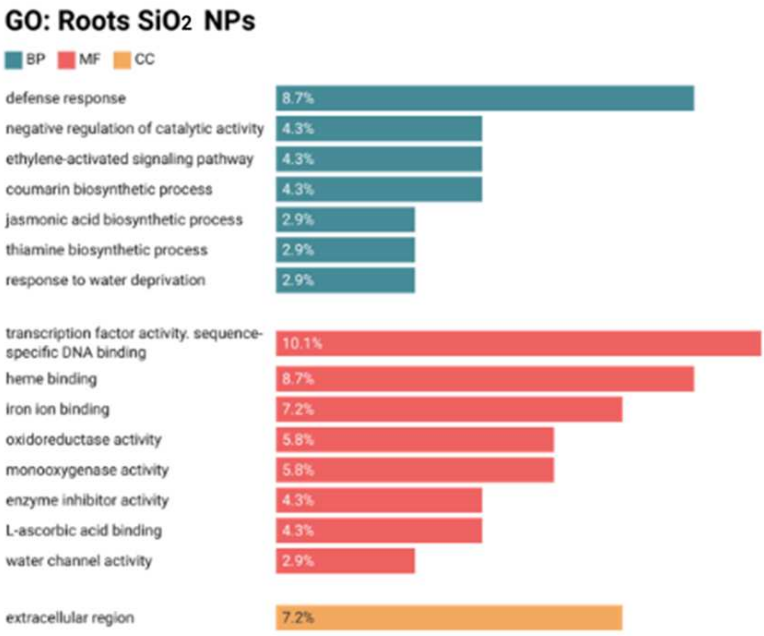

Figure 3.21-a: Cluster frequency (%) of GO enrichment performed with the Database for Annotation, Visualization, and Integrated Discovery (DAVID) of Differential Expressed Genes (DEGs) on tomato roots ($log_2FC>3$). Category of Biological Processes (BP, blue), Molecular Function (MF, pink) and Cellular Component (CC, yellow) are represented for the SiO_2 NPs condition.

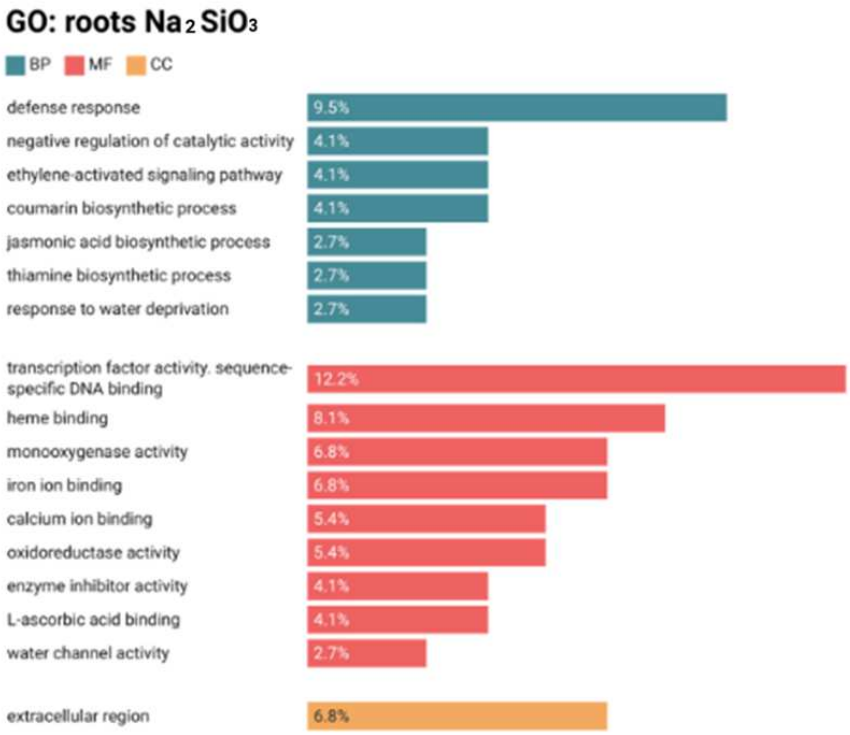

Figure 3.21-b: Cluster frequency (%) of GO enrichment performed with the Database for Annotation, Visualization, and Integrated Discovery (DAVID) of Differential Expressed Genes (DEGs) on tomato roots ($log_2FC>3$). Category of Biological Processes (BP, blue), Molecular Function (MF, pink) and Cellular Component (CC, yellow) are represented for the Na_2SiO_3 condition.

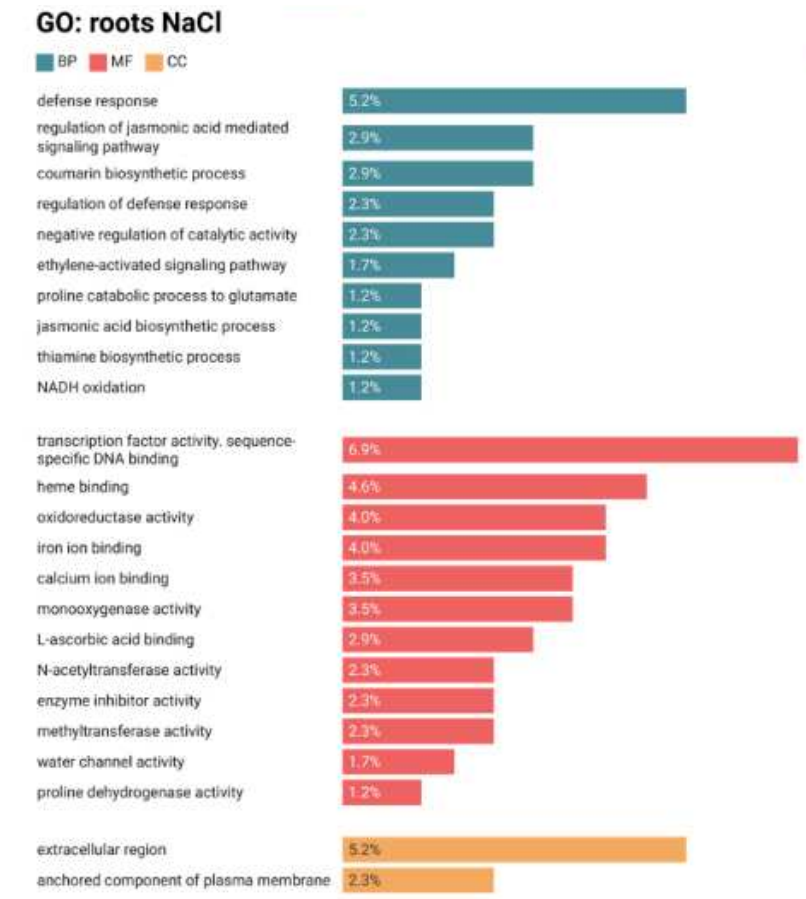

Figure 3.21-c: Cluster frequency (%) of GO enrichment performed with the Database for Annotation, Visualization, and Integrated Discovery (DAVID) of Differential Expressed Genes (DEGs) on tomato roots ($log_2FC>3$). Category of Biological Processes (BP, blue), Molecular Function (MF, pink) and Cellular Component (CC, yellow) are represented for the NaCl condition.

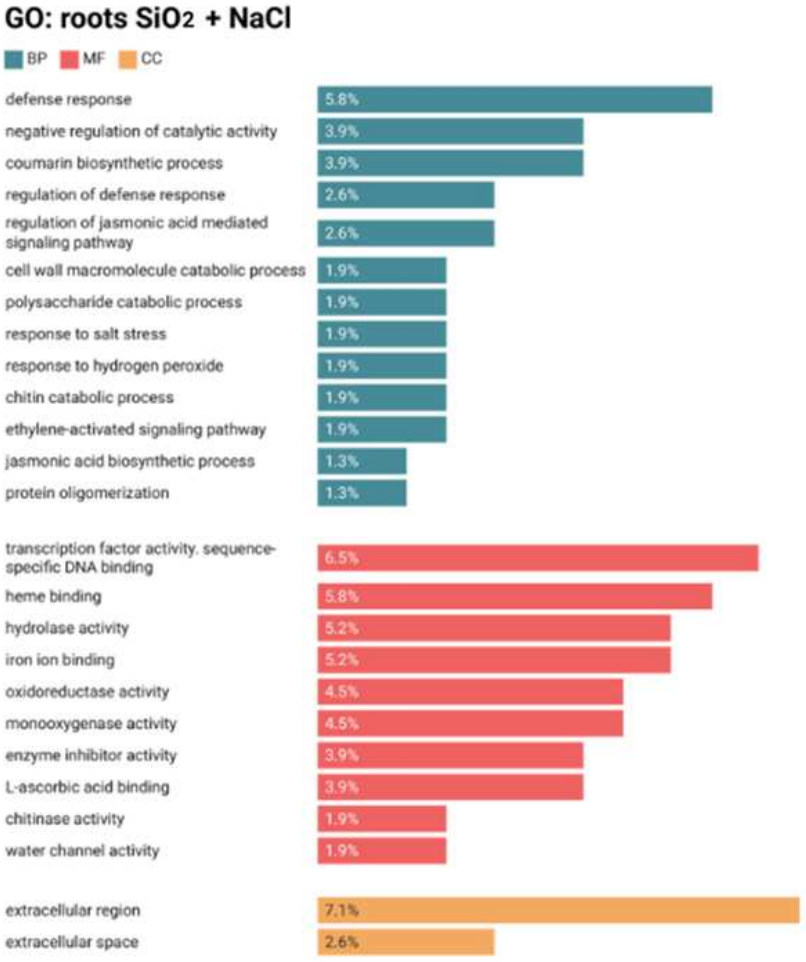

Figure 3.21-d: Cluster frequency (%) of GO enrichment performed with the Database for Annotation, Visualization, and Integrated Discovery (DAVID) of Differential Expressed Genes (DEGs) on tomato roots ($log_2FC>3$). Category of Biological Processes (BP, blue), Molecular Function (MF, pink) and Cellular Component (CC, yellow) are represented for the SiO_2 NPs + NaCl condition.

Observing the heatmap in **Figure 3.20-b**, no general differences in the modulation type between treatments are evident, but certain genes exhibit a more pronounced modulation under specific conditions compared to others. Specifically, the ethylene response factor D.5 (ERF-D5) and the gene encoding for protein TIFY 5A-like (LOC101252609) are significantly down-regulated only in plants exposed to salt stress, but this behavior is mitigated when SiO_2 NPs are applied to stressed plants. Notably, the TIFY gene family has been documented to play a crucial role in the salt stress response across various plant species, interacting with key genes and hormones (Heidari *et al.*, 2021; Tao *et al.,* 2022; Wang B. *et al.*, 2023). In soybean, it has been demonstrated that their down-regulation leads to increased salt stress sensitivity, while their overexpression enhances plant tolerance (Y. L. Liu *et al*., 2022). It is interesting to note that despite its reduced expression under salt stress conditions, the addition of nano-Si appears to act positively inhibiting this effect, playing an ameliorative role. Furthermore, chitinase activity is strongly up-regulated (CHI17, CHI3, CHI9) only in the salt stress condition when SiO_2 NPs are added. Chitinases constitute a group of proteins involved in chitin degradation, and it has been documented that they play a role in the response to abiotic stresses (Vaghela *et al*., 2022). Induction of chitinase activity is believed to contribute to the plant's ability to tolerate salt stress, and it has been demonstrated in various species that its overexpression can lead to an improved plant response to imbalances induced by exposure to saline soils (X. Liu *et al*., 2020; Takenaka *et al*., 2009).

Other key genes to analyze the response to salt stress include gibberellin 2-oxidase (GA2ox3), two jasmonate ZIM-domain proteins (JAZ2 and SLJAZ3), and two WRKY transcription factors (WRKY40 and WRKY41). Despite being down-regulated in all conditions, this behavior is approximately three times more pronounced in plants exposed to salt stress, but it is mitigated when nano-Si is added. It has been demonstrated that salt stress triggers the up-regulation of JAZ genes, which act as negative regulators of the jasmonate pathway, and the increased expression of these genes is associated with an improved plant stress response *(*Delgado *et al.*, 2021; Peethambaran *et al.,* 2018; Yoon *et al*., 2020). In this case, a down-regulation is observed under stress conditions, but the fact that the addition of nano-Si mitigates this type of response could be positive in terms of enhancing tolerance. Conversely, the aquaporin PIP2-4 (PIP2-4) and transcription factor MYB48 (LOC101262486) genes, despite being up-regulated in all conditions, exhibit an up-regulation of almost 50% only in the combined salt stress and nano-Si condition compared to other treatments. It is interesting to note that aquaporins under stress conditions generally tend to be down-regulated to limit water loss (Afzal *et al*., 2016; Jia *et al*., 2020; Yepes-Molina *et al*., 2020; Yi *et al*., 2022). However, it has been demonstrated in wheat that increasing their gene expression would be favorable for maintaining ion balance, thereby enhancing the plant's tolerance to saline environments (Hu *et*

al., 2012). Finally, the MYB transcription factor family serves as key regulators of salt stress tolerance, and it has been shown that overexpression of certain MYB genes improves resistance to saline conditions through their interaction with the DREB and ABA signaling pathways (Chen N. *et al*., 2023; Sukumaran *et al*., 2023; Wang X. *et al*., 2021). In general, it appears that at the leaves level, the plant's response is primarily influenced by salt stress, which involves the modulation of genes mainly associated with sugar metabolism and photosynthetic activity, confirming the common plant response to salt stress. The use of SiO_2 NPs does not seem to play a role in mitigating these effects. Conversely, at the root level, various genes involved in the salt stress response are strongly up-regulated or down-regulated and a direct effect of silicon nanoparticles is observed, which seems to mitigate this response when applied under stress conditions. Despite not showing a significant contribution of nano-Si at the systemic level, it is essential to consider the impact that nanoparticles have at the root level, given that this represents the plant's first point of contact. A confirmation of salt stress induced genes will be performed on tomato roots and leaves in condition of treatments with microbial consortia, alone and combined with nano-Si.

3.3.3 X-ray fluorescence elemental maps analyses on roots and leaves samples

The distribution of different elements in leaves and roots of tomato plants, was investigated through X-ray fluorescence elemental maps analyses, with the aim to clarify the interactions between the applied nanomaterials and the plants response to saline conditions. The details revealed by this analysis provide a perspective on the molecular dynamics governing the plants response to stress factors, for a deeper understanding of the underlying mechanisms in this complex interaction.

The μ-XRF maps reveal an increase in silicon uptake in both tissues when used in the form of salt (Na_2SiO_3). In the roots, the signal increased compared to the control in plants treated with nano-Si, but triplicate compared to the control in the presence of sodium metasilicate (**Figure 3.22-a**). Interestingly, in the leaves, despite silicon increased fivefold compared to the control when plants are treated with Na_2SiO_3, it remained substantially unchanged when compared to the control in plants treated with SiO_2 NPs, suggesting an absence of silicon translocation to the aerial part when used in its nanometric form (**Figure 3.22-b**). Despite this, sodium, which drastically increased under salt stress conditions compared to unstressed conditions, was significantly reduced both in the leaves and roots, demonstrating the effect of nano-Si in decreasing intracellular sodium ion content.

The observation was consistent with what has been reported in the literature: silicon has been identified as a key factor influencing the accumulation of sodium ions in plants, especially in the presence of salt stress conditions. Recent research has demonstrated that silicon effectively diminishes the absorption of sodium ions (Na^+) by plant roots, resulting in improved ion homeostasis and reduced sodium accumulation in the shoots (Shen *et al*., 2022). This beneficial effect is attributed to silicon's role in reinforcing the mechanical strength of the root cell wall, thereby limiting the uptake of sodium ions. Additionally, the deposition of silicon on the root cell wall acts as a physical barrier, further impeding the entry of sodium into the plant (Lunevich *et al.*, 2016). Moreover, silicon has been found to facilitate the excretion of sodium from the cell, decreasing sodium translocation and minimizing damage to plants (Jam *et al*., 2023). These findings suggest that silicon plays a significant role in mitigating the negative effects of salt stress by reducing the accumulation of sodium ions in plant tissues, making it a valuable tool for mitigating the detrimental impact of salt stress on plants.

a) Roots µ-XRF maps

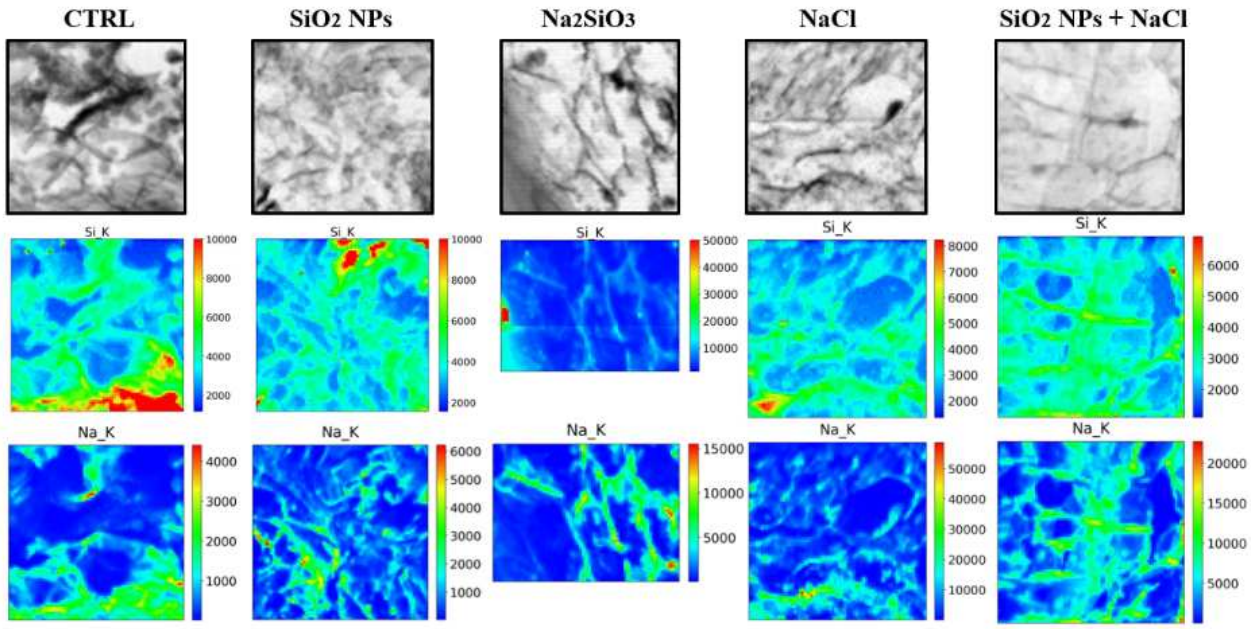

Figure 3.22-a: µ-XRF maps of roots from tomato plants treated with SiO_2 NPs, Na_2SiO_3, NaCl, SiO_2 NPs + NaCl. In the first row, the black and white 20x images of roots and leaf sections are presented, followed by the silicon maps in the second row, and the sodium maps in the third row.

b) Leaves µ-XRF maps

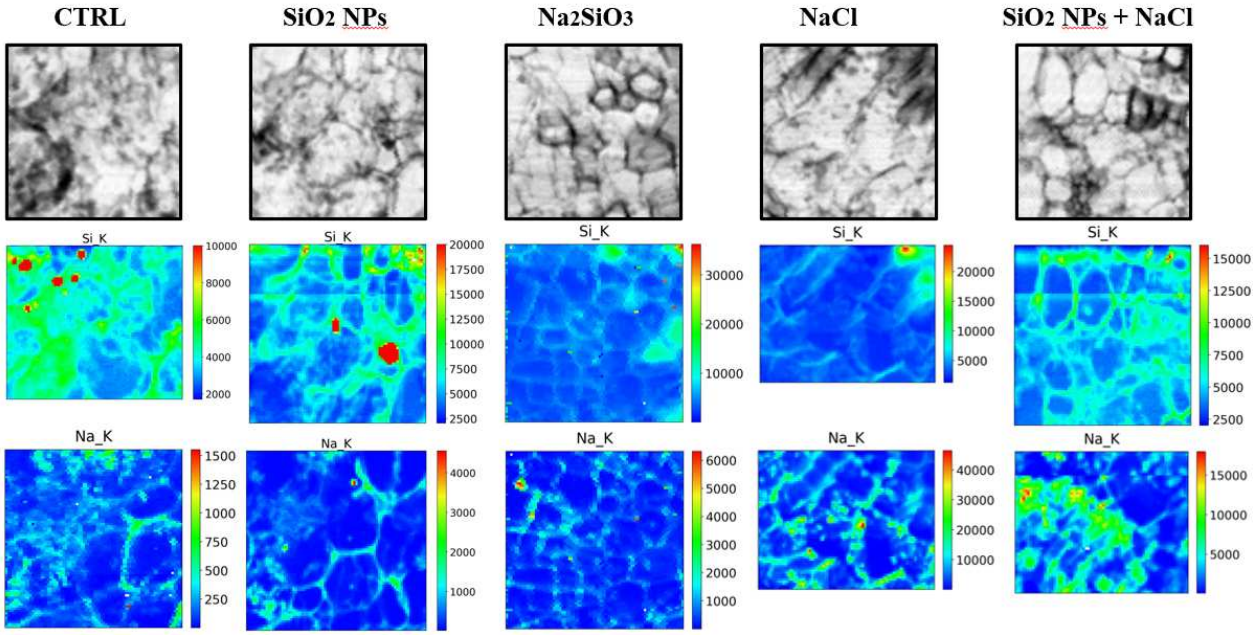

Figure 3.22-b: µ-XRF maps of leaves from tomato plants treated with SiO_2 NPs, Na_2SiO_3, NaCl, SiO_2 NPs + NaCl. In the first row, the black and white 20x images of roots and leaf sections are presented, followed by the silicon maps in the second row, and the sodium maps in the third row.

3.4 *Zea mays* L.

Iron is a fundamental element for the growth and development of plants, as it participates in vital physiological, biochemical, and molecular processes. It plays a crucial role in electron transport within the photosynthetic system, is involved in cellular respiration processes, and serves as an essential component of various enzymes. (Rout & Sahoo, 2015). Nevertheless, the plant's uptake and utilization of iron are closely tied to various environmental factors. Iron can only be transported into tissues in its Fe^{3+} form through specific transporters, following the interaction with specific chelators that facilitate uptake through dedicated transporters. The bioavailability of iron is thus correlated with the physicochemical characteristics of the soil (e.g., redox potential, pH) or the presence of a microbiota capable of enhancing its bioavailability. (Morrissey & Guerinot, 2009). To address iron deficiency in plants, several strategies are employed. These include the application of external iron sources as well as efforts to increase the bioavailability of existing iron in the soil or enhance the plant's ability to absorb it (Shenker & Chen, 2005).

In this study, the effect of Fe_3O_4 NPs on maize plants was assessed to determine the feasibility and safety of their use in the field of nano-fertilization for gradual iron release. Previous studies have suggested that certain nanoparticles, when used at appropriate concentrations, can act as effective nutrient sources to support crop growth (Anderson *et al.*, 2018). However, at excessive concentrations, nanoparticles could induce toxicity in plant crops, leading to reduced biomass, damage to the photosynthetic system, and disruption of defense mechanisms (Rizwan *et al*., 2017). Moreover, they may penetrate the root epidermis cell wall and membrane, enter the xylem, and migrate towards the shoots, potentially accumulating or undergoing biotransformation in various plant tissues. During their application, it is crucial to assess not only the impact on plant yield but also to understand the influence on biochemical and molecular pathways to identify potential signs of phytotoxicity. The evaluation of uptake and biotransformation in different tissues also helps verify the safety of their application in agri-food supply chain, especially when applied to crops of agronomic interest.

3.4.1 Morphological and physiological effects of nano-Fe in *Zea mays* L.

Maize plants were exposed to treatments with Fe_3O_4 NPs and $FeCl_3$, which were homogenized into the soil, starting from the V_2 stage (two visible leaf collars). At the end of the vegetative phase (three months after emergence), the plants entered the flowering stage (Vt) with the appearance of the tassel (**Figure 3.23-left**). During this phase, it was observed that in the control plants, the tassel remained enclosed within the flag leaf, while in the plants treated with iron, it was already exposed (**Figure 3.23-right**). Specifically, in plants treated with Fe_3O_4 NPs, unlike those treated with iron salt ($FeCl_3$), anther dehiscence appeared to be already in progress, highlighting an influence of iron-based treatments on the transition from the vegetative phase to the reproductive phase.

Figure 3.23: Maize plants three month after emergence (Vt stage) treated with Fe_3O_4 NPs 500 mg/kg and $FeCl_3$ 75 mg/kg (left). To the right, the tassels after three months of treatment are displayed for each condition.

In this phase, parameters such as plant height, stomatal transpiration, and photosynthetic activity were monitored. Despite the plants exposed to iron-based treatments appearing visually taller than the control, statistical analysis using One-way ANOVA did not reveal significant differences on the plant height among the three conditions. On the other hand, the photosynthetic activity of plants treated with $FeCl_3$ was significantly higher than the control. Furthermore, a significant increase in stomatal transpiration (reduction in resistance) was observed in maize plants treated with Fe_3O_4 NPs and $FeCl_3$ compared to the control (**Figure 3.24**).

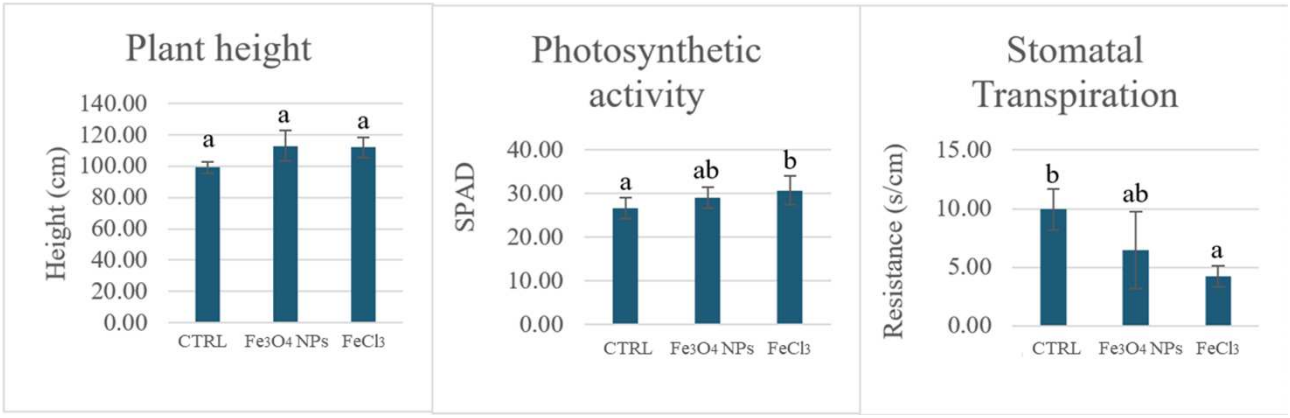

Figure 3.24: Means and standard deviations of plants height, photosynthetic activity and stomatal transpiration after three months of iron treatments. Stomatal resistance is the inverse of stomatal conductance: increased values of stomatal resistance indicate decreased stomatal transpiration. The letters (a and b) represent significant differences was obtained using One-way analysis of variance (ANOVA) followed by Tukey's HSD (Honestly Significant Difference).

One week after flowering, the emergence of silks was observed for all treatments, and after other 10 days, kernel development started. Two months after the appearance of silks (5 months after emergence), the ears were formed, and the analysis of non-invasive physiological and morphological parameters, followed by the sampling of roots, leaves, and seeds, was conducted (**Figure 3.25**).

Figure 3.25: Maize plants five month after emergence, treated with Fe_3O_4 NPs 500 mg/kg and $FeCl_3$ 75 mg/kg (left). To the right, the ears and silks after three months of treatment are displayed for each condition.

From the data collected at the end of the 5-month iron treatment, no significant differences were observed among the conditions for most of the parameters considered (**Figure 3.26**). Both the final yield (in terms of dry and fresh weight of shoots and roots, and plant height) and cellular respiration did not show significant differences in plants treated with iron compared to control plants. These results contrast with some studies reporting positive effects of Fe_3O_4 NPs on plant growth and development (Palmqvist *et al.*, 2017; Servin A. *et al.*, 2015), attributed to the peroxidase (POD) stimulatory activity of Fe_3O_4 NPs. However, it has also been demonstrated that iron-based nanomaterials may lead to plant growth deficits by blocking water and nutrient absorption at the root level (Zuverza-Mena *et al*., 2017). This can be attributed to the formation of aggregates that create plaques in the outer layer of the root inhibiting water and nutrient uptake.

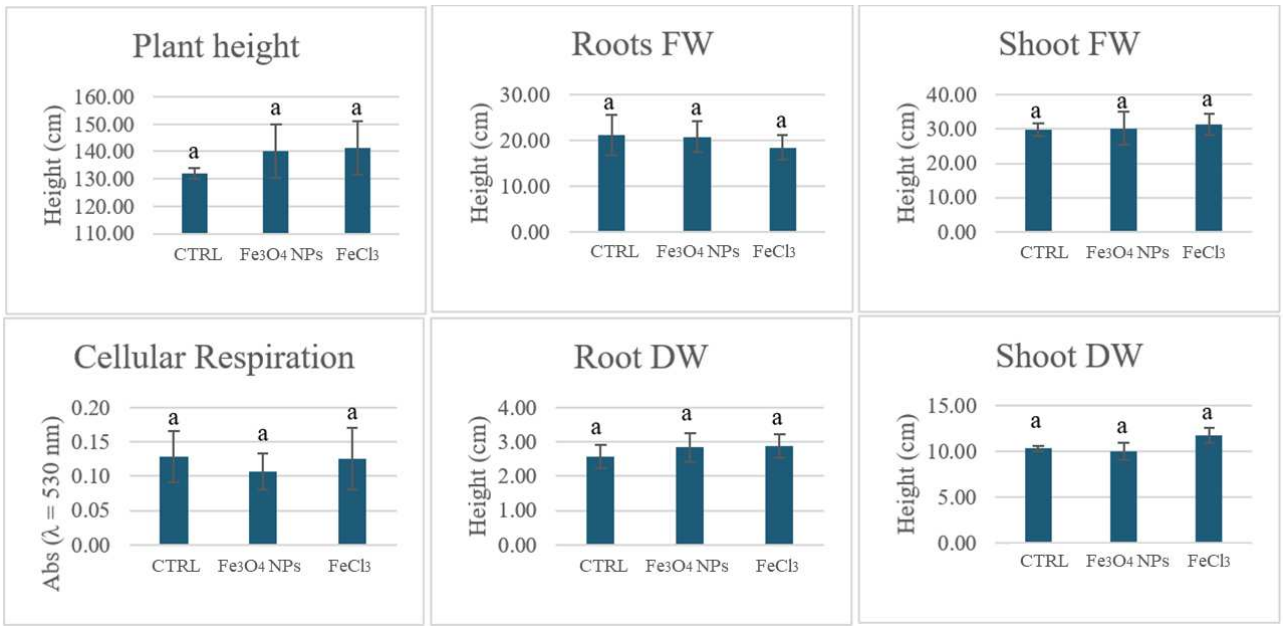

Figure 3.26: Means and standard deviations of plants height, roots and shoots fresh and dry weight (FW and DW) and cellular respiration after five months of iron treatments. The letters (a) represent significant differences was obtained using One-way analysis of variance (ANOVA) followed by Tukey's HSD (Honestly Significant Difference).

On the other hand, both stomatal transpiration and photosynthetic activity were modulated by iron exposure, with the same behavior observed during the flowering stage (**Figure 3.27-a** and **3.27-b**). The observed reduction in chlorophyll content seems in contrast with the findings reported in the literature. Several studies have demonstrated that the application of iron nanoparticles can lead to an increase in chlorophyll content in leaves, enhancing the photosynthetic activity of plants such as maize (Jalali et al., 2016), soybean (Ghafariyan *et al.*, 2013), and basil (Souad A. Elfeky, 2013). It has been hypothesized that this increase might be related to the role of iron in stimulating the activity of enzymes involved in chlorophyll synthesis (Souad A. Elfeky, 2013). The results obtained in this study may potentially be induced by stress caused by the release of ferric ions, considering that the observed effects on plants treated with nano-Fe exhibit an intermediate behavior between the untreated control and plants treated with $FeCl_3$. A similar pattern was observed in the results of MDA quantification (**Figure 3.27-c**). The presence of $FeCl_3$ resulted in an increase in lipid peroxidation compared to the control, while the cellular response of plants exposed to Fe_3O_4 NPs was intermediate between the two treatments. Several studies have observed the induction of stress in plants exposed to nano-Fe, characterized by an increase in lipid peroxidation and the activity of antioxidant enzymes. One of the hypothesized reasons is that Fe_3O_4 NPs absorbed by the root surface disrupt the physiological activity of the plant causing oxidative stress (H. Wang *et al.*, 2011), or they may form plaques around the roots that cause clogging and reduce their functionality. It is therefore suggested that the increase in antioxidant enzymes is linked to an imbalance in nutrient supply rather than direct effects (Zuverza-Mena *et al.*, 2017).

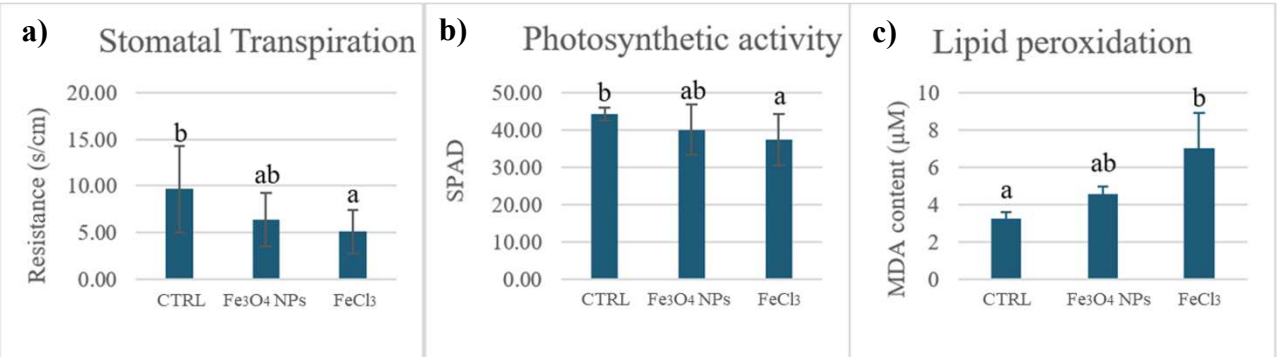

Figure 3.27: Means and standard deviations of stomatal transpiration (**a**), photosynthetic activity (**b**) and lipid peroxidation (**c**) after five months of iron treatments. The letters (a and b) represent significant differences was obtained using One-way analysis of variance (ANOVA) followed by Tukey's HSD (Honestly Significant Difference).

3.4.2 Transcriptional analysis in Real Time q-PCR on target genes

Understanding the impact of nano-Fe treatments on maize plants requires not only the assessment of morphological and physiological variations in treated plants but also the evaluation of iron-induced modulation of key genes in response to both iron uptake in tissues and potential oxidative stress induced by nanomaterials. In this study, seven genes (GSR1, MATE1, PRO1, SOD1, NAS3, FER1, AAS13) were selected to provide an overview of the plant's response to the treatments. It is well-known that sweet grasses like maize employ Strategy II for the uptake of dissolved Fe^{3+} from the soil. This involves the secretion of phytosiderophores (PS) from the roots through the TOM1 transporter. Once in the soil, these PS chelate trivalent iron, which can then be transported into the root by yellow stripe 1 (YS1) (Curie & Mari, 2017; Naranjo-Arcos & Bauer, 2016). Among the main PS produced by the plant for this purpose are those belonging to the mugineic acid family, with nicotianamine (NA) as a precursor. The synthesis of nicotianamine is catalyzed by nicotianamine synthase (NAS), playing a key role in the plant's response to iron availability or deficiency in the soil (Sharma *et al.*, 2021). In the context of plants, ferritin also serves various key functions related to iron regulation. When the plant absorbs iron from the soil through the roots, ferritin helps store the excess iron safely within cells, avoiding the risk of iron toxicity. Excess free iron can react with cellular molecules, producing harmful free radicals. Ferritin helps prevent these damages by protecting against excess reactive iron. In general, precise regulation of iron levels is essential for the proper functioning of plants, and ferritin plays a crucial role in ensuring that iron is available when needed without accumulating at harmful levels (Nguyen *et al*., 2022; Zhang *et al.*, 2023).

To inhibit cellular damage induced by free iron, another strategy adopted by plants is to chelate or bind it to metalloproteins. In extracellular fluids, citrate plays a key role in chelating iron for xylem transport. Among the elements contributing to maintaining iron homeostasis, transporters for citrate efflux, such as ferric reductase defective3 (FDR3) in *A. thaliana*, being part of the multidrug and toxic compound extrusion (MATE) transporters, are also crucial (Roschzttardtz *et al*., 2011). The modulation of genes encoding enzymes involved in the cellular response to oxidative stress, such as glutathione reductase 1 (GSR1) and superoxide dismutase 1 (SOD1), as well as in the regulation of proline biosynthesis, such as proline responding 1 (PRO1), could provide an indication of the potential cytotoxic damage caused by plant exposure to nanomaterials and the subsequent plant response (Naranjo-Arcos & Bauer, 2016; Yan *et al*., 2020). It is also important to focus on abiotic stress-induced signal transduction mediated by phytohormones.

Among these, JA plays an essential role in the plant's response to abiotic stresses, interacting with other hormones such as ethylene, auxin, and gibberellic acid, regulating the balance of resources between plant growth and defense (Wang Yun *et al*., 2021), as well as enhancing the maintenance of cellular integrity through the modulation of genes involved in oxidative stress response (Raza *et al*., 2021). For this purpose, in this study, we chose to investigate the potential modulation of the auxin amido synthetase13 (AAS13) gene. This gene encodes the enzyme jasmonic acid-amido synthetase (JAR1), which plays a key role in converting JA into its active form (7-iso-JA-Ile) that accumulates under stress conditions, thus initiating the JA signaling pathway (Wang Yun *et al*., 2021)

In **Figure 3.28**, heatmaps representing the gene expression analysis obtained through Real Time qPCR are depicted, using actin (ACT2) as the housekeeping gene and normalized to the control. At the root level (**Figure 3.28-a**), there were not very pronounced variations in gene expression, except for MATE1. Indeed, MATE1 was significantly up-regulated in the roots of plants treated with $FeCl_3$, to a much greater extent than in plants treated with nano-Fe. Considering the role of MATE1 in citrate efflux and, therefore, its involvement in xylem transport of chelated iron, it could be hypothesized that its up-regulation could be linked to a higher presence of available Fe^{3+} when used in saline form compared to nanometric form. To support this hypothesis, in leaves (**Figure 3.28-b**), both MATE1 and PRO1 are down-regulated in plants treated with Fe_3O_4 NPs and up-regulated in plants treated with $FeCl_3$. This suggests a potential greater internalization and accumulation of ions following salt treatments compared to nanomaterials.

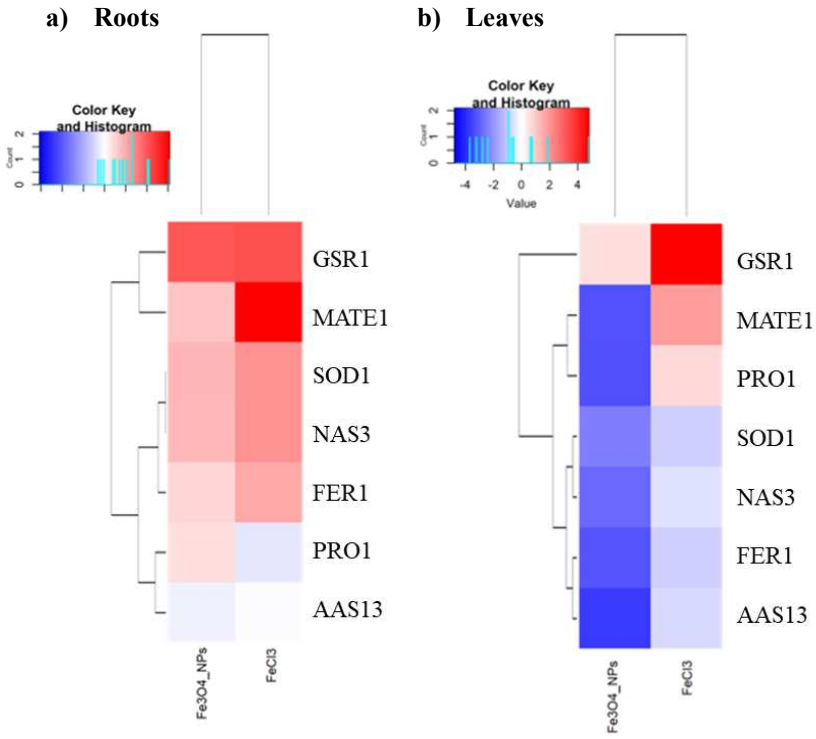

Figure 3.28: Modulation of roots (**a**) and leaves (**b**) genes of maize plants treated with Fe_3O_4 NPs and $FeCl_3$. Data were obtained through Real Time qPCR using actin (ACT2) as housekeeping gene, and normalized to the control condition.

Additionally, the response to abiotic stress seems to be more associated with salt than with nanomaterial use: the expression of the AAS13 gene, involved in triggering the JA pathway, is down-regulated in plants treated with Fe_3O_4 NPs, while GSR1 and consequently the antioxidant response is strongly up-regulated only in plants treated with $FeCl_3$. The results thus suggest a more pronounced molecular response when plants are treated with iron in ionic form compared to nanometric form, both in terms of factors related to iron uptake and in terms of the response to abiotic stress. It remains to be investigated whether this could be due to lower toxicity of iron in nanometric form or to its reduced uptake and/or translocation.

3.4.3 Iron uptake: quantitative and qualitative analyses

The results obtained, both at the physiological and molecular levels, suggest a more pronounced response of the plant when iron is administered in the form of salt compared to its nanometric form. However, it is still unclear to what extent this is related to the interaction with plant tissues and how much is attributed to the ability of iron to be internalized and translocated in its two forms. Given that maize is an agronomically significant plant, evaluating the potential accumulation of iron within the grain becomes crucial for assessing its applicability for fertilization purposes. In this context, tissues of roots, leaves, and seeds were analyzed to assess the iron content within specific tissue sections and the total content of the entire tissue. This was accomplished by generating μ-XRF maps illustrating the iron localization in tissues and its signal intensity, followed by quantification through FA-AAS of the homogenized whole tissue (**Figure 3.29**).

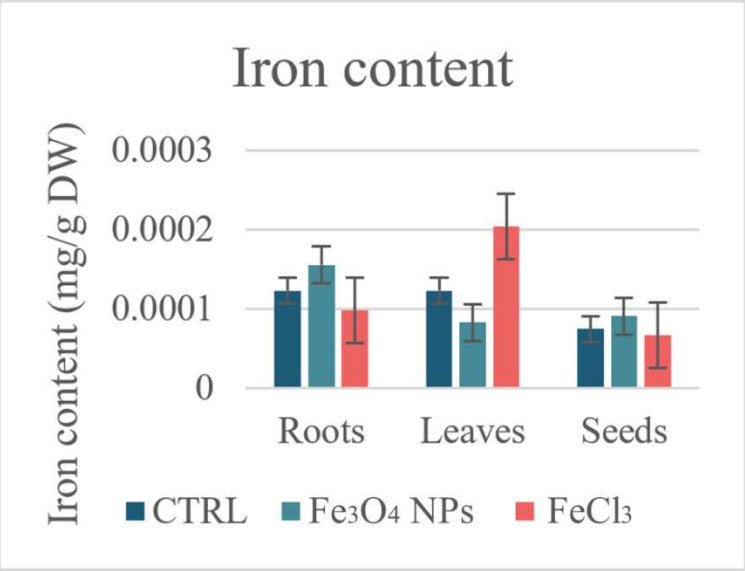

Figure 3.29-a: Iron quantification of roots, leaves and seed from tomato plants treated with Fe_3O_4 NPs and $FeCl_3$ through flame atomic absorption spectroscopy (FA-AAS).

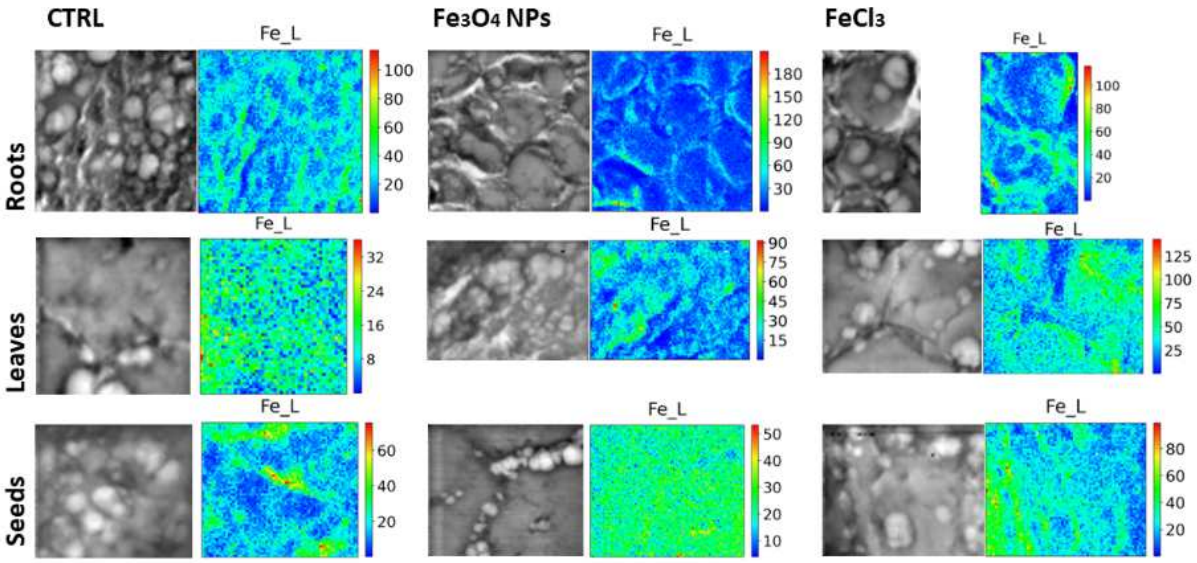

Figure 3.29-b: μ-XRF maps of roots, leaves and seed from tomato plants treated with Fe_3O_4 NPs and $FeCl_3$. The black and white 20x images of roots, leaves and seeds sections are presented, next to the iron distribution maps.

From the results of both analyses, a higher presence of iron at the root level emerged in plants treated with Fe_3O_4 NPs compared to the other two conditions, while in leaves, the iron content was significantly higher in plants treated with $FeCl_3$. In seeds, the iron content was very low for all conditions, and the differences were negligible. This evidence supports the hypotheses derived from the results of gene expression analysis. Specifically, at the root level, there was observed limited modulation of genes related to accumulation and oxidative stress response, coupled with the up-regulation of MATE1 (associated with xylematic transport) in plants treated with $FeCl_3$. In leaves, the modulation of genes involved in oxidative stress response and ion accumulation increased in plants treated with $FeCl_3$, and a greater physiological response in terms of photosynthetic activity and stomatal transpiration was observed. All these variables together reinforce the hypothesis that, when iron is applied in the form of Fe_3O_4 NPs, it tends to remain in the roots, and its translocation is significantly reduced. This results in a diminished plant response, both at the cellular and systemic levels, compared to the application of iron in the form of $FeCl_3$. Several studies have demonstrated that the use of nano-Fe as a soil amendment could, in some cases, lead to the formation of aggregates at the root level (Wang Yi *et al.*, 2021). The attractive forces between magnetite nanoparticles could create iron plaques around the roots, thus explaining the absence of evidence for iron accumulation and translocation when applied in nanometric form. However, it is essential to consider that this study utilized a concentration of Fe_3O_4 NPs of 500 mg/kg, which is quite high and may have influenced these outcomes. Indeed, it has been shown that different concentrations of Fe_3O_4 NPs can elicit diverse plant responses, ranging from being practically negligible at high concentrations to being beneficial in terms of antioxidant response and promising for nanofertilizer use at lower doses (Elanchezhian *et al.*, 2017).

4 Conclusions and future perspectives

In the context of ongoing climate emergencies and the diminishing arable lands, this study has explored alternative agro-biotechnologies, focusing on the application of biostimulants such as silicon-based nanomaterials and microbial consortia to alleviate salt stress in tomatoes, as well as iron-based nanomaterials for the gradual release of micronutrients in maize. These approaches aim to address the pressing need for sustainable agricultural practices capable of ensuring food security in despite the evolving environmental challenges. The contemporary agricultural methods are deemed unsustainable, necessitating the exploration of alternative systems. However, the utilization of such technologies is not without controversies, particularly concerning the fate of nanomaterials in the environment and their potential ecological impacts. The reduction in arable lands, coupled with unfavorable climate change projections, prompt for innovative solutions. This study contributes to the understanding of the efficacy and potential risks associated with the use of these technologies, emphasizing the need for a comprehensive evaluation of their impact on biological systems and the environment to achieve a balanced assessment of their benefits and risks.

The results obtained on tomato plants exposed to salt stress suggest a potential beneficial action of PGPMs, particularly MC_B combined with AMF, in mitigating the effect of high concentrations of NaCl-induced salt stress. Specifically, an increase in plant biomass was observed in the absence of stress, indicating a role of the microbial consortium in plant yield regardless of stress induction. On the other hand, key parameters for assessing salt stress, such as proline content and MDA content, are modulated in plants inoculated with MC_B+AMF under stress conditions. Proline content is reduced compared to other conditions in the presence of stress, while an interesting impact is noted regarding MDA content. Lipid peroxidation is indeed reduced in all conditions where microbial inoculation was applied, restoring its level under stress conditions to that present in unstressed conditions. These results suggest a potential mitigation effect on damage caused by salt stress, mediated by the microbial consortium, but further analyses are necessary to clarify the mode of action through which this effect is exerted. At the physiological level, the action of SiO_2 NPs appears to be less impactful compared to that observed with the use of the microbial consortium. However, a reduction in lipid peroxidation under stress conditions is still evident (although it remains higher compared to the control in unstressed conditions), along with an influence on cellular respiration, which shows an increase, suggesting a higher energy demand from the plant.

From a molecular perspective, a greater modulation of gene expression at the root level compared to the leaves is observed, supported by the idea that silicon, when used in nanometric form, has limited translocation capacity in the aerial part of the plant, as suggested by µ-XRF maps. In addition to the down-regulation of various HSPs in the presence of nano-Si, most effects observed in the leaves are associated with the induction of salt stress, involving the modulation of genes related to photosynthetic activity, sugar metabolism, and the cellular ion accumulation response. However, under stress conditions, these genes maintain the same level of modulation in the presence or absence of nano-Si. Conversely, at the root level, µ-XRF maps reveal an increase in silicon signal when used in nanometric form compared to the control, although still lower than that observed with Na_2SiO_3. The presence of silicon at the root level is also reflected at the molecular level, where the modulation of genes involved in the response to salt stress, such as TIFY 5A-like, various chitinase-coding genes (CHI17, CHI3, CHI9), genes involved in the jasmonate pathway (JAZ2 and SLJAZ3), aquaporins (PIP2-4), and transcription factors involved in the salt stress response (WRKY40, WRKY41, MYB48), is quite pronounced in the presence of NaCl but is significantly mitigated when SiO_2 NPs are added. Furthermore, both in leaves and roots, the sodium signal in µ-XRF maps is reduced under conditions of combined stress with nano-Si, suggesting its influence in modulating the internalization and accumulation of ions in the presence of strong osmotic imbalance, potentially playing a role in limiting the cytotoxic damage that ion accumulation could cause. However, these observations require confirmation: the modulation of key genes identified through RNA-seq must be validated through RT-qPCR, and a quantitative measurement of silicon and sodium content within the tissues is also necessary. This quantitative data will provide greater robustness to the observations drawn from µ-XRF maps.

In a parallel study, the use of Fe_3O_4 NPs as a fertilizer on maize plants was also investigated to understand its mode of action, potential accumulation, and the level of potential risk associated with its use. From physiological and molecular results, it appears that the plant's response to treatments is more dependent on the potential release of Fe^{3+} than on the use of nano-Fe. Both stomatal transpiration, photosynthetic activity, and lipid peroxidation are significantly impacted by $FeCl_3$ treatment, while plants exposed to Fe_3O_4 NPs exhibit an intermediate behavior between iron salt and the control. This finding is reinforced by gene expression analysis results, iron content quantification through FA-AAS, and observation of µ-XRF maps. The results suggest limited internalization and translocation of iron in nanometric form, while the plant's response appears to be primarily influenced by the Fe^{3+} ion. It remains to be clarified whether this behavior may be due to potential agglomeration of Fe_3O_4 NPs at the root level or potential biotransformation, which could inhibit its internalization.

In conclusion, the detailed examination of alternative agricultural technologies presented in this study has yielded positive outcomes. The potential mitigation of salt stress in tomatoes through the application of silicon-based nanomaterials and microbial consortia, as well as the use of nano-Fe in maize, underscore the potentialities of these biostimulants to contribute to the innovation of agricultural practices. While these results are promising, it is essential to acknowledge the ongoing debates surrounding the environmental fate of nanomaterials and their potential long-term impacts. The outcomes obtained in this study contribute to the knowledge supporting the adoption of biostimulants in agriculture, but ongoing research and a careful understanding of these technologies are crucial for establishing a responsible and effective framework for their widespread use, with a proper balance between implications and applications. In addressing climate challenges and declining arable lands, these solutions offer a path toward a more resilient and sustainable agricultural landscape.

5 Acknowledgements

I would like to thank all my colleagues of the Unit of Biotechnology of the Department of Chemistry, Life Science, and Environmental Sustainability (University of Parma) for their support and guidance throughout my PhD. They significantly contributed to my personal and professional growth. It is through their support that navigating through every challenge encountered along this path has made this experience truly unique and unforgettable.

I would also like to thank Dr. Andrea Zappettini and Dr. Marco Villani of IMEM-CNR (Parma, Italy) for providing certified Fe_3O_4 NPs.

Special thanks to Alessandra Gianoncelli and Valentina Bonanni of Elettra synchrotron (Trieste, Italy) for their assistance in obtaining μ-X-ray fluorescence elemental maps at the TwinMic beamline.

Finally, I am deeply grateful to all my loved ones, my family, and my friends, for their support, understanding, and encouragement in every step of the way. Without them, none of this would have been possible.

6 References

Abdelgawad, H., Zinta, G., M. Hegab, M., Pandey, R., Asard, H., & Abuelsoud, W. (2016). High Salinity Induces Different Oxidative Stress and Antioxidant Responses in Maize Seedlings Organs. *Frontiers in Plant Science*, *2*(276). https://doi.org/10.3389/fpls.2016.00276

Afzal, Z., Howton, T. C., Sun, Y., & Mukhtar, M. S. (2016). The roles of aquaporins in plant stress responses. *Journal of Developmental Biology*, *4*(1), 1–22. https://doi.org/10.3390/jdb4010009

Anderson, A. J., McLean, J. E., Jacobson, A. R., & Britt, D. W. (2018). CuO and ZnO Nanoparticles Modify Interkingdom Cell Signaling Processes Relevant to Crop Production. *Journal of Agricultural and Food Chemistry*, *66*(26), 6513–6524. https://doi.org/10.1021/ACS.JAFC.7B01302

Andorf, C., Beavis, W. D., Hufford, · Matthew, Smith, S., Suza, W. P., Wang, · Kan, Woodhouse, M., Yu, J., & Lübberstedt, T. (2019). Technological advances in maize breeding: past, present and future. *Theoretical and Applied Genetics*, *132*, 817–849. https://doi.org/10.1007/s00122-019-03306-3

Ashkavand, P., Tabari, M., Zarafshar, M., Tomášková, I., & Struve, D. (2015). Effect of SiO 2 nanoparticles on drought resistance in hawthorn seedlings . *Forest Research Papers*, *76*(4), 350–359. https://doi.org/10.1515/frp-2015-0034

Atkin, O. K., & Macherel, D. (2009). The crucial role of plant mitochondria in orchestrating drought tolerance. *Annals of Botany*, *103*(4), 581–597. https://doi.org/10.1093/aob/mcn094

Augé, R. M., Toler, H. D., & Saxton, A. M. (2015). Arbuscular mycorrhizal symbiosis alters stomatal conductance of host plants more under drought than under amply watered conditions: a meta-analysis. *Mycorrhiza*, *25*, 13–24. https://doi.org/10.1007/s00572-014-0585-4

Bao-shan, L., shao-qi, D., Chun-hui, L., Li-jun, F., Shu-chun, Q., & Min, Y. (2004). Effect of TMS (nanostructured silicon dioxide) on growth of Changbai larch seedlings. *Journal of Forestry Research*, *15*(2), 138–140.

Bergougnoux, V. (2014). The history of tomato: From domestication to biopharming. *Biotechnology Advances*, *32*(1), 170–189. https://doi.org/10.1016/J.BIOTECHADV.2013.11.003

Birhane, E., Sterck, F. J., Fetene, M., Bongers, F., & Kuyper, T. W. (2012). Arbuscular mycorrhizal fungi enhance photosynthesis, water use eYciency, and growth of frankincense seedlings under pulsed water availability conditions. *Oecologia*, *169*, 895–904. https://doi.org/10.1007/s00442-012-2258-3

Burello, E., & Worth, A. P. (2015). A rule for designing safer nanomaterials: do not interfere with the cellular redox equilibrium. *Nanotoxicology*, *9*(S1), 116–117. https://doi.org/10.3109/17435390.2013.828109

Buzea, C., & Pacheco, I. (2017). Nanomaterials and their classification. In *Advanced Structured Materials* (Vol. 62). Springer (India) Pvt. Ltd. 2017 A.K. Shukla (ed.), EMR/ESR/EPR Spectroscopy for Characterization of Nanomaterials, Advanced Structured Materials 62. https://doi.org/10.1007/978-81-322-3655-9_1

Caldara, M., Gullì, M., Graziano, S., Riboni, N., Maestri, E., Mattarozzi, M., Bianchi, F., Careri, M., & Marmiroli, N. (2024). Microbial consortia and biochar as sustainable biofertilisers: Analysis of their impact on wheat growth and production. *Science of The Total Environment*, 170168. https://doi.org/10.1016/J.SCITOTENV.2024.170168

Calestani, C., Moses, M. S., Maestri, E., Marmiroli, N., & Bray, E. A. (2015). Constitutive Expression of the Barley Dehydrin Gene aba2 Enhances Arabidopsis Germination in Response to Salt Stress. *International Journal of Plant Biology 2015, Vol. 6, Page 5826*, *6*(1), 5826. https://doi.org/10.4081/PB.2015.5826

Chen, N., Pan, L., Yang, Z., Su, M., Xu, J., Jiang, X., Yin, X., Wang, T., Wan, F., & Chi, X. (2023). A MYB-related transcription factor from peanut, AhMYB30, improves freezing and salt stress tolerance in transgenic Arabidopsis through both DREB/CBF and ABA-signaling pathways. *Frontiers in Plant Science*, *14*(February), 1–10. https://doi.org/10.3389/fpls.2023.1136626

Chen, T., & Zhang, B. (2016). Measurements of Proline and Malondialdehyde Content and Antioxidant Enzyme Activities in Leaves of Drought Stressed Cotton. *BIO-PROTOCOL*, *6*(17). https://doi.org/10.21769/BIOPROTOC.1913

Choudhary, D. K., Prakash, A., & Johri, · B N. (2007). Induced systemic resistance (ISR) in plants: mechanism of action. *Indian J. Microbiol*, *47*, 289–297.

Curie, C., & Mari, S. (2017). New routes for plant iron mining. *New Phytologist*, *214*(2), 521–525. https://doi.org/10.1111/nph.14364

Davies, K. J. A. (2000). Oxidative stress, antioxidant defenses, and damage removal, repair, and replacement systems. *IUBMB Life*, *50*(4–5), 279–289. https://doi.org/10.1080/15216540051081010

De La Cruz-Perera, C. I., Ren, D., Blanchet, M., Dendooven, L., Marsch, R., Sørensen, S. J., & Burmølle, M. (2013). The ability of soil bacteria to receive the conjugative IncP1 plasmid, pKJK10, is different in a mixed community compared to single strains. *FEMS Microbiol Lett*, *338*, 95–100. https://doi.org/10.1111/1574-6968.12036

Delgado, C., Mora-poblete, F., Ahmar, S., Chen, J. T., & Figueroa, C. R. (2021). Jasmonates and

plant salt stress: Molecular players, physiological effects, and improving tolerance by using genome-associated tools. *International Journal of Molecular Sciences*, *22*(6), 1–26. https://doi.org/10.3390/ijms22063082

du Jardin, P. (2015). Plant biostimulants: Definition, concept, main categories and regulation. *Scientia Horticulturae*, *196*, 3–14. https://doi.org/10.1016/J.SCIENTA.2015.09.021

El-Kady, M. E. ;, El-Boray, M. S., Shalan, ; A M, & Mohamed, L. M. (2017). Effect of Silicon Dioxide Nanoparticles on Growth Improvement of Banana Shoots In Vitro within Rooting Stage. *J. Plant Production, Mansoura Univ*, *8*(9), 913–916.

Elanchezhian, R., Kumar, D., Ramesh, K., Biswas, A. K., Guhey, A., & Patra, A. K. (2017). Morpho-physiological and biochemical response of maize (Zea mays L.) plants fertilized with nano-iron (Fe3O4) micronutrient. *Journal of Plant Nutrition*, *40*(14), 1969–1977. https://doi.org/10.1080/01904167.2016.1270320

Elhakem, A. H. (2020). Salicylic acid ameliorates salinity tolerance in maize by regulation of phytohormones and osmolytes. *Plant, Soil and Environment*, *66*(10), 533–541. https://doi.org/10.17221/441/2020-PSE

Elmer, W., & White, J. C. (2018). The Future of Nanotechnology in Plant Pathology. *Annual Review of Phytopathology*, *56*, 111–133. https://doi.org/10.1146/ANNUREV-PHYTO-080417-050108

EU Commission. (2022). Commission Recommendation of 10 June 2022 on the definition of nanomaterial. *Official Journal of the European Union*, *36237*(October 2011), 1–5. https://doi.org/10.2788/36237

Evelin, H., Kapoor, R., & Giri, B. (2009). Arbuscular mycorrhizal fungi in alleviation of salt stress: a review. *Annals of Botany*, *104*, 1263–1280. https://doi.org/10.1093/aob/mcp251

Fellet, G., Pilotto, L., Marchiol, L., & Braidot, E. (2021). Tools for nano-enabled agriculture: Fertilizers based on calcium phosphate, silicon, and chitosan nanostructures. *Agronomy*, *11*(6). https://doi.org/10.3390/agronomy11061239

Fujita, Y., Yoshida, T., & Yamaguchi-Shinozaki, K. (2013). Pivotal role of the AREB ABF-SnRK2 pathway in ABRE-mediated transcription in.pdf. *Physiologia Plantarum*, *147*, 15–27. https://doi.org/doi:10.1111/j.1399-3054.2012.01635.x

Ghafariyan, M. H., Malakouti, M. J., Dadpour, M. R., Stroeve, P., & Mahmoudi, M. (2013). Effects of Magnetite Nanoparticles on Soybean Chlorophyll. *Environ. Sci. Technol*, *47*, 25. https://doi.org/10.1021/es402249b

Gill, S. S., & Tuteja, N. (2010). Reactive oxygen species and antioxidant machinery in abiotic stress tolerance in crop plants. *Plant Physiology and Biochemistry*, *48*(12), 909–930. https://doi.org/10.1016/j.plaphy.2010.08.016

Goswami, P., & Mathur, J. (2022). Application of agro-waste-mediated silica nanoparticles to sustainable agriculture. *Bioresources and Bioprocessing*, *9:9*. https://doi.org/10.1186/s40643-022-00496-5

Gray, E. J., & Smith, D. L. (2005). Intracellular and extracellular PGPR: Commonalities and distinctions in the plant-bacterium signaling processes. *Soil Biology and Biochemistry*, *37*(3), 395–412. https://doi.org/10.1016/j.soilbio.2004.08.030

Graziano, S., Caldara, M., Gullì, M., Bevivino, A., Maestri, E., & Marmiroli, N. (2022). A Metagenomic and Gene Expression Analysis in Wheat (T. durum) and Maize (Z. mays) Biofertilized with PGPM and Biochar. *International Journal of Molecular Sciences*, *23*(18), 10376. https://doi.org/10.3390/IJMS231810376/S1

Hashem, A., Tabassum, B., & Fathi Abd_Allah, E. (2019). Bacillus subtilis: A plant-growth promoting rhizobacterium that also impacts biotic stress. *Saudi Journal of Biological Sciences*, *26*(6), 1291–1297. https://doi.org/10.1016/j.sjbs.2019.05.004

Hattori, T., Inanaga, S., Araki, H., An, P., Morita, S., Luxová, M., & Lux, A. (2005). Application of silicon enhanced drought tolerance in Sorghum bicolor. *Physiologia Plantarum*, *123*(4), 459–466. https://doi.org/10.1111/J.1399-3054.2005.00481.X

Heidari, P., Faraji, S., Ahmadizadeh, M., Ahmar, S., & Mora-Poblete, F. (2021). New Insights Into Structure and Function of TIFY Genes in Zea mays and Solanum lycopersicum: A Genome-Wide Comprehensive Analysis. *Frontiers in Genetics*, *12*, 657970. https://doi.org/10.3389/FGENE.2021.657970/BIBTEX

Hett, J., Döring, T. F., Bevivino, A., & Neuhoff, D. (2023). Impact of microbial consortia on organic maize in a temperate climate varies with environment but not with fertilization. *European Journal of Agronomy*, *144*, 126743. https://doi.org/10.1016/J.EJA.2023.126743

Hett, J., Neuhoff, D., Döring, T. F., Masoero, G., Ercole, E., & Bevivino, A. (2022). Effects of Multi-Species Microbial Inoculants on Early Wheat Growth and Litterbag Microbial Activity. *Agronomy*, *12*(4), 899. https://doi.org/10.3390/AGRONOMY12040899/S1

Hodges, D. M., DeLong, J. M., Forney, C. F., & Prange, R. K. (1999). Improving the thiobarbituric acid-reactive-substances assay for estimating lipid peroxidation in plant tissues containing anthocyanin and other interfering compounds. *Planta* , *207*, 604–611. https://doi.org/10.1007/s004250050524

Holden, P. A., Gardea-Torresdey, J. L., Klaessig, F., Turco, R. F., Mortimer, M., Hund-Rinke, K.,

Cohen Hubal, E. A., Avery, D., Barceló, D., Behra, R., Cohen, Y., Deydier-Stephan, L., Ferguson, P. L., Fernandes, T. F., Herr Harthorn, B., Henderson, W. M., Hoke, R. A., Hristozov, D., Johnston, J. M., … Nel, A. E. (2016). Considerations of Environmentally Relevant Test Conditions for Improved Evaluation of Ecological Hazards of Engineered Nanomaterials. *Environmental Science and Technology*, *50*(12), 6124–6145. https://doi.org/10.1021/ACS.EST.6B00608/SUPPL_FILE/ES6B00608_SI_001.PDF

Hu, W., Yuan, Q., Wang, Y., Cai, R., Deng, X., Wang, J., Zhou, S., Chen, M., Chen, L., Huang, C., Ma, Z., Yang, G., & He, G. (2012). Overexpression of a wheat aquaporin gene, TaAQP8, enhances salt stress tolerance in transgenic tobacco. *Plant and Cell Physiology*, *53*(12), 2127–2141. https://doi.org/10.1093/pcp/pcs154

Huang, D. W., Sherman, B. T., & Lempicki, R. A. (2008). Systematic and integrative analysis of large gene lists using DAVID bioinformatics resources. *Nature Protocols 2009 4:1*, *4*(1), 44–57. https://doi.org/10.1038/nprot.2008.211

Hussain, B., Lin, Q., Hamid, Y., Sanaullah, M., Di, L., Laeeq, M., Hashmi, R., Bilal Khan, M., He, Z., & Yang, X. (2020). Foliage application of selenium and silicon nanoparticles alleviates Cd and Pb toxicity in rice (Oryza sativa L.). *Science of the Total Environment*, *712*, 136497. https://doi.org/10.1016/j.scitotenv.2020.136497

Iavicoli, I., Leso, V., Beezhold, D. H., & Shvedova, A. A. (2017). Nanotechnology in agriculture: Opportunities, toxicological implications, and occupational risks. *Toxicology and Applied Pharmacology*, *329*, 96. https://doi.org/10.1016/J.TAAP.2017.05.025

Ilangumaran, G., & Smith, D. L. (2017). Plant Growth Promoting Rhizobacteria in Amelioration of Salinity Stress: A Systems Biology Perspective. *Front. Plant Sci*, *8*, 1768. https://doi.org/10.3389/fpls.2017.01768

IPCC. (2023). Summary for Policymakers: Synthesis Report. *Climate Change 2023: Synthesis Report. Contribution of Working Groups I, II and III to the Sixth Assessment Report of the Intergovernmental Panel on Climate Change*, 1–34.

Jacott, C. N., Murray, J. D., & Ridout, C. J. (2017). Trade-Offs in Arbuscular Mycorrhizal Symbiosis: Disease Resistance, Growth Responses and Perspectives for Crop Breeding. *Agronomy*, *7*(75). https://doi.org/10.3390/agronomy7040075

Jalali, M., Ghanati, | F, Modarres-Sanavi, | A M, & Khoshgoftarmanesh, | A H. (2017). Physiological effects of repeated foliar application of magnetite nanoparticles on maize plants. *J Agro Crop Sci.*, *203*, 593–602. https://doi.org/10.1111/jac.12208

Jalali, M., Ghanati, F., & Modarres-Sanavi, A. M. (2016). Effect of Fe3O4 nanoparticles and iron chelate on the antioxidant capacity and nutritional value of soil-cultivated maize (Zea mays) plants. *Crop and Pasture Science*, *67*(6), 621–628. https://doi.org/10.1071/CP15271

Jam, B. J., Shekari, F., Andalibi, B., Fotovat, R., Jafarian, V., Najafi, J., Uberti, D., & Mastinu, A. (2023). Impact of Silicon Foliar Application on the Growth and Physiological Traits of Carthamus tinctorius L. Exposed to Salt Stress. *Silicon*, *15*(3), 1235–1245. https://doi.org/10.1007/S12633-022-02090-Y/METRICS

Janni, M., Maestri, E., Gullì, M., Marmiroli, M., & Marmiroli, N. (2024). Plant responses to climate change, how global warming may impact on food security: a critical review. *Frontiers in Plant Science*, *14*, 1297569. https://doi.org/10.3389/FPLS.2023.1297569

Jia, J., Liang, Y., Gou, T., Hu, Y., Zhu, Y., Huo, H., Guo, J., & Gong, H. (2020). The expression response of plasma membrane aquaporins to salt stress in tomato plants. *Environmental and Experimental Botany*, *178*(February), 104190. https://doi.org/10.1016/j.envexpbot.2020.104190

Jiao, Y., Peluso, P., Shi, J., Liang, T., Stitzer, M. C., Wang, B., Campbell, M. S., Stein, J. C., Wei, X., Chin, C. S., Guill, K., Regulski, M., Kumari, S., Olson, A., Gent, J., Schneider, K. L., Wolfgruber, T. K., May, M. R., Springer, N. M., … Ware, D. (2017). Improved maize reference genome with single-molecule technologies. *Nature*, *546*(7659), 524–527. https://doi.org/10.1038/nature22971

Ke, Q., Kim, H. S., Wang, Z., Ji, C. Y., Jeong, J. C., Lee, H. S., Choi, Y. I., Xu, B., Deng, X., Yun, D. J., & Kwak, S. S. (2017). Down-regulation of GIGANTEA-like genes increases plant growth and salt stress tolerance in poplar. *Plant Biotechnology Journal*, *15*(3), 331–343. https://doi.org/10.1111/PBI.12628

Khan, M. I. R., Iqbal, N., Masood, A., & Khan, N. A. (2012). Variation in Salt Tolerance of Wheat Cultivars: Role of Glycinebetaine and Ethylene. *Pedosphere*, *22*(6), 746–754. https://doi.org/10.1016/S1002-0160(12)60060-5

Kim, J. A., Jung, H., Ki Hong, J., Hermand, V., Robertson McClung, C., Lee, Y.-H., Yeol Kim, J., In Lee, S., Jeong, M.-J., Kim, J., Yun, D., Kim, W., Robertson McClung CRobertsonMcClung, C., & Yeon-Hee Lee, dartmouthedu. (2008). Reduction of GIGANTEA expression in transgenic Brassica rapa enhances salt tolerance. *Plant Cell Rep*, *35*, 1943–1954. https://doi.org/10.1007/s00299-016-2008-9

Krishna, R., Jaiswal, D. K., Ansari, W. A., Singh, S., Soumia, P. S., Singh, A. K., Kumari, B., Singh, M., & Verma, J. P. (2022). Potential Microbial Consortium Mitigates Drought Stress in Tomato (Solanum lycopersicum L.) Plant by Up-regulating Stress-Responsive Genes and Improving Fruit Yield and Soil Properties. *Journal of Soil Science and Plant Nutrition*, *22*(4), 4598–4615. https://doi.org/10.1007/s42729-022-00929-2

Kumar Tripathi, D., Singh, S., Singh, V. P., Prasad, S. M., Dubey, N. K., & Chauhan, D. K. (2017). Silicon nanoparticles more effectively alleviated UV-B stress than silicon in wheat (Triticum aestivum) seedlings *. *Plant Physiology and Biochemistry*, *110*, 70–81. https://doi.org/10.1016/j.plaphy.2016.06.026

Läuchli, A., & Grattan, S. R. (2011). Plant responses to saline and sodic conditions. *Agricultural Salinity Assessment and Management: Second Edition*, 169–205. https://doi.org/10.1061/9780784411698.ch06

Liang, Y., Sun, W., Zhu, Y.-G., & Christie, P. (2007). Mechanisms of silicon-mediated alleviation of abiotic stresses in higher plants: A review. *Environmental Pollution*, *147*, 422–428. https://doi.org/10.1016/j.envpol.2006.06.008

Liu, W., Liu, K., Chen, D., Zhang, Z., Li, B., El-Mogy, M. M., Tian, S., & Chen, T. (2022). Solanum lycopersicum, a Model Plant for the Studies in Developmental Biology, Stress Biology and Food Science. *Foods 2022, Vol. 11, Page 2402*, *11*(16), 2402. https://doi.org/10.3390/FOODS11162402

Liu, X., Yu, Y., Liu, Q., Deng, S., Jin, X., Yin, Y., Guo, J., Li, N., Liu, Y., Han, S., Wang, C., & Hao, D. (2020). A Na2CO3-Responsive Chitinase Gene From Leymus chinensis Improve Pathogen Resistance and Saline-Alkali Stress Tolerance in Transgenic Tobacco and Maize. *Frontiers in Plant Science*, *11*(April), 1–12. https://doi.org/10.3389/fpls.2020.00504

Liu, Y. L., Zheng, L., Jin, L. G., Liu, Y. X., Kong, Y. N., Wang, Y. X., Yu, T. F., Chen, J., Zhou, Y. Bin, Chen, M., Wang, F. Z., Ma, Y. Z., Xu, Z. S., & Lan, J. H. (2022). Genome-Wide Analysis of the Soybean TIFY Family and Identification of GmTIFY10e and GmTIFY10g Response to Salt Stress. *Frontiers in Plant Science*, *13*(March), 1–17. https://doi.org/10.3389/fpls.2022.845314

Lunevich, L., Sanciolo, P., Smallridge, A., & Gray, S. R. (2016). Silica scale formation and effect of sodium and aluminium ions - 29 Si NMR study. *Environmental Science: Water Research & Technology*, *2*(1), 174–185. https://doi.org/10.1039/C5EW00220F

Ma, C., White, J. C., Dhankher, O. P., & Xing, B. (2015). Metal-Based Nanotoxicity and Detoxification Pathways in Higher Plants. *Environmental Science and Technology*, *49*(12), 7109–7122. https://doi.org/10.1021/ACS.EST.5B00685/SUPPL_FILE/ES5B00685_SI_001.PDF

Ma, C., White, J. C., Zhao, J., Zhao, Q., & Xing, B. (2018). Uptake of Engineered Nanoparticles by Food Crops: Characterization, Mechanisms, and Implications. *Annual Review of Food Science and Technology*, *9*, 129–153. https://doi.org/10.1146/ANNUREV-FOOD-030117-012657

Ma, L., Liu, X., Lv, W., & Yang, Y. (2022). Molecular Mechanisms of Plant Responses to Salt Stress. *Frontiers in Plant Science*, *13*(June), 1–17. https://doi.org/10.3389/fpls.2022.934877

Ma, Y., Prasad, M. N. V., Rajkumar, M., & Freitas, H. (2011). Plant growth promoting rhizobacteria and endophytes accelerate phytoremediation of metalliferous soils. *Biotechnology Advances*, *29*(2), 248–258. https://doi.org/10.1016/j.biotechadv.2010.12.001

Ma, Y., Rajkumar, M., Oliveira, R. S., Zhang, C., & Freitas, H. (2019). Potential of plant beneficial bacteria and arbuscular mycorrhizal fungi in phytoremediation of metal-contaminated saline soils. *Journal of Hazardous Materials*, *379*(March), 120813. https://doi.org/10.1016/j.jhazmat.2019.120813

Magarelli, R. A., Trupo, M., Ambrico, A., Larocca, V., Martino, M., Palazzo, S., Balducchi, R., Joutsjoki, V., Pihlanto, A., & Bevivino, A. (2022). Designing a Waste-Based Culture Medium for the Production of Plant Growth Promoting Microorganisms Based on Cladodes Juice from Opuntia ficus-indica Pruning. *Fermentation 2022, Vol. 8, Page 225*, *8*(5), 225. https://doi.org/10.3390/FERMENTATION8050225

Marmiroli, M., Mussi, F., Gallo, V., Gianoncelli, A., Hartley, W., & Marmiroli, N. (2022). Combination of Biochemical, Molecular, and Synchrotron-Radiation-Based Techniques to Study the Effects of Silicon in Tomato (Solanum Lycopersicum L.). *International Journal of Molecular Sciences*, *23*(24), 15837. https://doi.org/10.3390/IJMS232415837/S1

Marmiroli, M., Mussi, F., Imperiale, D., Lencioni, G., & Marmiroli, N. (2017). Abiotic stress response to As and As+Si, composite reprogramming of fruit metabolites in tomato cultivars. *Frontiers in Plant Science*, *8*, 310257. https://doi.org/10.3389/FPLS.2017.02201/BIBTEX

Marmiroli, M., Mussi, F., Pagano, L., Imperiale, D., Lencioni, G., Villani, M., Zappettini, A., White, J. C., & Marmiroli, N. (2020). Cadmium sulfide quantum dots impact Arabidopsis thaliana physiology and morphology. *Chemosphere*, *240*, 124856. https://doi.org/10.1016/J.CHEMOSPHERE.2019.124856

Marmiroli, M., Pagano, L., Rossi, R., De, R., Torre-Roche, L., Lepore, G. O., Ruotolo, R., Gariani, G., Bonanni, V., Pollastri, S., Puri, A., Gianoncelli, A., Aquilanti, G., D'acapito, F., White, J. C., & Marmiroli, N. (2021). Copper Oxide Nanomaterial Fate in Plant Tissue: Nanoscale Impacts on Reproductive Tissues. *Cite This: Environ. Sci. Technol*, *55*, 10769–10783. https://doi.org/10.1021/acs.est.1c01123

Marmiroli, M., Pagano, L., Savo Sardaro, M. L., Villani, M., & Marmiroli, N. (2014). Genome-wide approach in Arabidopsis thaliana to assess the toxicity of cadmium sulfide quantum dots. *Environmental Science and Technology*, *48*(10), 5902–5909. https://doi.org/10.1021/ES404958R/SUPPL_FILE/ES404958R_SI_001.PDF

Metzler, D. M., Erdem, A., Tseng, Y. H., & Huang, C. P. (2012). Responses of algal cells to engineered nanoparticles measured as algal cell population, chlorophyll a, and lipid peroxidation: Effect of particle size and type. *Journal of Nanotechnology*. https://doi.org/10.1155/2012/237284

Morrissey, J., & Guerinot, M. Lou. (2009). Iron uptake and transport in plants: The good, the bad, and the ionome. *Chem Rev.*, *109*(10), 4553–4567. https://doi.org/10.1021/cr900112r

Mourdikoudis, S., Pallares, R. M., & Thanh, N. T. K. (2018). Characterization techniques for

nanoparticles: comparison and complementarity upon studying nanoparticle properties. *Nanoscale*, *10*, 12871. https://doi.org/10.1039/c8nr02278j

Mukarram, M., Petrik, P., Mushtaq, Z., Khan, M. M. A., Gulfishan, M., & Lux, A. (2022). Silicon nanoparticles in higher plants: Uptake, action, stress tolerance, and crosstalk with phytohormones, antioxidants, and other signalling molecules. *Environmental Pollution*, *310*, 119855. https://doi.org/10.1016/J.ENVPOL.2022.119855

Munns, R., & Tester, M. (2008). Mechanisms of salinity tolerance. *Annual Review of Plant Biology*, *59*, 651–681. https://doi.org/10.1146/annurev.arplant.59.032607.092911

Murali, M., Gowtham, H. G., Singh, S. B., Shilpa, N., Aiyaz, M., Niranjana, S. R., & Amruthesh, K. N. (2021). Bio-prospecting of ACC deaminase producing Rhizobacteria towards sustainable agriculture: A special emphasis on abiotic stress in plants. *Applied Soil Ecology*, *168*, 104142. https://doi.org/10.1016/J.APSOIL.2021.104142

Murshed, R., Lopez-Lauri, F., & Sallanon, H. (2014). Effect of salt stress on tomato fruit antioxidant systems depends on fruit development stage. *Physiology and Molecular Biology of Plants*, *20*(1), 15–29. https://doi.org/10.1007/s12298-013-0209-z

Nadarajah, K. K. (2020). Ros homeostasis in abiotic stress tolerance in plants. *International Journal of Molecular Sciences*, *21*(15), 1–29. https://doi.org/10.3390/ijms21155208

Naranjo-Arcos, M. A., & Bauer, P. (2016). Iron Nutrition, Oxidative Stress, and Pathogen Defense. *Nutritional Deficiency*, *June*. https://doi.org/10.5772/63204

Nguyen, N. K., Wang, J., Liu, D., Hwang, B. K., & Jwa, N. S. (2022). Rice iron storage protein ferritin 2 (OsFER2) positively regulates ferroptotic cell death and defense responses against Magnaporthe oryzae. *Frontiers in Plant Science*, *13*(October), 1–24. https://doi.org/10.3389/fpls.2022.1019669

Okeke, E. S., Nweze, E. J., Ezike, T. C., Nwuche, C. O., Ezeorba, T. P. C., & Nwankwo, C. E. I. (2023). Silicon-based nanoparticles for mitigating the effect of potentially toxic elements and plant stress in agroecosystems: A sustainable pathway towards food security. *Science of The Total Environment*, *898*, 165446. https://doi.org/10.1016/J.SCITOTENV.2023.165446

Pagano, L., Marmiroli, M., Villani, M., Magnani, J., Rossi, R., Zappettini, A., White, J. C., & Marmiroli, N. (2022). Engineered Nanomaterial Exposure Affects Organelle Genetic Material Replication in Arabidopsis thaliana. *ACS Nano*, *16*(2), 2249–2260. https://doi.org/10.1021/ACSNANO.1C08367/SUPPL_FILE/NN1C08367_SI_001.PDF

Pagano, L., Pasquali, F., Majumdar, S., De La Torre-Roche, R., Zuverza-Mena, N., Villani, M., Zappettini, A., Marra, R. E., Isch, S. M., Marmiroli, M., Maestri, E., Dhankher, O. P., White, J. C., & Marmiroli, N. (2017). Exposure of Cucurbita pepo to binary combinations of engineered

nanomaterials: physiological and molecular response. *Environmental Science: Nano*, *4*(7), 1579–1590. https://doi.org/10.1039/C7EN00219J

Pagano, L., Rossi, R., White, J. C., Marmiroli, N., & Marmiroli, M. (2023). Nanomaterials biotransformation: In planta mechanisms of action. *Environmental Pollution*, *318*, 120834. https://doi.org/10.1016/J.ENVPOL.2022.120834

Palmqvist, N. G. M., Seisenbaeva, G. A., Svedlindh, P., & Kessler, V. G. (2017). Maghemite Nanoparticles Acts as Nanozymes, Improving Growth and Abiotic Stress Tolerance in Brassica napus. *Nanoscale Research Letters*, *12*. https://doi.org/10.1186/s11671-017-2404-2

Park, H. J., Kim, W.-Y., & Yun, D.-J. (2016). A New Insight of Salt Stress Signaling in Plant. *Mol. Cells*, *39*(6), 447–459. https://doi.org/10.14348/molcells.2016.0083

Parveen, A., Mumtaz, S., Saleem, M. H., Hussain, I., Perveen, S., & Thind, S. (2022). Silicon and nanosilicon mediated heat stress tolerance in plants. *Silicon and Nano-Silicon in Environmental Stress Management and Crop Quality Improvement: Progress and Prospects*, 153–159. https://doi.org/10.1016/B978-0-323-91225-9.00001-7

Pavlicevic, M., Elmer, W., Zuverza-Mena, N., Abdelraheem, W., Patel, R., Dimkpa, C., O'Keefe, T., Haynes, C. L., Pagano, L., Caldara, M., Marmioli, M., Maestri, E., Marmiroli, N., & White, J. C. (2023). Nanoparticles and biochar with adsorbed plant growth-promoting rhizobacteria alleviate Fusarium wilt damage on tomato and watermelon. *Plant Physiology and Biochemistry*, *203*, 108052. https://doi.org/10.1016/J.PLAPHY.2023.108052

Pavlicevic, M., Pagano, L., Villani, M., Zappettini, A., Paesano, L., Bonas, U., Marmiroli, N., & Marmiroli, M. (2023). Comparison of effect of CdS QD and ZnS QD and their corresponding salts on growth, chlorophyll content and antioxidative capacity of tomato. *International Journal of Phytoremediation*. https://doi.org/10.1080/15226514.2023.2270692

Peethambaran, P. K., Glenz, R., Höninger, S., Shahinul Islam, S. M., Hummel, S., Harter, K., Kolukisaoglu, Ü., Meynard, D., Guiderdoni, E., Nick, P., & Riemann, M. (2018). Salt-inducible expression of OsJAZ8 improves resilience against salt-stress. *BMC Plant Biology*, *18*(1), 1–15. https://doi.org/10.1186/s12870-018-1521-0

Prasanna, B. M. (2012). Diversity in global maize germplasm: Characterization and utilization. *J. Biosci.*, *37*(5), 843–855. https://doi.org/10.1007/s12038-012-9227-1

Raiola, A., Rigano, M. M., Calafiore, R., Frusciante, L., & Barone, A. (2014). Enhancing the health-promoting effects of tomato fruit for biofortified food. *Mediators of Inflammation*, *2014*. https://doi.org/10.1155/2014/139873

Rajput, V. D., Minkina, T., Feizi, M., Kumari, A., Khan, M., Mandzhieva, S., Sushkova, S., El-ramady, H., Verma, K. K., Singh, A., van Hullebusch, E. D., Singh, R. K., Jatav, H. S., &

Choudhary, R. (2021). Effects of Silicon and Silicon-Based Nanoparticles on Rhizosphere Microbiome, Plant Stress and Growth. *Biology 2021, Vol. 10, Page 791*, *10*(8), 791. https://doi.org/10.3390/BIOLOGY10080791

Rastogi, A., Tripathi, D. K., Yadav, S., Chauhan, D. K., Živčák, M., Ghorbanpour, M., El-Sheery, N. I., & Brestic, M. (2019). Application of silicon nanoparticles in agriculture. *3 Biotech*, *9*(3), 1–11. https://doi.org/10.1007/s13205-019-1626-7

Raza, A., Charagh, S., Zahid, Z., Mubarik, M. S., Javed, R., Siddiqui, M. H., & Hasanuzzaman, M. (2021). Jasmonic acid: a key frontier in conferring abiotic stress tolerance in plants. *Plant Cell Reports*, *40*(8), 1513–1541. https://doi.org/10.1007/s00299-020-02614-z

Ren, D., Madsen, J. S., Sørensen, S. J., & Burmølle, M. (2014). High prevalence of biofilm synergy among bacterial soil isolates in cocultures indicates bacterial interspecific cooperation. *The ISME Journal*, *9*, 81–89. https://doi.org/10.1038/ismej.2014.96

Rico, C. M., Majumdar, S., Duarte-Gardea, M., Peralta-Videa, J. R., & Gardea-Torresdey, J. L. (2011). Interaction of nanoparticles with edible plants and their possible implications in the food chain. *Journal of Agricultural and Food Chemistry*, *59*(8), 3485–3498. https://doi.org/10.1021/jf104517j

Rizwan, M., Ali, S., Qayyum, M. F., Ok, Y. S., Adrees, M., Ibrahim, M., Zia-ur-Rehman, M., Farid, M., & Abbas, F. (2017). Effect of metal and metal oxide nanoparticles on growth and physiology of globally important food crops: A critical review. *Journal of Hazardous Materials*, *322*(Pt A), 2–16. https://doi.org/10.1016/J.JHAZMAT.2016.05.061

Rocha, I., Ma, Y., Soluza-Alonso, P., Vosàtka, M., Freitas, H., & Oliveira, R. S. (2019). Seed Coating: A Tool for Delivering Beneficial Microbes to Agricultural Crops. *Frontiers in Plant Science*, *10*. https://doi.org/10.3389/fpls.2019.01357

Romero-Aranda, M. R., Jurado, O., & Cuartero, J. S. (2006). Silicon alleviates the deleterious salt effect on tomato plant growth by improving plant water status ARTICLE IN PRESS. *Journal of Plant Physiology*, *163*, 847–855. https://doi.org/10.1016/j.jplph.2005.05.010

Roohizadeh, G., Majd, A., & Arbabian, S. (2015). The effect of sodium silicate and silica nanoparticles on seed germination and growth in the Vicia faba L. *Tropical Plant Research*, *2*(2), 85–89. www.tropicalplantresearch.com

Roschzttardtz, H., Séguéla-Arnaud, M., Briat, J. F., Vert, G., & Curie, C. (2011). The FRD3 citrate effluxer promotes iron nutrition between symplastically disconnected tissues Throughout Arabidopsis development. *Plant Cell*, *23*(7), 2725–2737. https://doi.org/10.1105/tpc.111.088088

Rout, G. R., & Sahoo, S. (2015). ROLE OF IRON IN PLANT GROWTH AND METABOLISM

REVIEWS OPEN ACCESS. *Reviews in Agricultural Science*, *3*, 1–24. https://doi.org/10.7831/ras.3.1

Ruotolo, R., Maestri, E., Pagano, L., Marmiroli, M., White, J. C., & Marmiroli, N. (2018). Plant Response to Metal-Containing Engineered Nanomaterials: An Omics-Based Perspective. *Environmental Science and Technology*, *52*(5), 2451–2467. https://doi.org/10.1021/acs.est.7b04121

Salajegheh, M., Yavarzadeh, M., Payandeh, A., & Akbarian, M. M. (2020). Effects of titanium and silicon nanoparticles on antioxidant enzymes activity and some biochemical properties of Cuminum cyminum L. under drought stress. *Banat's Journal of Biotechnology*, *XI*(21), 19–25. https://doi.org/10.7904/2068-4738-XI(21)-19

Santoyo, G., Guzmán-Guzmán, P., Isela Parra-Cota, F., de los Santos-Villalobos, S., del Carmen Orozco-Mosqueda, M., Glick, B. R., Flores-Félix, D., Velazquez, E., & González-Andrés, F. (2021). Plant Growth Stimulation by Microbial Consortia. *Agronomy*, *11*(219). https://doi.org/10.3390/agronomy11020219

Saradadevi, R., Palta, J. A., & Siddique, K. H. M. (2017). ABA-mediated stomatal response in regulating water use during the development of terminal drought in wheat. *Frontiers in Plant Science*, *8*(July), 1–14. https://doi.org/10.3389/fpls.2017.01251

Sato, S., Tabata, S., Hirakawa, H., Asamizu, E., Shirasawa, K., Isobe, S., Kaneko, T., Nakamura, Y., Shibata, D., Aoki, K., Egholm, M., Knight, J., Bogden, R., Li, C., Shuang, Y., Xu, X., Pan, S., Cheng, S., Liu, X., … Gianese, G. (2012). The tomato genome sequence provides insights into fleshy fruit evolution. *Nature 2012 485:7400*, *485*(7400), 635–641. https://doi.org/10.1038/nature11119

Servin, A. D., De la Torre-Roche, R., Castillo-Michel, H., Pagano, L., Hawthorne, J., Musante, C., Pignatello, J., Uchimiya, M., & White, J. C. (2017). Exposure of agricultural crops to nanoparticle CeO2 in biochar-amended soil. *Plant Physiology and Biochemistry*, *110*, 147–157. https://doi.org/10.1016/J.PLAPHY.2016.06.003

Servin, A., Elmer, W., Mukherjee, A., De la Torre-Roche, R., Hamdi, H., White, J. C., Bindraban, P., & Dimkpa, C. (2015). A review of the use of engineered nanomaterials to suppress plant disease and enhance crop yield. *J Nanopart Res*, *17*(92). https://doi.org/10.1007/s11051-015-2907-7

Shah, A., Nazari, M., Antar, M., Msimbira, L. A., Naamala, J., Lyu, D., Rabileh, M., Zajonc, J., & Smith, D. L. (2021). PGPR in Agriculture: A Sustainable Approach to Increasing Climate Change Resilience. *Frontiers in Sustainable Food Systems*, *5*(July), 1–22. https://doi.org/10.3389/fsufs.2021.667546

Sharifi, M., Ghorbanli, M., & Ebrahimzadeh, H. (2007). Improved growth of salinity-stressed soybean after inoculation with salt pre-treated mycorrhizal fungi. *Journal of Plant Physiology*,

164(9), 1144–1151. https://doi.org/https://doi.org/10.1016/j.jplph.2006.06.016

Sharma, D., Chhabra, R., Muthusamy, V., Zunjare, R. U., & Hossain, F. (2021). Molecular characterization of elite maize (Zea mays L.) inbreds using markers associated with iron and zinc transporter genes. *Genetic Resources and Crop Evolution*, *68*(4), 1545–1556. https://doi.org/10.1007/s10722-020-01084-2

Shen, Z., Pu, X., Wang, S., Dong, X., Cheng, X., & Cheng, M. (2022). Silicon improves ion homeostasis and growth of liquorice under salt stress by reducing plant Na+ uptake. *Scientific Reports 2022 12:1*, *12*(1), 1–13. https://doi.org/10.1038/s41598-022-09061-8

Shenker, M., & Chen, Y. (2005). Increasing Iron Availability to Crops: Fertilizers, Organo-Fertilizers, and Biological Approaches. *Soil Science and Plant Nutrition*, *51*(1), 1–17. https://doi.org/10.1111/J.1747-0765.2005.TB00001.X

Sherman, B. T., Hao, M., Qiu, J., Jiao, X., Baseler, M. W., Lane, H. C., Imamichi, T., & Chang, W. (2022). DAVID: a web server for functional enrichment analysis and functional annotation of gene lists (2021 update). *Nucleic Acids Research*, *50*(W1), W216–W221. https://doi.org/10.1093/NAR/GKAC194

Siddiqui, M. H., & Al-Whaibi, M. H. (2014). Role of nano-SiO2 in germination of tomato (Lycopersicum esculentum seeds Mill.). *Saudi Journal of Biological Sciences*, *21*(1), 13–17. https://doi.org/10.1016/j.sjbs.2013.04.005

Slomberg, D. L., & Schoenfisch, M. H. (2012). Silica nanoparticle phytotoxicity to Arabidopsis thaliana. *Environmental Science & Technology*, *46*(18), 10247–10254. https://doi.org/10.1021/ES300949F

Smith, S. E., & Read, D. (2008). *Mycorrhizal Symbiosis* (Third). Elsevier Ltd. https://doi.org/https://doi.org/10.1016/B978-0-12-370526-6.X5001-6

Sol Genomics Network. (n.d.). Retrieved January 19, 2024, from https://solgenomics.net/organism/Solanum_lycopersicum/genome

Souad A. Elfeky, M. A. M. M. S. K. Y. A. H. O. E. E. (2013). Effect of magnetite Nano-Fertilizer on Growth and yield of Ocimum basilicum L. *International Journal of Indigenous Medicinal Plants*, *64*(3).

Su, X., Wang, B., Geng, X., Du, Y., Yang, Q., Liang, B., Meng, G., Gao, Q., Yang, W., Zhu, Y., & Lin, T. (2021). A high-continuity and annotated tomato reference genome. *BMC Genomics*, *22*(1), 1–12. https://doi.org/10.1186/S12864-021-08212-X/FIGURES/5

Sukumaran, S., Lethin, J., Liu, X., Pelc, J., Zeng, P., Hassan, S., & Aronsson, H. (2023). Genome-

Wide Analysis of MYB Transcription Factors in the Wheat Genome and Their Roles in Salt Stress Response. *Cells*, *12*(10). https://doi.org/10.3390/cells12101431

Sunita, K., Mishra, I., Mishra, J., Prakash, J., & Arora, N. K. (2020). Secondary Metabolites From Halotolerant Plant Growth Promoting Rhizobacteria for Ameliorating Salinity Stress in Plants. *Frontiers in Microbiology*, *11*, 22. https://doi.org/10.3389/fmicb.2020.567768

Suriyaprabha, R., Karunakaran, G., Yuvakkumar, R., Rajendran, V., & Kannan, N. (2014). Foliar Application of Silica Nanoparticles on the Phytochemical Responses of Maize (Zea mays L.) and Its Toxicological Behavior. *Synthesis and Reactivity in Inorganic, Metal-Organic, and Nano-Metal Chemistry*, *44*(8), 1128–1131. https://doi.org/10.1080/15533174.2013.799197

Tabacchioni, S., Passato, S., Ambrosino, P., Huang, L., Caldara, M., Cantale, C., Hett, J., Fiore, A. Del, Fiore, A., Schlüter, A., Sczyrba, A., Maestri, E., Marmiroli, N., Neuhoff, D., Nesme, J., Sørensen, S. J., Aprea, G., Nobili, C., Presenti, O., … Bevivino, A. (2021). Identification of Beneficial Microbial Consortia and Bioactive Compounds with Potential as Plant Biostimulants for a Sustainable Agriculture. *Microorganisms*, *9*, 426. https://doi.org/10.3390/microorganisms9020426

Taïbi, K., Taïbi, F., Abderrahim, L. A., Ennajah, A., Belkhodja, M., & Mulet, J. M. (2016). Effect of salt stress on growth, chlorophyll content, lipid peroxidation and antioxidant defence systems in Phaseolus vulgaris L. *South African Journal of Botany*, *105*, 306–312. https://doi.org/https://doi.org/10.1016/j.sajb.2016.03.011

Takenaka, Y., Nakano, S., Tamoi, M., Sakuda, S., & Fukamizo, T. (2009). Chitinase gene expression in response to environmental stresses in arabidopsis thaliana: Chitinase inhibitor allosamidin enhances stress tolerance. *Bioscience, Biotechnology and Biochemistry*, *73*(5), 1066–1071. https://doi.org/10.1271/bbb.80837

Tanveer, K., Gilani, S., Hussain, Z., Ishaq, R., Adeel, M., & Ilyas, N. (2020). Effect of salt stress on tomato plant and the role of calcium. *Journal of Plant Nutrition*, *43*(1), 28–35. https://doi.org/10.1080/01904167.2019.1659324

Tao, J., Jia, H., Wu, M., Zhong, W., Jia, D., Wang, Z., & Huang, C. (2022). Genome-wide identification and characterization of the TIFY gene family in kiwifruit. *BMC Genomics*, *23*(1). https://doi.org/10.1186/S12864-022-08398-8

Trovato, M., Mattioli, R., & Costantino, P. (2008). Multiple roles of proline in plant stress tolerance and development. *Rendiconti Lincei*, *19*(4), 325–346. https://doi.org/10.1007/s12210-008-0022-8

Uçarlı, C., & Uçarlı, C. (2020). Effects of Salinity on Seed Germination and Early Seedling Stage. *Abiotic Stress in Plants*. https://doi.org/10.5772/INTECHOPEN.93647

Vaghela, B., Vashi, R., Rajput, K., & Joshi, R. (2022). Plant chitinases and their role in plant defense: A comprehensive review. *Enzyme and Microbial Technology*, *159*(April), 110055. https://doi.org/10.1016/j.enzmictec.2022.110055

Vassura, I., Fabbri, D., Rombolà, A. G., Rizzi, B., Menichetti, A., Cornali, S., Pagano, L., Reggiani, R., Vecchi, M. R., & Marmiroli, N. (2023). Multi-analytical techniques to study changes in carbon and nitrogen forms in a tomato-cultivated soil treated with biochar and biostimulants. *Soil & Environmental Health*, *1*(4), 100050. https://doi.org/10.1016/J.SEH.2023.100050

Verma, K. K., Zeng, Y., Song, X. P., Singh, M., Wu, K. C., Rajput, V. D., & Li, Y. R. (2022). Nanosilicon: An approach for abiotic stress mitigation and sustainable agriculture. *Frontiers in Plant Science*, *13*(December), 1–9. https://doi.org/10.3389/fpls.2022.1025974

Volkmar, K. M., Hu, Y., & Steppuhn, H. (2011). Physiological responses of plants to salinity: A review. *Https://Doi.Org/10.4141/P97-020*, *78*(1), 19–27. https://doi.org/10.4141/P97-020

Wang, B., Wang, J., Yang, T., Wang, J., Dai, Q., Zhang, F., Xi, R., Yu, Q., & Li, N. (2023). The transcriptional regulatory network of hormones and genes under salt stress in tomato plants (Solanum lycopersicum L.). *Frontiers in Plant Science*, *14*, 1115593. https://doi.org/10.3389/FPLS.2023.1115593/BIBTEX

Wang, H., Kou, X., Pei, Z., Xiao, J. Q., Shan, X., & Xing, B. (2011). Physiological effects of magnetite (Fe3O4) nanoparticles on perennial ryegrass (Lolium perenne L.) and pumpkin (Cucurbita mixta) plants. *Nanotoxicology*, *5*(1), 30–42. https://doi.org/10.3109/17435390.2010.489206

Wang, P., Lombi, E., Zhao, F. J., & Kopittke, P. M. (2016). Nanotechnology: A New Opportunity in Plant Sciences. *Trends in Plant Science*, *21*(8), 699–712. https://doi.org/10.1016/J.TPLANTS.2016.04.005

Wang, X., Niu, Y., & Zheng, Y. (2021). Multiple functions of myb transcription factors in abiotic stress responses. *International Journal of Molecular Sciences*, *22*(11). https://doi.org/10.3390/ijms22116125

Wang, Y., Chen, S., Deng, C., Shi, X., Cota-Ruiz, K., White, J. C., Zhao, L., & Gardea-Torresdey, J. L. (2021). Metabolomic analysis reveals dose-dependent alteration of maize (Zea mays L.) metabolites and mineral nutrient profiles upon exposure to zerovalent iron nanoparticles. *NanoImpact*, *23*(March), 100336. https://doi.org/10.1016/j.impact.2021.100336

Wang, Y., Mostafa, S., Zeng, W., & Jin, B. (2021). Function and mechanism of jasmonic acid in plant responses to abiotic and biotic stresses. *International Journal of Molecular Sciences*, *22*(16). https://doi.org/10.3390/ijms22168568

Yan, L., Li, P., Zhao, X., Ji, R., & Zhao, L. (2020). Physiological and metabolic responses of maize

(Zea mays) plants to Fe3O4 nanoparticles. *Science of the Total Environment*, *718*, 137400. https://doi.org/10.1016/j.scitotenv.2020.137400

Yancey, P. H. (2005). Organic osmolytes as compatible, metabolic and counteracting cytoprotectants in high osmolarity and other stresses. *Journal of Experimental Biology*, *208*(15), 2819–2830. https://doi.org/10.1242/JEB.01730

Yang, N., Nesme, J., Lyng Røder, H., Li, X., Zuo, Z., Petersen, M., Burmølle, M., & Johannes Sørensen, S. (2021). Emergent bacterial community properties induce enhanced drought tolerance in Arabidopsis. *Npj Biofilms and Microbiomes*, *7:82*. https://doi.org/10.1038/s41522-021-00253-0

Yang, Y., & Guo, Y. (2018). Elucidating the molecular mechanisms mediating plant salt-stress responses. *New Phytologist*, *217*, 523–539. https://nph.onlinelibrary.wiley.com/doi/full/10.1111/nph.14920

Yepes-Molina, L., Bárzana, G., & Carvajal, M. (2020). Controversial regulation of gene expression and protein transduction of aquaporins under drought and salinity stress. *Plants*, *9*(12), 1–18. https://doi.org/10.3390/plants9121662

Yi, X., Sun, X., Tian, R., Li, K., Ni, M., Ying, J., Xu, L., Liu, L., & Wang, Y. (2022). Genome-Wide Characterization of the Aquaporin Gene Family in Radish and Functional Analysis of RsPIP2-6 Involved in Salt Stress. *Frontiers in Plant Science*, *13*(July). https://doi.org/10.3389/fpls.2022.860742

Yoon, Y., Seo, D. H., Shin, H., Kim, H. J., Kim, C. M., & Jang, G. (2020). The role of stress-responsive transcription factors in modulating abiotic stress tolerance in plants. *Agronomy*, *10*(6), 1–23. https://doi.org/10.3390/agronomy10060788

Zarafshar, M., Akbarinia, M., & Hosseini, S. M. (2015). Toxicity Assessment of SiO2 Nanoparticles to Pear Seedlings. *International Journal of Nanoscience and Nanotechnology*, *11*, 13–22.

Zhang, H., Song, J., Dong, F., Li, Y., Ge, S., Wei, B., & Liu, Y. (2023). Multiple roles of wheat ferritin genes during stress treatment and TaFER5D-1 as a positive regulator in response to drought and salt tolerance. *Plant Physiology and Biochemistry*, *202*(March), 107921. https://doi.org/10.1016/j.plaphy.2023.107921

Zhao, S., Zhang, Q., Liu, M., Zhou, H., Ma, C., & Wang, P. (2021). Regulation of plant responses to salt stress. *International Journal of Molecular Sciences*, *22*(9), 1–16. https://doi.org/10.3390/ijms22094609

Zmeeva, O. N., Daibova, E. B., Proskurina, L. D., Petrova, L. V., Kolomiets, N. E., Svetlichny, V. A., Lapin, I. N., & Karakchieva, N. I. (2017). Effects of Silicon Dioxide Nanoparticles on

Biological and Physiological Characteristics of Medicago sativa L. nothosubsp. varia (Martyn) in Natural Agroclimatic Conditions of the Subtaiga Zone in Western Siberia. *BioNanoScience*, *7*(4), 672–679. https://doi.org/10.1007/S12668-017-0395-1

Zuverza-Mena, N., Martínez-Fernández, D., Du, W., Hernandez-Viezcas, J. A., Bonilla-Bird, N., López-Moreno, M. L., Komárek, M., Peralta-Videa, J. R., & Gardea-Torresdey, J. L. (2017). Exposure of engineered nanomaterials to plants: Insights into the physiological and biochemical responses-A review. *Plant Physiology and Biochemistry : PPB*, *110*, 236–264. https://doi.org/10.1016/J.PLAPHY.2016.05.037

7 Appendix

Description of target genes analyzed by Real Time qPCR in *Zea mays*

GSR1 (glutathione reductase 1): encode enzyme involved in ROS scavenging by converting oxidized glutathione back to its active form.

https://www.maizegdb.org/gene_center/gene/57211

SOD1 (superoxide dismutase 1): encode enzyme involved in cellular defense against oxidative stress, catalyzing the dismutation of superoxide radicals into oxygen and hydrogen peroxide.

https://www.maizegdb.org/gene_center/gene/12645

NAS3 (nicotianamine synthase 3): encodes the enzyme (NAS) that synthesizes nicotinamine (NA), that is the precursor of mugineic acid (phytosiderophore).

https://www.maizegdb.org/gene_center/gene/952741

FER1 (ferritin1): product synthesis in response to increased iron concentration. Also involved in the formation of ferrihydrite.

https://www.maizegdb.org/gene_center/gene/25281

MATE1 (multidrug and toxic compound extrusion 1): ortholog of *A. thaliana* FDR3 gene. Located in root pericycle, mediates citrate efflux into xylem to chelate and transport iron. It is part of response pathways to abiotic stimuli and stress.

https://www.maizegdb.org/gene_center/gene/Zm00001eb261140

PRO1 (proline responding 1): encodes Δ1-pyrroline-5-carboxylate synthetase (P5CS), involved in proline biosynthesis for osmoregulation in plants.

https://www.maizegdb.org/gene_center/gene/12559

AAS13 (auxin amido synthetase13): also known as Jasmonic acid-amido synthetase (JAR1), encodes for enzyme that catalyzes the biosynthesis of 7-iso-JA-Ile (represses jasmonate signaling pathway, activates abiotic stress response pathway).

https://www.maizegdb.org/gene_center/gene/9042110

List of primers for target genes in *Z. mays*

GENE NAME	GENE ID	REFSEQ	PRIMER	PRIMER SEQ.
GSR1	Zm00001eb004790	NM_001305818.1	F	CAACCTGACACCAGTTGCAC
			R	GGGAGAACACAGCAGAAGGT
SOD1	Zm00001eb008850	NM_001155647.1	F	TCCATTCTGGGAAGGGCAGT
			R	GCTCCTGCGTTTCCTGTTGA
NAS3	Zm00001eb052890	XM_008666956.4	F	TGTCTACACCACATGCGTGA
			R	GCTCGGACTTCGACTTCTACC
FER1	Zm00001eb195010	NM_001112093.2	F	CAACTCTGGGTCGGTGGATT
			R	GACCGAACTGACACATCGCA
MATE1	Zm00001eb261140	NM_001170581.1	F	TCCTTGTTGCCGTTGTCAGT
			R	AAACATCCGGAGGCTCATGT
PRO1	Zm00001eb347680	NM_001319696.1	F	CCTTCCCTTACAATGAGGCTGT
			R	ACCATTCTATGCTCCTGCCTG
AAS13	Zm00001eb358430	NM_001174342.1	F	CGTTTAGCAGCCGTGTCATC
			R	TCGAGTGAGTTCGCTGCTTC
HK_ACT2	Zm00001d012277	NM_001154731.2	F	ACGCCGAGAACACTTTGAGG
			R	AAACCCGCCTTGACCATTCC

Value of log_2 Fold Change of common Differentially Expressed Genes (DEGs) in *S. lycopersicum* leaves for all treatments, obtained with RNA-seq analysis

Gene_ID	*SiO_2_NPs*	*Na_2SiO_3*	*NaCl*	*SiO_2_NPs_NaCl*
ACO1	-1.05255	-1.50145	-1.48738	-1.655283614
CNX61,0	-0.84227	-0.62389	-0.97765	-0.918798505
ELIP	0.639439	0.906074	1.046083	1.327393618
hsc70_1	-0.73131	-0.96245	-0.82007	-0.803919527
HSP21	1.414632	3.235802	3.612434	2.619760288
LOC100191114	-0.69192	-0.8227	-0.82535	-1.302143545
LOC101055516	-0.85602	-1.0128	-1.43277	-0.774796768
LOC101246665	0.652958	1.371206	1.581755	0.936388704
LOC101253759	1.075824	0.943386	-1.66621	-1.447364172
LOC101254946	-1.50381	0.830617	2.125847	1.332267422
LOC101255185	-0.89253	0.967727	2.336325	1.545016894
LOC101262853	-0.97191	-1.03674	-1.14082	-1.604162498
LOC101268271	0.64877	1.795353	1.752498	1.793161067
LOC101268307	-0.73784	1.40199	1.570437	1.16417925
LOC543848	-1.1251	1.15448	1.504838	1.177776038
loxF	-0.61405	-1.12007	-0.87383	-1.308241026
SlFBA1	0.758448	1.071412	1.623637	1.839782219
TAS14	1.196787	1.728512	0.693358	0.958709219
TIL	2.955646	3.330648	2.505128	2.718828373
TIL'	-2.20028	-2.11603	-2.48436	-1.806298916
yfe37	-2.474	-1.21081	1.650148	0.980896958

Value of log_2 Fold Change of common Differentially Expressed Genes (DEGs) in *S. lycopersicum* roots for all treatments, obtained with RNA-seq analysis

Gene_ID	*SiO_2_NPs*	*Na_2SiO_3*	*NaCl*	*SiO_2_NPs_NaCl*
AOC	-4.22219	-4.44101	-5.59891	-4.649312383
aos	-3.07755	-3.43924	-7.79344	-5.552631571
DES	-4.65472	-5.93421	-6.62753	-4.857984445
ER5	-3.53779	-3.31551	-4.78325	-4.839609204
ERF5	3.756572	3.59653	4.195141	3.868115678
Fad7	-3.92539	-3.95874	-5.44464	-4.017318507
ht2	-6.33303	-7.14747	-5.28789	-4.803623959
LOC100736472	-5.06295	-4.9404	-4.98721	-4.760990198
LOC101244366	-3.51682	-3.67409	-4.35859	-4.544900974
LOC101244496	-3.15316	-3.57934	-4.79085	-3.408304258
LOC101245039	-4.0181	-4.29497	-5.9034	-4.4102741
LOC101245157	-3.09233	-3.75428	-4.466	-6.218734701
LOC101245181	-3.42635	-3.53707	-3.73414	-3.726699615
LOC101245814	-4.13304	-4.06501	-4.66907	-4.359162609
LOC101246255	-3.34019	-3.68618	-20.4249	-5.539394501
LOC101246755	-5.91561	-8.15451	-20.7068	-6.557769075
LOC101246971	3.209938	3.358488	4.408529	4.36363059
LOC101247100	-6.55026	-8.98825	-15.5502	-10.16910929
LOC101247124	-4.623	-4.67636	-5.99133	-5.460907205
LOC101247816	-4.00559	-5.60841	-20.0326	-20.03263397
LOC101248084	-8.69256	-9.87952	-21.3502	-21.35017579

LOC101248306	-4.36999	-4.45347	-21.4221	-6.104996472
LOC101248628	-7.68423	-7.24678	-20.5211	-8.380140487
LOC101248631	-3.79758	-3.99429	-21.5854	-4.376553335
LOC101248653	-4.08627	-4.02059	-5.49377	-5.069558841
LOC101248655	-3.77326	-4.30121	-6.61065	-7.562703522
LOC101248770	-3.8146	-4.29551	-3.76448	-3.385423668
LOC101248856	-4.21763	-3.79034	-6.84187	-5.495266427
LOC101248953	-3.06873	-3.26687	-20.2241	-3.876941513
LOC101250382	-3.31503	-3.5642	-5.01005	-3.494617546
LOC101251084	-6.05876	-6.87383	-4.9036	-4.762045135
LOC101251208	-3.07685	-3.77657	-5.45005	-3.976865176
LOC101252146	-3.47995	-3.18823	-4.16974	-3.31819583
LOC101252232	4.51192	4.643574	4.759608	4.775758821
LOC101252571	-4.09147	-7.17957	-21.2451	-5.193122046
LOC101252574	-4.41821	-5.37965	-5.95439	-6.089639568
LOC101252609	-3.58362	-3.00478	-21.5225	-5.405317138
LOC101252898	4.037486	3.941003	5.051598	4.980695044
LOC101253225	4.367526	4.354979	5.072024	5.310462251
LOC101253387	-4.26559	-3.85206	-20.5251	-8.274826461
LOC101253648	3.907257	4.223132	4.308368	4.900645256
LOC101253836	4.124858	3.891552	3.702594	3.859420002
LOC101253883	-5.05693	-6.60686	-8.66253	-8.088402857
LOC101254783	3.311302	3.08755	3.900692	4.434969442
LOC101255971	-3.18057	-3.25413	-4.3445	-5.744530957

LOC101256077	-4.04567	-4.4627	-4.58218	-3.198863233
LOC101256185	-4.97536	-5.55387	-5.35581	-4.930719126
LOC101256762	-4.19152	-3.29756	-7.90984	-4.150137809
LOC101257192	3.805085	3.154261	3.126527	3.624335301
LOC101257443	-4.20236	-4.13986	-5.46178	-7.933826361
LOC101257731	-3.93325	-3.02772	-4.56222	-5.138518642
LOC101257981	-4.11017	-4.63405	-20.0043	-4.566835614
LOC101258429	4.360166	4.907681	6.504739	5.675551773
LOC101258434	3.82498	3.891	4.373541	4.043900081
LOC101258933	3.822907	4.048011	4.134844	4.420961381
LOC101259198	3.242967	3.469003	4.54342	3.736426367
LOC101260345	-4.19544	-5.2627	-6.60841	-6.206439173
LOC101260391	-3.22144	-3.54184	-5.02135	-5.781135912
LOC101260455	-5.68575	-8.3112	-19.9638	-5.971694535
LOC101260710	-3.68076	-5.12307	-20.4012	-6.008757608
LOC101260960	-4.069	-4.40793	-5.79396	-4.6091007
LOC101262486	3.66665	3.307528	3.712442	5.747043369
LOC101262853	-3.03561	-3.3568	-4.1711	-3.980928901
LOC101263697	-9.07292	-21.6961	-21.6961	-21.69612924
LOC101263899	-9.25592	-8.43387	-20.7233	-10.09571849
LOC101264708	3.060003	3.040327	3.259962	3.399866401
LOC101264862	-3.26038	-3.41614	-4.3772	-3.675976478
LOC101265262	-3.2427	-3.57119	-4.10863	-4.590233134
LOC101265618	-3.48096	-3.35514	-4.11126	-3.375087113

LOC101266402	-3.83964	-3.89948	-3.82423	-3.969597287
LOC101266443	-3.23442	-3.71602	-5.75702	-3.791971311
LOC101266542	-4.98294	-5.17759	-20.9756	-8.073571484
LOC101266736	-3.23157	-3.7083	-4.51446	-5.127311442
LOC101267111	-4.16558	-3.85888	-5.06843	-8.037261645
LOC101267231	-3.0179	-3.31215	-3.778	-3.109275937
LOC101267253	-3.59541	-3.6633	-3.40289	-3.086823004
LOC101267367	-4.61895	-4.47166	-5.24049	-4.741714807
LOC101267393	-3.95575	-4.41621	-6.1096	-5.36182949
LOC101267599	-3.18485	-3.00748	-20.4798	-4.709122055
LOC104645999	-3.89803	-3.83322	-4.42087	-5.867697838
LOC104647284	-3.25007	-3.32458	-5.81346	-6.123121521
LOC112940299	4.093119	4.225338	4.738208	4.831558231
LOC543607	-3.3372	-3.71674	-6.32425	-4.107965433
NR	-3.41085	-3.27624	-5.4898	-5.295179833
opr2	-3.58308	-4.91895	-5.47241	-5.372479875
PIP1-5	3.20753	3.032937	3.15948	3.745226326
PLDb2	-3.42984	-3.3119	-5.37695	-3.909490577
PPO	-3.68392	-3.54651	-6.46894	-4.852183925
SlDMR6-1	-3.07267	-3.39147	-4.35674	-4.367029376
SlERFD2	-3.93453	-3.91446	-4.44077	-3.004351807
SlVPE3	3.366143	3.398788	3.188155	3.585994956
VAHOX1	3.021178	3.216854	3.766823	4.663133429
VIF	3.91624	4.113189	4.799626	4.419675095

Wiv-1	-4.16138	-4.92068	-5.85417	-8.782036063
XSP10	3.756011	4.317089	4.544373	4.974582467

Genes that, in at least one of the four conditions (SiO_2 NPs, Na_2SiO_3, NaCl, SiO_2 NPs + NaCl), fall within functional annotations with high frequency in leaves

Ensembl_ID	***ENTREZ_ID***	***Gene_ID***	***Gene_info***
Solyc07g049530.3	544052	ACO1	1-aminocyclopropane-1-carboxylate oxidase 1(ACO1)
Solyc01g105030.3	101256629	CAB-10A	Chlorophyll a-b binding protein CP24 10A, chloroplastic(CAB-10A)
Solyc12g011450.2	101243766	CAB13	chlorophyll a-b binding protein 13, chloroplastic(CAB13)
Solyc05g056070.3	544310	CAB6A	chlorophyll a/b binding protein precursor(CAB6A)
Solyc06g068440.3	100125904	CCR1	cinnamoyl-CoA reductase(CCR1)
Solyc07g042250.3	543643	Cpn21	chaperonin 21 precursor(Cpn21)
Solyc01g008110.3	100736446	CYP51	sterol C14-demetylase(CYP51)
Solyc09g082690.3	101257109	ELIP	early light inducible protein(ELIP)
Solyc11g020330.1	544205	er-sHSP	small heat shock protein(er-sHSP)
Solyc06g051400.3	544203	Fad7	omega-3 fatty acid desaturase(Fad7)
Solyc02g081550.3	778337	ftsH6	FtsH protease(ftsH6)
Solyc06g076020.3	100736433	hsc70	heat shock protein cognate 70(Hsc70.1)
Solyc12g015880.2	543902	Hsp90-1	molecular chaperone Hsp90-1(Hsp90-1)
Solyc02g036350.3	100125909	LOC100125909	1-aminocyclopropane-1-carboxylate oxidase(ACO6)
Solyc04g015750.3	101244176	LOC101244176	magnesium-chelatase subunit ChlH, chloroplastic(LOC101244176)
Solyc12g044280.2	101244751	LOC101244751	photosystem I reaction center subunit VI, chloroplastic-like(LOC101244751)
Solyc02g069490.3	101244831	LOC101244831	sterol side chain reductase 2(SSR2)
Solyc02g069460.3	101245121	LOC101245121	photosystem I reaction center subunit III, chloroplastic(LOC101245121)
Solyc05g007780.3	101245163	LOC101245163	photosynthetic NDH subunit of lumenal location 2, chloroplastic(LOC101245163)
Solyc09g064500.3	101245880	LOC101245880	photosystem II reaction center Psb28 protein(LOC101245880)
Solyc01g088610.3	101246758	LOC101246758	10 kDa chaperonin 1, chloroplastic(LOC101246758)
Solyc07g019460.3	101247036	LOC101247036	NADPH--cytochrome P450 reductase(LOC101247036)
Solyc04g057980.3	101247812	LOC101247812	NAD(P)H-quinone oxidoreductase subunit M, chloroplastic(ORR)
Solyc09g014520.3	101249002	LOC101249002	chlorophyll a-b binding protein CP29.1, chloroplastic(LOC101249002)
Solyc09g075020.3	101249208	LOC101249208	ABC transporter C family member 9(ABCC9)
Solyc12g013810.2	101249435	LOC101249435	thioredoxin 1(LOC101249435)
Solyc11g065740.2	101249788	LOC101249788	chaperonin-like RbcX protein 2, chloroplastic(LOC101249788)
Solyc09g011080.3	101250725	LOC101250725	ribulose bisphosphate carboxylase/oxygenase activase 1, chloroplastic(LOC101250725)

Solyc05g056050.3	101253380	LOC101253380	chlorophyll a-b binding protein 6A, chloroplastic(LOC101253380)
Solyc03g115230.3	101254583	LOC101254583	chaperone protein ClpB1(LOC101254583)
Solyc12g056830.1	101254882	LOC101254882	ATP synthase delta chain, chloroplastic(LOC101254882)
Solyc01g102960.3	101254946	LOC101254946	22.7 kDa class IV heat shock protein-like(LOC101254946)
Solyc07g043460.3	101255011	LOC101255011	GLYCOALKALOID METABOLISM 6(GAME6)
Solyc03g117630.1	101255185	LOC101255185	heat shock 70 kDa protein 5(LOC101255185)
Solyc04g071990.3	101255788	LOC101255788	protein GIGANTEA(LOC101255788)
Solyc06g071920.3	101255800	LOC101255800	glyceraldehyde-3-phosphate dehydrogenase, cytosolic(LOC101255800)
Solyc06g074090.3	101256596	LOC101256596	7-dehydrocholesterol reductase(DWF5-2)
Solyc06g084045.1	101257676	LOC101257676	photosystem II reaction center W protein, chloroplastic(LOC101257676)
Solyc06g005750.3	101258266	LOC101258266	4-methylsterol oxidase(SMO4)
Solyc12g056650.2	101258346	LOC101258346	protein GIGANTEA-like(LOC101258346)
Solyc09g007270.3	101258987	LOC101258987	L-ascorbate peroxidase 2, cytosolic(LOC101258987)
Solyc12g006460.2	101261488	LOC101261488	GLYCOALKALOID METABOLISM 4(GAME4)
Solyc04g048900.3	101262304	LOC101262304	calreticulin-3-like(LOC101262304)
Solyc07g066150.1	101263732	LOC101263732	photosystem I reaction center subunit V, chloroplastic(LOC101263732)
Solyc04g082630.3	101264004	LOC101264004	glyceraldehyde-3-phosphate dehydrogenase B, chloroplastic(LOC101264004)
Solyc02g086180.3	101264777	LOC101264777	delta(7)-sterol-C5(6)-desaturase(C5-SD)
Solyc06g082940.3	101265249	LOC101265249	photosystem I reaction center subunit XI, chloroplastic(LOC101265249)
Solyc04g081570.3	101265819	LOC101265819	endoplasmin homolog(LOC101265819)
Solyc11g069790.2	101266598	LOC101266598	ruBisCO large subunit-binding protein subunit alpha(LOC101266598)
Solyc09g063130.3	101266666	LOC101266666	photosystem I reaction center subunit IV B, chloroplastic(LOC101266666)
Solyc04g009030.3	101266713	LOC101266713	glyceraldehyde-3-phosphate dehydrogenase A, chloroplastic(LOC101266713)
Solyc03g006870.3	101267287	LOC101267287	phosphoglucomutase, chloroplastic(LOC101267287)
Solyc04g014480.3	101268271	LOC101268271	15.7 kDa heat shock protein, peroxisomal(LOC101268271)
Solyc08g013670.3	101268297	LOC101268297	photosystem I reaction center subunit(LOC101268297)
Solyc03g034220.3	543974	LOC543974	ribulose bisphosphate carboxylase small chain 2A, chloroplastic(LOC543974)
Solyc07g043420.3	544002	LOC544002	2-oxoglutarate-dependent dioxygenase 2(gad2)
Solyc08g062450.1	544282	LOC544282	class II small heat shock protein Le-HSP17.6(LOC544282)
Solyc04g082010.1	544053	PETE	plastocyanin, chloroplastic(PETE)
Solyc07g054210.3	543647	POR2	protochlorophyllide reductase(POR2)
Solyc02g065400.3	544299	PSBO	oxygen-evolving enhancer protein 1, chloroplastic(PSBO)
Solyc02g079950.3	543931	PsbQ	photosystem II oxygen-evolving complex protein 3(PsbQ)
Solyc07g066310.3	778297	PSBR	PSII polypeptide(PSBR)

Solyc06g060340.3	101260830	psbS	photosystem II subunit S(psbS)
Solyc02g063150.3	543973	rbcS1	ribulose bisphosphate carboxylase small chain 1, chloroplastic(rbcS1)
Solyc02g085950.3	101268337	Rbcs-3B	ribulose bisphosphate carboxylase small chain 3B, chloroplastic-like(RBCS4)
Solyc12g010320.2	100736439	TIL	temperature-induced lipocalin(TIL)
Solyc01g073640.3	543760	yfe37	yfe37 protein(yfe37)

Genes that, in at least one of the four conditions (SiO_2 NPs, Na_2SiO_3, NaCl, SiO_2 NPs + NaCl), fall within functional annotations with high frequency in roots

Ensembl_ID	*ENTREZ_ID*	*Gene_ID*	*Gene_info*
Solyc02g085730.3	544306	AOC	allene oxide cyclase(AOC)
Solyc04g079730.1	606711	aos	allene oxide synthase(aos)
Solyc02g082930.3	544147	CHI17	chitinase(CHI17)
Solyc02g082920.3	544149	CHI3	chitinase(CHI3)
Solyc10g055810.2	544148	CHI9	chitinase(CHI9)
Solyc01g109140.3	543675	DES	divinyl ether synthase(DES)
Solyc06g051400.3	544203	Fad7	omega-3 fatty acid desaturase(Fad7)
Solyc01g079200.3	100134888	GA2ox3	gibberellin 2-oxidase(GA2ox3)
Solyc12g009220.2	100134911	LOC100134911	jasmonate ZIM-domain protein 2(JAZ2)
Solyc06g011350.3	100529106	LOC100529106	aquaporin PIP2-4(PIP2-4)
Solyc03g116890.3	101246812	LOC101246812	probable WRKY transcription factor 40(LOC101246812)
Solyc08g007830.1	101248897	LOC101248897	dehydration-responsive element-binding protein 1F-like(LOC101248897)
Solyc04g071770.3	101251084	LOC101251084	ethylene-responsive transcription factor ERF84(ERF84)
Solyc10g017510.3	101252232	LOC101252232	cytochrome P450 71BE8(CYP71BE8)
Solyc08g036620.3	101252609	LOC101252609	protein TIFY 5A-like(LOC101252609)
Solyc02g080410.3	101256444	LOC101256444	15.4 kDa class V heat shock protein(LOC101256444)
Solyc02g093600.3	101256536	LOC101256536	class I heat shock protein(LOC101256536)
Solyc03g114940.3	101258933	LOC101258933	cytochrome P450 78A5-like(LOC101258933)
Solyc11g073120.2	101262486	LOC101262486	transcription factor MYB48(LOC101262486)
Solyc08g078340.3	101262741	LOC101262741	transcription factor KUA1(LOC101262741)
Solyc01g079260.3	101263542	LOC101263542	WRKY transcription factor 23(LOC101263542)
Solyc04g051360.3	101263697	LOC101263697	ethylene response factor D.1(ERF-D1)
Solyc04g012050.3	101263899	LOC101263899	ethylene response factor D.5(ERF-D5)
Solyc12g056220.2	101264708	LOC101264708	aquaporin PIP1-3(PIP1-3)
Solyc02g089630.3	101268445	LOC101268445	proline dehydrogenase 2, mitochondrial(LOC101268445)
Solyc08g007820.1	104648613	LOC104648613	dehydration-responsive element-binding protein 1E-like(LOC104648613)
Solyc02g069310.3	543940	NML1	NIM1-like protein 1(NML1)
Solyc09g075440.3	544279	NR	ethylene receptor NR(NR)
Solyc01g103390.3	543762	opr2	12-oxophytodienoate reductase 2(opr2)
Solyc02g089620.3	778202	PDH	proline dehydrogenase(PDH)
Solyc08g081190.3	544086	PIP1-5	aquaporin PIP1-5(PIP1-5)
Solyc03g080190.3	100736526	SlDMR6-1	protein DMR6-like oxygenase(DMR6-1)
Solyc03g120475.1	101055566	SlTIP2-2	tonoplast intrinsic protein 2.2(TIP2-2)
Solyc03g122190.3	100301927	SRG1	jasmonate-ZIM domain protein 3(SLJAZ3)
Solyc03g117980.3	543603	Wfi1	whitefly-induced gp91-phox(Wfi1)
Solyc09g015770.3	101259967	WRKY81	WRKY transcription factor 41(WRKY41)